

THE EFFECT OF ALTERED WORK-REST RATIOS ON PORCINE
STIFLES

DAMJANA MILICEVIC

**THE EFFECT OF REST INSERTIONS DURING LOADING ON STIFLE
JOINT MECHANICS AND CARTILAGE DAMAGE IN A PORCINE
MODEL**

BY: DAMJANA MILICEVIC B.Sc. Kin (Hons)

**A Thesis Submitted to the School of Graduate Studies in Partial Fulfillment of the
Requirements for the Degree Master of Science**

McMaster University © Copyright by Damjana Milicevic, Sept 2016

MASTER OF SCIENCE (2016)

McMaster University

(Department of Kinesiology)

Hamilton, Ontario

TITLE:

The Effect of Rest Insertions during Loading on
Stifle Joint Mechanics and Cartilage Damage in a
Porcine Model

AUTHOR:

Damjana Milicevic B.Sc. (Hons) (University of
Waterloo)

SUPERVISOR:

Dr. Monica Maly, PhD

NUMBER OF PAGES:

xvii, 134

Lay Abstract

Repetitive loading of the knee joint is linked to breakdown of knee cartilage leading to the development and progression of knee osteoarthritis (OA). For example, over-exposure to physically demanding tasks in the workplace (*i.e.* squatting, bending, lifting etc.) increases knee OA risk. However, it is possible that rest breaks can prevent cartilage damage by allowing the tissue to recover and maintain proper function. Therefore, the purpose of this work was to determine the influence of rest on knee joint mechanics and cartilage quality by repetitively loading pig knee joints and exposing them to varying periods of rest. Rest up to sixty seconds did not allow for tissue recovery, nor did it assist with joint function. This work suggests that longer periods of rest may be required to mitigate the damaging effects of loading, or that rest may not mitigate the effects of loading at all.

Abstract

Background: Knee osteoarthritis (OA) is a prevalent disease that contributes to lower limb immobility and pain resulting in lost productivity in the work place. Repetitive loading of the knee joint, particularly in occupational settings, significantly increases OA risk. However, rest may promote tissue recovery and increase tissue tolerance to load. Therefore rest should be examined as a mechanism to prevent the development of knee OA.

Purpose: The primary objective was to determine if rest can mitigate mechanical deformation of the stifle (knee) joint and articular cartilage damage during loading compared to an unloaded control in an intact porcine stifle model.

Methods: A randomized controlled trial was conducted. Among 18 pairs of porcine hind limbs, one limb in each pair was randomly assigned to receive a loading intervention; while the matched pair served as control. Stifles in both groups were dissected, mounted into the loading apparatus, and pre-loaded. Intervention joints were then randomized into one of three loading protocols: no rest, 3:2 work:rest, and 1:1 work:rest; all of these protocols exposed joints to the same amount of cumulative load. Following loading, all joints were dissected to expose the cartilage. Cartilage damage was scored on a categorical scale. Deformation and energy dissipation were calculated for intervention limbs from data obtained from the loading apparatus.

Results: Rest did not mitigate displacement or energy dissipation in the stifles exposed to loading. Rest was associated with reduced cartilage damage scores in the lateral femur in the 1:1 condition.

Conclusion: Rest had little impact on joint mechanics and cartilage damage in this model. The small sample size may explain these results. Future investigations involving larger samples should assess if longer periods of rest are need to minimize joint damage as a result of loading.

Acknowledgements

Firstly, I would like to thank my supervisor Dr. Monica Maly for providing me with this wonderful learning opportunity. I am coming out of this degree a better researcher and I thank you for that. And I truly appreciate the countless hours you have dedicated to my work so that I may achieve my academic goals. Thank you to my collaborators Dr. Jack Callaghan and Dr. Joe Quadrilatero for the use of their lab space and expertise that have really made this project possible. I'd like to sincerely thank Mamiko Noguchi for her support and guidance throughout this project. Mamiko, you have been the best mentor I could have asked for! Thank you for all of the lessons you have taught me. I would also like to thank Dr. Gregory Wohl and Dr. Peter Keir for their investment in my project and their input that has helped to improve this work. Thank you to my amazing MacMobilize team members, both past and present: Sarah, Nick, Anthony, Elora, Jackie, Brittany, Alex, Emily, and Steph. You have made the past two years a real pleasure. Finally, I would like to thank my family and friends for their support and encouragement. I could not have done this without the help of my parents and grandparents. Without their selfless sacrifices and life-long support this achievement may only have been a dream for me. This work is their accomplishment, as much as it is mine. And last but certainly not least – thank you to my rock, Mike, for all of the little things you have done for me to make the toughest days easier. I will always appreciate your effort and love.

Contents

Lay Abstract	iii
Abstract	iv
Acknowledgements	vi
List of Tables	x
List of Figures:	xii
List of Abbreviations	xvi
Declaration of Academic Achievement	xvii
Chapter One: Introduction & Review of the Literature	1
1.0 Introduction	2
1.1 A Review of the Literature.....	5
1.1.1 Articular Cartilage of the Tibiofemoral Joint	5
1.1.2 The Loading Response of Healthy Articular Cartilage.....	6
1.1.3 Tibiofemoral Knee Osteoarthritis	10
1.1.4 Injury Mechanisms of Articular Cartilage – The Development of Tibiofemoral OA.....	12
1.1.5 Risk Factors for the Development of Tibiofemoral OA	14
1.1.6 Mechanical Determinants of OA in the Workplace.....	19
1.1.7 <i>Ex Vivo</i> Mechanical Loading and Tibiofemoral Cartilage Degeneration	22
1.2 References	36
Chapter Two: The Presence of Articular Cartilage Damage is not associated with Restrictions in End-Range Extension in Porcine Stifles.....	45
2.0 Introduction.....	46
2.1 Methodology	48
2.1.1 Specimen Preparation	48
2.1.2 Goniometry	49
2.1.3 Line Bisection	50
2.1.4 Articular Cartilage Assessment.....	50

2.1.5 Statistical Analyses	51
2.2 Results.....	52
2.2.1 Goniometry and Line Bisection Measures of Maximum Extension.....	52
2.2.2 Reliability of the Macroscopic Scoring System for Cartilage Damage.....	54
2.2.3 Differences between Extension Groups in Cartilage Damage Scores	55
2.4 Discussion	56
2.5 Conclusion	59
2.6 References.....	61
Chapter Three: The Effect of Mechanical Cyclical Loading on Porcine Stifle Deformation and Cartilage Quality	65
3.0 Introduction.....	66
3.1 Methodology	70
3.1.1 Specimen Preparation	72
3.1.2 The Loading Jig	79
3.1.3 Loading Protocols	79
3.1.4 Outcome Measures.....	89
3.1.5 Statistical Analysis.....	94
3.2 Results.....	97
3.2.1 Stifle Deformation within the No Rest, 3:2, and 1:1 Conditions throughout Loading	97
3.2.2 Energy Dissipation within the No Rest, 3:2, and 1:1 Conditions throughout Loading	99
3.2.4 Initial and Post-Loading Cartilage Damage Scores for No Rest, 3:2, and 1:1 Conditions.....	101
3.3 Discussion	102
3.4 Conclusion	111
3.5 References.....	112
Chapter Four: Discussion.....	117
4.0 Thesis Summary.....	118
4.1 Scientific Contributions	119
4.2 Future Directions	121
4.3 References.....	123

Appendix A.....	125
Macroscopic Cartilage Damage Score – A Guide to Scoring Images	125
Appendix B	129
Supplementary Figures and Tables	129
Appendix C	133
Thesis Collection Sheet.....	133

List of Tables

Table 2. 1: Macroscopic articular cartilage scoring for the medial and lateral tibial and femoral compartment of the canine stifle joint. Scores range from 0 to 4, where 0 representing no cartilage damage, and 4 representing large areas of severe damage.	42
Table 2.2: Descriptive characteristics of maximum extension angle data obtained by goniometry and line bisection including: mean, median, minimum, and maximum angle for 32 porcine stifles.	44
Table 2.3: Cartilage damage scores of the medial and lateral tibia and femur, ranging between 0 (no damage/smooth surface) to 4 (large areas of damage including the presence of cartilage lesions and fibrillation). Scores in this sample of 32 porcine stifles ranged from 0 – 4 with the majority of stifles receiving scores between 0 – 2.	46
Table 2.4: Maximum extension angle representing minor and major restrictions in extension are not related to cartilage damage score for both goniometer and line bisection measures in a sample of 32 porcine stifle joints.	47
Table 3.1: Details of the loading protocol for each condition (no rest, 3:2, 1:1) including cumulative exposure to work and rest, the work to rest ratio, and the overall duration of each loading protocol. Work, or cumulative load exposure is constant for all 3 loading protocols. The cumulative exposure to rest varies between protocols and increases from zero rest in the no rest condition to equal amounts of work and rest in the 1:1 condition.	65
Table 3.2: Categorical scores and articular cartilage surface descriptions for the qualitative macroscopic scoring system, representing cartilage damage, for a canine model (Cook et al., 2010). Scores range from 0-4, with higher scores being associated with greater cartilage damage	79
Table 3.3A: Medial femur damage scores were negatively associated with energy dissipation at the beginning of the loading protocol.....	87
Table 3.3B: Medial tibia damage scores were positively associated with energy dissipation at the end of the loading protocol	87
Table 3.4: Cartilage damage scores were significantly higher in intervention joints compared to control joints across all 4 joint compartments indicating that the loading protocol induced cartilage damage	88

Table 3.5: Lateral femur damage scores differed between the 3:2 and 1:1 loading conditions88

Table B.1: Cartilage damage scores for all intervention and control specimens and for all 4 joint compartments. Damage scores increase from no damage (0) to large areas of severe damage (4). Boxes coloured in green indicate a score of 0. Blue boxes represent scores of 1. Yellow boxes represent a score of 2, and orange represents a score of 3. The colour red represents a score of 4..... 120

List of Figures:

Figure 2.1: Goniometer and line bisection measures have poor agreement when measuring sagittal maximum extension angle. The Bland-Altman plot features a wide spread of data across the vertical axis (y), indicating large variance in angle measures...45

Figure 3.1: A methodological outline depicting the study protocol. Paired stifles were randomized to either the control or intervention groups. All specimens were dissected, mounted, and preloaded at 200 N. Intervention joints were randomized into 1 of 3 loading protocols that all produced 7,200 cycles of the same loading curve. Throughout the protocol, position data were obtained. Qualitative cartilage damage scores were also obtained for both control and intervention joints.....58

Figure 3.2: Anterior view of a specimen prior to dissection. This includes the entire limb and in intact joint, from the head of the femur to the distal portion of the tibia and fibula. The marked numbers denote anatomical landmarks where: 1) femur, 2) patella, 3) tibia and fibula.59

Figure 3.3: Example of a specimen following dissection. (A) Anterior view. This includes the entire limb and in intact joint, from the head of the femur to the distal portion of the tibia and fibula. The marked numbers denote anatomical landmarks where: 1) femur, 2) patella, 3) tibia and fibula. (B) Posterior view of a specimen following dissection where: 1) femur, 2) intact posterior joint capsule, 3) tibia and fibula.....61

Figure 3.4: (A) Anterior view of a dissected specimen resting in a custom-built vice prior to removal of excess bone. This was used to ensure that the shaft of the femur, tibia, and fibula are parallel with one another to maximize sawing accuracy and to obtain a parallel cut for mounting. (B) Anterior view of a dissected and sawed specimen where the femoral, tibial, and fibular shafts have been cut down to prepare for mounting. The anatomical landmarks are as follows: 1) femur, 2) patella, 3) tibia and fibula.....61

Figure 3.5: The femur from a bird's eye view perspective. Holes have been drilled obliquely relative to the anterior/posterior portions of the joint and the tibial condyles. Wire was inserted into these holes and folded in preparation for mounting the specimen into an aluminum cup.....62

Figure 3.6: (A) Lateral view of a dissected specimen who’s mounted on the femoral side (bottom). Wire and wood screws hold the specimen in place. Wood screws were drilled into the sides and posterior aspect of the bone. (B) Lateral view of a fully dissected and mounted specimen prior to the addition of dental plaster.63

Figure 3.7: Anterior view of a fully mounted specimen, including dental plaster, placed in the Instron for loading where: 1) femur and 2) patella. The femur is placed superiorly to the tibia such that the top cup holds the femur.64

Figure 3.8: One cycle of work. The loading cycle is a vertical GRF curve for one entire stride obtained from one representative human subject with knee OA. Loading begins at 10 N of compression and the peak load is 2400 N, or three times body weight. Ten N of compression were applied during the swing phase. The cycle was normalized to be 1 sec in duration.67

Figure 3.9: One cycle of rest where a constant load of 10 N is applied. The cycle was time normalized to be 1 s in duration.68

Figure 3.10: (A) One loading period for the no rest condition. This includes 60 repetitions of individual work cycles with no rest, which equals 1 min of loading. 120 periods of work, which each include 60 cycles of work, are repeated in the no rest loading protocol. This yields a cumulative load of 7,200 work cycles. (B) A schematic of the no rest condition. One period of work includes 60 repetitions of the work loading curve with no rest that equals 1 min of loading. This is repeated 120 times for a total cumulative load of 7200 work cycles.69

Figure 3.11: (A) One work-rest period for the 3:2 condition. This includes 60 repetitions of individual work cycles, followed by 40 repetitions of the rest cycle. Both are repeated 120 times, in an intermittent fashion (work-rest-work-rest...). However, cumulative exposure to work and rest is disproportionate with this condition having 7,200 cycles of work and 2,880 cycles of rest exposure overall. (B) A schematic of the 3:2 condition. One period of work includes 60 repetitions of the work loading curve with no rest that equals 1 min of loading. This is repeated 120 times for a total cumulative load of 7,200 work cycles. Each period of work is followed by a period of rest where 40 rest cycles are repeated for each period resulting in 40 s of rest per period. This protocol includes 120 periods of rest, with 40 rest cycles in each period. Work and rest are intermittent such that the specimen is exposed to 1 min of work followed by 40 s of rest.71

Figure 3.12: (A) One work-rest period for the 1:1 condition. This includes 60 repetitions of individual work cycles, followed by 60 repetitions of the rest cycle. Both are repeated 120 times, in an intermittent fashion (work-rest-work-rest...) so that cumulative exposure to work and rest is identical (a total of 7200 cycles of work and rest). (B) A schematic of the 1:1 condition. One period of work includes 60 repetitions of the work loading curve with no rest that equals 1 min of loading. This is repeated 120 times for a total cumulative load of 7,200 work cycles. Each period of work is followed by a period of rest where 60 rest cycles are repeated for each period resulting in 1 min of rest per period. This protocol includes 120 periods of rest, with 60 rest cycles in each period. Work and rest are intermittent such that the specimen is exposed to 1 min of work followed by 1 min of rest.73

Figure 3.13: Change in position, or displacement of a representative of mean deformation over the loading protocol (120 periods).....76

Figure 3.14: A typical load deformation curve for a representative specimen. The loading portion of the curve, beginning at the start of each cycle and ending at the peak loading magnitude (2,400 N), represents a specimen's response to loading. The unloading portion of the curve, beginning after the peak compressive value and ceasing at the end of a cycle, represents a specimen's response to unloading. The hysteresis, or area under each curve, represents energy dissipation. Dissipated energy can be calculated by subtracting the area under the unloading region from the loading region77

Figure 3.15: To address the third purpose, Spearman's Rho correlations were computed between energy dissipation at the start of the protocol and initial cartilage damage (obtained from the cartilage damage scores from the control joint – a surrogate measure of initial damage) (seen in red). Correlations were also done for energy dissipation at the end of the loading protocol and final cartilage damage (obtained from the cartilage damage scores of the intervention limb) (seen in blue).81

Figure 3.16: Mean deformation over (A) the entire loading protocol, (B) stage I, and (C) stage II for all intervention stifles in all 3 loading conditions is not affected by rest. Mean rate of deformation (D) for all intervention stifles in all 3 loading conditions is not affected by rest.84

Figure 3.17: Mean energy dissipation decreased as a function of time for all intervention stifles in all 3 loading conditions. Energy dissipation, both at the start and end of the loading protocol was not mitigated by rest.86

Figure B.1: The frequency of cartilage damage scores for all 4 joint compartments in control specimens. Damage scores increase from no damage (0) to large areas of severe damage (4)..... 122

Figure B.2: The frequency of cartilage damage scores for all 4 joint compartments in intervention specimens. Damage scores increase from no damage (0) to large areas of severe damage (4)..... 123

List of Abbreviations

OA	Osteoarthritis
GRF	Ground reaction force
PG	Proteoglycan
ECM	Extracellular matrix
GAG	Glycosaminoglycan
MRI	Magnetic resonance imaging
ACL	Anterior cruciate ligament
KAM	Knee adduction moment
PCL	Posterior cruciate ligament
OARSI	Osteoarthritis Research Society International

Declaration of Academic Achievement

This thesis is the original work of Damjana Milicevic, Master of Science candidate in the Department of Kinesiology at McMaster University. Damjana is the primary author of this document including the two manuscripts presented in this work. Damjana conducted the literature review and was involved in the following aspects of both studies: study conception and design, pilot work, development of a standardized methodological protocol, specimen sourcing, data collection and analysis, and preparation of this thesis work.

Important contributors to this work included: Dr. Monica Maly, Mamiko Noguchi, Dr. Jack Callaghan, Dr. Joe Quadrilatero, Dr. Peter Keir, and Dr. Gregory Wohl. Dr. Monica Maly is the supervisor of this thesis and the principal investigator of both studies who secured funding and oversaw study design and conduction, in addition to manuscript preparation. Mamiko Noguchi was involved in study design, pilot work, data collection and participating as an additional rater for cartilage damage scores in study one. Dr. Jack Callaghan provided the use of his laboratory and was also involved in study conception and design due to his expertise in tissue loading. Dr. Joe Quadrilatero provided guidance regarding study design and pilot work. Dr. Peter Keir provided guidance and input on study design and data analysis. Dr. Gregory Wohl provided expertise in the field of mechanical engineering in addition to input on study design and data analysis.

Chapter One: Introduction & Review of the Literature

1.0 Introduction

The degradation of articular surfaces, leading to osteoarthritis (OA), is largely due to mechanical loading of the joint (Radin et al., 1991). A clear relationship exists between exposure to mechanical loading in the workplace and the degradation of knee joint structures, ultimately leading to knee OA (Rossignol et al., 2005). This phenomenon has been shown in an overwhelming body of work (Jensen, 2008). High repetitions of tasks that load the knee joint, including prolonged standing, lifting, kneeling, and bending are linked to greater OA incidence in a variety of occupations (Jensen, 2008; Rossignol et al., 2005). Additionally, excessive amounts of heavy physical activity further OA progression, particularly in elderly and obese populations (Cheng et al., 2000). In those with pre-existing structural joint changes indicative of early knee OA, high levels of physical activity appear to facilitate further joint damage (Dore et al., 2013).

Knee OA is the leading cause of disability, immobility and pain in older adults (Felson, 2004). Additionally, OA is a large burden for the economy. Osteoarthritis costs \$33 billion per year in indirect costs, including lost productivity in the workplace (Arthritis Alliance of Canada, 2011). Thus, OA is a huge concern for employers – one of three individuals suffering from arthritis are expected to be out of work (Bradley & Glazier, 2004). There is also no known cure for OA, making understanding disease development crucial, so that its incidence can be minimized.

Although a clear link has been established between repetitive mechanical loading of the knee joint and the degradation of articular cartilage, it is unknown how work:rest, or duty cycles, impact the degradation of articular cartilage in the knee joint. It is possible that adequate rest periods between loading exposures will enable knee articular cartilage to be more resilient to loading, and therefore reduce tissue degradation. The purpose of this Master's thesis was to examine the effect of altering work:rest on the mechanical behavior of the stifle (porcine knee) and articular cartilage damage in an *ex vivo* porcine model.

Eighteen pairs of porcine stifle joints were assessed. One joint was randomized to the intervention group and the matching pair was considered a control. The intervention joint was loaded at one of three ratios: no rest, 3:2, and 1:1 work:rest, whereas the control joint was not loaded. The total exposure to load was kept constant in all three conditions, so that specimens in all condition were all exposed to 7200 cycles of loading. The axial compression profile replicated a ground reaction force experienced during gait obtained from one representative human subject with knee OA. During this loading profile, “work” is the term used to describe the joint when it was loaded, including both the stance and swing phases of gait. During “rest,” the joint was unloaded such that it was no longer subjected to compression. This rest condition assumes minimal forces are acting on the joint structure. Specimen load and position data during loading were obtained from the loading apparatus for the intervention limb and use to compute specimen deformation and energy dissipation. Additionally, macroscopic assessments of the control and intervention cartilage took place post loading to compare the effects of no

rest, 3:2 and 1:1 on cartilage damage. Focus was placed on the quality of the cartilage surface, including the presence of fibrillation and lesions.

Such evidence is necessary to develop an understanding of optimal work-rest ratios that can help to reduce OA risk or progression. Evidence from this thesis can aid in the secondary prevention of OA. This work can be applied to the workplace as these data may provide the background to eventually initiate guidelines for work duty cycles within occupational settings. Eventually, these data can be used to provide insights into ideal development of safer exercise programs, particularly in individuals suffering from OA because rest can be incorporated into the workout program to enable resilience of cartilage tissue.

In order to make the primary study of this thesis possible, a pilot study was done to address methodological considerations (cartilage damage scoring reliability and the range of damage scores) in addition to investigating the impact of minor vs major restrictions in knee extension on cartilage damage. Two measures (goniometry and line bisection) were used to measure extension angle and their agreeability was examined in this study as well.

1.1 A Review of the Literature

1.1.1 Articular Cartilage of the Tibiofemoral Joint

The tibiofemoral joint is a synovial joint (Mansour, 2003). Synovial joints are enclosed in a capsule comprised of fibrous tissue. The inner surface of the capsule is lined with a membrane that secretes synovial fluid. This synovial fluid provides lubrication for the articular surfaces of the joint. Articular cartilage covers the surface of the femur and tibia. The cartilage of the tibiofemoral joint improves the congruency of a load bearing surface, and due to its low friction and wear, it allows the articulating bones to move along one another with minimal resistance. As a result of its compliance, articular cartilage also assists in distributing the loads between articulating bones within a joint (Mansour, 2003).

Understanding the components that comprise articular cartilage is crucial to understanding its mechanical properties. Articular cartilage is made up of three main components: 1) chondrocytes, which are the cells of the cartilage, 2) solid structural components including collagen and proteoglycans (PG), and 3) fluid (Choi & Gold, 2011; Felson, 2004; Mansour, 2003). The structural components and fluid are found in the extracellular matrix (ECM) that surround the cells. Water comprises roughly 80% of the ECM.

The role of the chondrocytes is to produce and secrete components of the ECM, particularly the type II collagen and PGs (Mansour, 2003). The chondrocytes also give cartilage adaptive capacity – they are sensitive to changes in the mechanical environment,

including increased joint load, and are able to alter metabolic activity in response (Andriacchi et al., 2004). Thus, these cells are crucial in maintaining homeostasis between degenerative and synthesizing processes within the cartilage, hereby maintaining its health.

Proteoglycans, one of the structural components of cartilage, are comprised of glycosaminoglycans (GAG) – negatively charged molecules that attach to a protein core and bind to hyaluronic acid (Mansour, 2003). The negatively charged molecules in PG endow the cartilage with its load-bearing properties, including defining its compressive strength and stiffness (Felson, 2004).

The solid structure of articular cartilage varies based on the depth of the tissue. Cartilage is described in four zones that range from the articular surface to the subchondral bone: the superficial tangential zone, the intermediate or middle zone, the deep or radiate zone, and the calcified zone (Choi & Gold, 2011). The border between the deep zone and the calcified area of bone is called the tidemark. Water and proteoglycan content vary depending on the depth of the tissue (Mansour, 2003). Near the articular surface, proteoglycan content is low, whereas the water content is high. In the deeper regions, as the subchondral bone is approached, the proteoglycan content is greatest whereas the water content is lowest.

1.1.2 The Loading Response of Healthy Articular Cartilage

Compressive loading of the tibiofemoral joint causes fluid (mainly water) flow from the ECM of the articular cartilage, into the synovial space (Choi & Gold, 2011).

The expulsion of fluid out of the cartilage under load and alterations in collagen fiber arrangement leads to a reduction in cartilage volume and thickness, which is referred to as deformation (Choi & Gold, 2011). The exudation of tissue is initially rapid, resulting in large initial cartilage deformations (Nordin & Frankel, 2012). This gradually slows as the concentration of fluid outside of the cartilage increases until cessation of flow occurs. The expulsion of fluid out of the cartilage results in the negatively charged PGs to become densely packed, thereby increasing repulsive forces between the molecules. The repulsive force generated also increases the compressive stiffness of articular cartilage (Mansour, 2003). Cartilage membrane permeability is reduced as a function of increasing deformation, increasing stiffness, and applied fluid pressure from the joint cavity that limits fluid flow back into the cartilage (Nordin & Frankel, 2012).

Articular cartilage is a viscoelastic tissue. The response of articular cartilage to load varies with time and the rate of load application (Nordin & Frankel, 2012). Typically viscoelastic materials respond to load with rapid deformations initially, followed by a slower, steadier rate of deformation. This initial period of rapid deformation is referred to as the toe region of the load deformation curve and the slower deformation occurring after is called the linear region of the load deformation curve. The behaviour of articular cartilage under load is determined by the flow of fluid out of the cartilage during compressive loading (Ateshian et al., 1997; Mow et al., 1980, 1984). Cartilage compression is resisted in healthy cartilage, as the ECM is able to limit water permeability that allows water to dissipate the energy imparted on the cartilage during

compressive loading, giving the cartilage its “shock absorbing” properties (Mansour, 2003).

Once the compressive load has been removed from the joint, the articular cartilage has the ability to recover. The repulsive forces generated as a result of a high concentration of negatively charged molecules is hydrophilic; which causes fluid to be drawn back into the cartilage following the removal of load (Choi & Gold, 2011). Thus, the chemical equilibrium between the cartilage and synovial space is restored to normal, unloaded conditions. Cartilage stiffness and permeability are also restored to normal, unloaded ranges (Mansour, 2003).

Physical activity produces deformations in cartilage, representing an acute thinning or loss of cartilage volume in response to a bout of loading. For example, in humans, cartilage deformations occur from the loads presented on the tibiofemoral joint during running (Kessler, 2005; Kessler et al., 2008). However, deformation can occur from even mild to moderate physical activity. Normal, level walking for 5 minutes can produce deformations of $2.8 \pm 0.8\%$ (Eckstein et al., 2006). Doing 30 isometric squats has resulted in statistically significant deformations in cartilage as well (Eckstein et al., 2006). Eckstein et al. (1991) demonstrated that it takes roughly 45 minutes for articular cartilage to recover 50% of its volume following 100 knee bends, and over 90 minutes for full recovery to take place (Eckstein et al., 1999). Kessler et al (2008) also demonstrated that cartilage deformations are able to recover quickly following prolonged loading of the knee joint. Athletes ran 20 km and tibiofemoral cartilage volume was assessed via magnetic resonance imaging (MRI) scans taken prior to the run, immediately following

the run, and one hour after the run. Immediately following the run, there was a significant amount of cartilage deformation present. Cartilage volume was restored after one hour of rest, indicating that cartilage is able to adapt to the loads experienced during prolonged loading of the tibiofemoral joint. However, it should be noted that damaged cartilage often has a maladaptive response to loading (Choi & Gold, 2011). Damaged cartilage tends to respond negatively to load, in such a manner that promotes further cartilage degradation (Andriacchi, 2009).

Articular cartilage has the capacity to adapt to loads it is frequently exposed to (Andriacchi et al., 2004; Seedhom, 2005). Cartilage can be conditioned to greater loads with repeated exposure without damage, so long as no injuries occur. The threshold at that the tissue fails is determined by the most prevalent stresses the joint is exposed to (Seedhom, 2005). In fact, articular cartilage is thickest where contact pressure, or stress, is greatest (Carter & Wong, 2003). Common daily activities, or individual lifestyle, determine the stresses that the tibiofemoral joint is exposed to (Seedhom, 2005). Gait is the most common form of physical activity done by man (Seedhom, 2005). Thus, cartilage is often conditioned to the stresses incurred during walking. However, as lifestyles between individuals varies, the threshold for failure is different between individuals of varying ages (Seedhom, 2005). The threshold also differs for different regions of the joint (Seedhom, 2005).

Degeneration of the articular cartilage can be a result of high loads incurred in areas that are not normally exposed to loading. For example, the femur and patella can be damaged as a result of loading in postures that involve high flexion (Seedhom, 2005).

Injury to the knee joint can also alter joint kinematics, which in turn can alter joint motion and contact stress. As a result, cartilage degeneration can occur as areas of the cartilage that are not conditioned to repetitive loading may be loaded (Andriacchi et al., 2004; Seedhom, 2005).

Damaged articular cartilage responds poorly to load in comparison to healthy cartilage. The breakdown of articular cartilage during damage causes collagen and PG disruption, ultimately leading to the loss of PG molecules (Freeman, 1975).

Proteoglycans are essential to the maintenance of normal cartilage functioning under load as these molecules are responsible for endowing cartilage with its load bearing behaviour (Felson, 2004; Mansour, 2003). Cartilage permeability is increased following cartilage damage that alters fluid flow through cartilage as well (Nordin & Frankel, 2012). As a result of these phenomena, damaged cartilage responds poorly to any load compared to healthy cartilage that benefits from moderate levels of daily physical activity (Andriacchi, 2009; Akizuki et al., 1986). Progressive cartilage damage over time can lead to the development of OA.

1.1.3 Tibiofemoral Knee Osteoarthritis

Osteoarthritis refers to a loss of articular cartilage within a joint, accompanied by pathological changes in the underlying subchondral bone and all other joint tissues (Radin et al., 1991). Osteoarthritis is the most common form of arthritis, with knee OA being a prevalent form (Felson, 2004). Knee OA mainly affects middle-aged and older adults (Felson, 2004). It is also a prevalent disease among the obese. Because the Canadian population is aging and increasingly obese, the incidence of OA is expected to rise over

time. Osteoarthritis of the knee is also more common in women than in men (Felson, 2004). Disease development typically begins in areas that are exposed to the most loading (Pritzker et al., 2006). Progression occurs from this initial site of damage, indicating increased disease severity (Pritzker et al., 2006).

Knee OA is of great concern for several reasons. First, its prevalence is high: 4.6 million Canadian adults have arthritis and 13% of Canadians are affected with OA (ACREU, 2013). In fact, it is the most common chronic condition affecting women (ACREU, 2013). By 2036, it is estimated that 7.6 million Canadian adults will suffer from OA (ACREU, 2013). In addition to its high prevalence, OA is burdensome to its patients. Knee OA is a leading cause of lower limb disability, immobility, and pain (Felson, 2004). As a result, patients suffering from knee OA have a diminished quality of life (Arthritis Alliance of Canada, 2011). People with OA are twice as likely to report decreased activity within the home versus those suffering from other chronic illnesses, such as heart disease, cancer, high blood pressure etc. (ACREU, 2013). Individuals with OA are also more likely to develop mood disorders such as depression, which further contributes to reductions in quality of life (Han et al., 2015). Osteoarthritis also places a huge economic burden. In Canada, OA related health care costs and lost productivity in the workplace cost an estimated \$33 billion per year (Arthritis Alliance of Canada, 2011). Clearly, knee OA is a devastating disease on both a personal and economical level. It is particularly concerning as there is no cure; therefore, understanding the underlying mechanisms that lead to disease development and progression is crucial.

1.1.4 Injury Mechanisms of Articular Cartilage – The Development of Tibiofemoral OA

Overall, the health of articular cartilage is dependent on its ability to maintain a balance between degenerative and synthesizing processes, including the maintenance of collagen and PGs (Andriacchi et al., 2004). Once damaged, articular cartilage has a poor ability for repair as it is aneural and avascular in healthy mature adults (Mansour, 2003).

It has been theorized that two primary injury pathways exist for musculoskeletal tissues – tissues may be overloaded acutely or chronically (McGill, 1997). In the case of cartilage degradation and OA development, the chronic pathway is of importance. This model suggests that tissue fatigue is a mechanism of articular cartilage failure (Nordin & Frankel, 2012; Seedhom, 2005). In this pathway, damage to tissue is caused by repeated or sustained load that is not large enough to cause injury acutely (Nordin & Frankel, 2012). With repeated exposure, the tissue's ability to bear load, or its tolerance, is reduced. Therefore, tissue failure occurs when repetitive loads are incurred without proper recovery (McGill, 1997).

Cartilage degradation refers to the undesirable loss of materials from the solid cartilage surface due to mechanical actions including loading (Nordin & Frankel, 2012). This includes the disruption and loss of PGs and collagen fibers that alter mechanical properties of the joint (Freeman, 1975; Felson, 2004; Mansour, 2003). Cartilage wear occurs as a combination of two factors: 1) interfacial wear (resulting from interaction of articular load bearing surfaces) and 2) fatigue wear (resulting from repetitive or prolonged deformation under load) (Nordin & Frankel, 2012). In the case of the second point, the cartilage experiences microscopic damage as a result of repetitive cyclical loading and

can occur even in well lubricated joints (Aultman et al., 2004). Thus, although cartilage is able to resist compressive forces quite well under normal conditions, repetitive loading can weaken the tissue resulting in micro damage that propagates to cartilage surface fibrillation. Another cause of cartilage damage is the tensile failure of collagen fibers (Seedhom, 2005; Freeman, 1975).

Cartilage fatigue is sensitive to the presence of surface imperfections and discontinuities (Nordin & Frankel, 2012). Structural defects and reductions in cartilage volume and mass cause cartilage to become softer with an increased permeability (Akizuki et al, 1986). Surface discontinuities can also lead to the development of stress concentrations that can further propagate damage: fatigue behavior begins with a small crack on the cartilage surface that propagates when exposed to repetitive loading resulting in the formation of cartilage lesions and the development of OA (Nordin & Frankel, 2012).

However, it is possible that adequate rest periods between loading exposures will enable tissues, specifically tibiofemoral articular cartilage, to be more resilient to loading and therefore minimize tissue degradation (Grimsby & Rivard, 2008). With rest, the fluid expelled from the cartilage is drawn back into the tissue as a result of the swelling pressure generated by the negatively charged molecules that are pushed together during compressive loading. This allows for the cartilage to recover from any elastic deformations, thus improving its tolerance to injury. Therefore, implementing proper rest breaks can allow for tissue tolerance to recover that in turn can mitigate injury resulting from the chronic pathway.

1.1.5 Risk Factors for the Development of Tibiofemoral OA

The causes of knee OA are multifactorial. For the purposes of this work, risk factors will be dichotomised as either intrinsic or extrinsic factors. Examples of intrinsic risk factors include: age, sex, obesity, genetics, joint damage and laxity, reduced proprioception, muscle weakness, and joint misalignment (Felson, 2004). Extrinsic risk factors include: repetitive loading, body mass, and injurious activities (Felson, 2004; Jensen, 2008; Rossignol et al., 2005). Osteoarthritis most often occurs in adults over 50 years of age due to the decline of muscular strength and reduced ligament stiffness that go hand in hand with aging (Andriacchi et al., 2004). Knee OA is also more prevalent in women over the age of 50 (Felson, 2004; Felson et al., 2000). The hormonal changes associated with menopause compound the effects of aging and further reduce the ability of cartilage to adapt and repair (Andriacchi et al., 2004). The adipokines and cytokines associated with obesity negatively impact joint tissue health (Toussirost et al., 2007). However, body mass was regarded as an extrinsic factor as this is the physical load acting on the tibiofemoral joint that can result in cartilage damage. Higher body mass is linked to greater loads experienced by the tibiofemoral joint that can cause tissue failure and damage over time (King et al., 2013). Repetitive loading of the knee has also been demonstrated to cause cartilage degradation and ultimately OA development as knee OA is a mechanical disease (Radin et al., 1991; Mansour, 2003). This is particularly true in occupational settings that over load the knee (*i.e.* physically demanding work - tiling, construction, agriculture etc.) (Jensen, 2008; Rossignol et al., 2005).

Clearly, the causes of tibiofemoral cartilage degeneration and knee OA are complex as they typically involve a combination of factors. The prevention of knee OA and improvements to treatment regimens can be assisted by better understanding the factors that lead to disease onset and progression (Andriacchi et al., 2004; Mansour, 2003).

Two risk factors will be focused on in this thesis: 1) altered joint motion as a result of joint laxity, malalignment, and/or previous damage, and 2) mechanical loading of the tibiofemoral joint.

Kinematic Factors

Variations in joint structure or soft tissue (*i.e.* ligament) properties influence joint laxity and congruency, and as a result may alter joint motion, and therefore contact stress, impacting the mechanical environment of the cartilage (Andriacchi et al., 2004).

Degeneration of articular cartilage often occurs as a result of abnormal knee motion (Andriacchi et al., 2004). For example, knee OA is common in individuals with anterior cruciate ligament (ACL) injury (Andriacchi et al., 2004). The main role of the ACL is to provide stability in the anterior-posterior direction in addition to rotational stability at the knee (Andriacchi et al., 2004). The increased prevalence of knee OA in these individuals is likely due to joint laxity and abnormal motion that are associated with ACL deficiency (Andriacchi et al., 2004). Even following ACL reconstruction, knee OA is likely to occur. Reconstruction restores anterior-posterior stability, however it does not restore damaged proprioception, the relative position (angle) of the femur on the tibia that

influences contact area of the articular surfaces (rotational alignment) and motion to a healthy pre-injury state (Andriacchi et al., 2004).

Cartilage thickness varies with regional variations in the loads incurred at the tibiofemoral joint during gait (Carter & Wong, 2003). Therefore, abnormal rotational alignment and joint motion can shift the region of loading within the cartilage from regions with thicker cartilage that have adapted to facing the loads associated with heel strike, to other areas that are not conditioned to take these high loads (Andriacchi et al., 2004). Loading with altered contact mechanics can produce local degenerative changes within the articular cartilage as cartilage fibrillation is likely to occur when areas that are unconditioned become loaded as these areas do not readily adapt to the load (Andriacchi et al., 2004). Rotational alterations following ACL injury are a risk factor for the progression of knee OA (Andriacchi et al., 2004). This theory has yet to be investigated in a controlled model. Kinematics may play a large role in OA development following ACL injury, but have little influence on a healthy, structurally sound knee. Additional complications associated with ACL deficiency (*i.e.* joint laxity, reduced stability etc.), aside from limitations in extension, can also explain the development of knee OA, making it difficult to isolate limited extension as a cause.

This kinematic theory also suggests that abnormal excursions of knee flexion and extension may initiate degenerative processes by shifting load to areas of the articular cartilage that are infrequently, therefore poorly conditioned, to tolerate loading. These areas are not equipped to carry loads experienced during everyday activities, such as

walking, which may initiate a pathway of degenerative changes in the knee joint (Andriacchi et al., 2004).

Kinetic Factors

Kinetic factors, including force and energy dissipation observed during loading of the tibiofemoral joint, can lead to the development of knee OA as the degradation of articular surfaces is largely due to mechanical loading of the joint (Radin et al., 1991). Therefore, diseases that lead to the breakdown of articular cartilage, particularly OA, are thought to be mechanical in nature (Mansour, 2003).

When assessing knee joint loading during activities such as level walking, the external knee adduction moment (KAM) is commonly studied. The KAM represents the load distribution between the medial and lateral portions of the joint and while the KAM does not equate with actual medial contact force, the reliability and validity of the KAM as a representation of medial compartment loading within the tibiofemoral joint has been established (Hurwitz et al., 1999; Hurwitz et al., 2000; Jackson et al., 2004; Birmingham et al., 2007; Zhao et al., 2007; Meyer et al., 2013). The medial compartment of the tibiofemoral joint is of primary importance as this is the typical site of OA development (Hurwitz et al., 1999). From the KAM waveform, both the peak and the impulse (reflecting the duration and magnitude of loading) are implicated in knee OA (Miyazaki et al., 2002; Mündermann et al., 2005).

The KAM predicts medial compartment knee OA presence, severity, and progression, particularly during gait (Henriksen et al., 2012). Both the peak KAM and KAM impulse are increased in individuals with medial knee OA in comparison to healthy

controls (Hurwitz et al., 1991, Hurwitz et al., 2000; Foroughi et al., 2009). This indicates that the medial compartment is subject to higher loads in comparison to the lateral compartment in individuals with knee OA. The presence of increased loads can cause cartilage degeneration and knee OA. Prolonged exposure to increased loads in the medial compartment of the tibiofemoral joint also contributes to OA progression. A 25% increase in peak KAM over 6 years corresponds to a 6.46 times greater risk for knee OA progression, as determined by joint space narrowing (Miyazaki et al., 2002). The peak KAM has also been linked to knee OA severity. The peak KAM is correlated with the Kellgren-Lawrence score of radiograph severity for both the right and left knees ($r=0.68$ and $r = 0.6$ for the left and right knees respectively) (Sharma et al., 1998). A relationship also exists between the peak KAM and joint space width ($r = -0.45$ and $r = -0.47$ for the left and right knees respectively) (Sharma et al., 1998). An increase in KAM by one unit (% body weight x height) was associated with a 0.63 mm decrease in joint space width (Sharma et al., 1998).

The KAM also relates with cartilage thickness and quality. In a sample of 180 medial knee OA patients, higher peak KAM was associated with more severe cartilage defects (Creaby et al., 2010). A recent study that examined the relationship between cartilage morphology and the KAM found that the peak KAM explained 6.6% of variance in mean tibial cartilage thickness after adjusting for age, and the KAM impulse explained 5.1% of the variance in the same outcome (Maly et al., 2015). In the femur, the peak KAM explained 7.9% of the variance in mean femoral cartilage thickness in comparison to the KAM impulse that explained 8.4%. When examining the 5th percentile cartilage

thickness, or the thinnest regions of cartilage, the predictive power of the KAM increased. 12.3% and 15.6% of the variance in mean tibial cartilage thickness were explained by the peak KAM and the KAM impulse, respectively. In the femur, 12.5% and 10.5% of the variance in mean femoral cartilage thickness were explained by the peak KAM and KAM impulse, respectively (Maly et al., 2015). Therefore, in knee OA, both the peak KAM and the impulse are associated with tibial and femoral cartilage thickness, particularly in the thinnest regions of cartilage. However, the relationship between the KAM and cartilage damage is not straightforward. Bennell et al (2011) demonstrated that a higher KAM impulse, but not peak, is associated with a larger loss of mean tibial cartilage volume over twelve months in knee OA patients.

1.1.6 Mechanical Determinants of OA in the Workplace

A relationship exists between exposure to repetitive mechanical loading of the tibiofemoral joint in the workplace and the degradation of cartilage (Jensen, 2008; Rossignol et al., 2005). An extensive review published by Jensen (2008) examined 25 epidemiological studies to determine if an association exists between physical demand and knee OA. The studies included in the review examined three physical activities: heavy lifting, kneeling, and stair climbing, and their relationship with knee OA within the mining, construction, concrete-reinforcement, and floor laying industries. Exposure to all 3 activities were associated with an increased risk of knee OA in the majority of work. Dose-response relationships between exposure to heavy lifting and kneeling and knee OA were also found in the literature. Of the 17 studies examining the association between heavy lifting and knee OA, 9 showed that heavy lifting increased the odds ratio of

developing knee OA to 1.9 – 7.13 times. Twelve studies assessed the association between kneeling and knee OA and 8 found a significant association with an odds ratio between 2.2 to 6.9. Of the 5 studies examining stair climbing, 4 demonstrated that stair climbing significantly increased the risk of OA development in men. However, the role of stair or ladder climbing in knee OA incidence among women is not fully understood because few studies enrolled women with large exposures to physical work (Jensen, 2008).

When examining occupational demand, jobs involving very heavy, continuous manual work had odds ratio of 18.3 for OA risk compared to workers involved in sedentary work, mainly consisting of sitting and light manual work (odds ratio = 5.1) (Toivanen et al., 2010). It is thought that extreme physical stress in these occupations leads to micro, or even macro, joint injuries that make workers susceptible to secondary knee OA development (Toivanen et al., 2010).

Biomechanical factors impact a large range of occupations, exposing a great number of workers to the risk of OA development (Rossignol et al., 2005). Occupations with high prevalence of knee, hip, and hand OA were identified and OA severity and biomechanical stress exposures between the various occupations were compared. Symptomatic OA was assessed using questionnaires (Lequesne questionnaire was used for the knee). Occupations were split into 30 categories based on occupation type, sector, and professional status (self-employed or salaried). To assess OA prevalence in each occupation, the number of observed cases in each category was divided by the number of expected cases in the region (prevalence rate ratio). A total of 2848 patients participated

(54.9 % were male, mean age was 61.8 ± 9.3 years). Knee OA affected 59.3% of the patients recruited and the median age of OA detection was 55 years old. Differences in occupational exposures existed for males and females. For female workers, cleaners had the greatest prevalence of OA for all 3 joints and the lower limb was most affected (prevalence rate ratio= 6.2). Self-employed male construction workers, masons, and trades workers (*i.e.* plumbers, mechanics, carpenters etc.) had the highest rates of OA (prevalence ratio = 2.9). Employed men working in the same categories had a slightly lower prevalence (prevalence ratio = 1.9). Interestingly, males and females in agriculture had almost identical rates of OA (male prevalence ratio = 2.8, female prevalence ratio = 2.7) (Rossignol et al., 2005). Compared to other occupations, workers in the aforementioned occupations all reported lifting more heavy objects and maintaining uncomfortable positions. Thus, biomechanical factors play an important role in the development of knee OA (Rossignol et al., 2005).

Cumulative loading over the life span, or lifelong physical activity exposure from occupational and leisure time activities may play a role in the development of knee OA (Sandmark et al., 2000). A total of 264 Swedish males and 284 Swedish females partook in a study in that they answered questionnaires regarding physical loading exposure during occupational and house work. Kneeling, standing, sitting, whole-body vibration, stairs climbed, squatting and bending, jumps, and lifts were the exposures of interest. Exposures were classified into: no/low, medium, and high based on the duration and frequency for all activities. It was found that men and women who worked in occupations involving heavy loading of the knee joint for a minimum of 10 years had an

increased risk of developing knee OA (odds ratio = 2.5) compared to those workers who had not been exposed. Similarly to the Rossignol et al. (2005) study, male forestry (odds ratio = 3.1) and construction workers (odds ratio = 2.1) and farmers of both sexes (male odds ratio = 3.2, female odds ratio = 2.4) had the highest risk of developing knee OA (Sandmark et al., 2000). Men had higher exposure in the workplace in terms of lifting, jumps, and vibrations compared to their female counterparts, and these exposures were strongly associated with knee OA development. Exposure to physical loading, prolonged standing, and lifting were positively associated to knee OA development in women (Sandmark et al., 2000). Thus, cumulative load was identified as a risk factor for OA.

Epidemiological evidence provides some compelling evidence that physical loading of the knee joint increases the risk for knee OA progression. A variety of tasks, from prolonged standing to kneeling can contribute to OA risk, both within and outside of the workplace. Individuals who work in occupations with exposures to detrimental knee loading are at an increased risk for developing knee OA. Coupled with the fact that OA is extremely burdensome to the patient and economy, it is important to understand the underlying mechanical mechanisms that lead to knee cartilage degradation and knee OA development, and how these processes can be mitigated. *Ex vivo* studies are common ways of examining these mechanisms.

1.1.7 Ex Vivo Mechanical Loading and Tibiofemoral Cartilage Degeneration

Ex vivo studies are useful as they provide insight into fundamental mechanisms for physiological and biological effects that may be difficult to achieve in an *in vivo* study design. For example, an *ex vivo* model will allow for changes in cartilage to be assessed

at the tissue level. A larger degree of control is attainable in *ex vivo* studies, allowing for clearer connections to be made between the independent and dependent variables. In a porcine model, animals are exposed to the same diet, physical activity level, and are sacrificed at the same age. Therefore, the sample should be more homogenous (Gooyers, 2014). This homogeneity will allow for variability to be minimized within the sample, and thus, the effects of rest on articular cartilage can be more clearly established without the influence of confounding factors. Various animal knee models have been used *ex vivo* to assess the impact of mechanical loading, the independent variable, on dependant variables including histological outcomes, cartilage fissuring, and proteoglycan content.

The Porcine Model

Compared to their human counterparts, animal models are advantageous to use in *ex vivo* research because genetics, age, diet, body mass, and physical activity levels are often controlled (Gooyers, 2014). Additionally, human specimens are rare, and donors are typically elderly with poor joint quality, or young adults who have sustained trauma (Gooyers, 2014). Several other animal models are commonly used to study the knee joint including cow, sheep, goat, dog, rabbit, and guinea pig models (Proffen et al., 2012). Of these, a porcine model is a reasonable approach to explore the impact of loading on joint tissues. Specifically, the porcine stifle joint is comparable to a human knee joint.

First, the porcine hind limb is comparable to the lower limb of a human and the porcine stifle joint is the equivalent of a human knee joint (Sack, 1982). The collagen structure of the articular cartilage of the tibial plateau in a porcine stifle is also most similar to that of humans throughout the radial to superficial zones (Kääb et al., 1998).

There is no difference in the directly measured length of the ACL and posterior cruciate ligament (PCL) between humans and pigs and their function is identical (Fuss, 1991; Proffen et al., 2012). Although the menisci are of similar shape between the pig and human, the lateral menisci splits the ACL bundles in the pig resulting in the tibial insertion of the anterior and posterior medial ACL bundles to be separated (Proffen et al., 2012). This is the most striking anatomical difference between the human knee joint and the porcine stifle joint (Fuss, 1991). Despite this, functionally, the ACL of the human and pig behave similarly; pigs load the ACL in similar ways to humans (Xerogeanes et al., 1998). One functional difference found between the pig and human is that pigs cannot reach full knee extension (Fuss, 1991; Proffen et al., 2012). However, this is true for all of the aforementioned animal models as it is a feature expressed by all quadrupeds, and is thus a limitation of animal *ex vivo* models in general (Proffen et al., 2012).

The porcine model is also ideal for examining OA. Pigs that are bred for consumption reach their target body weight (80 kg) within the first 5-6 months of life, long before the skeleton has matured (Sack, 1982). The weight of the pig on the immature skeletal structure causes the degradation of articular cartilage within the stifle joint, as well as bone deformity. Finally, the use of porcine stifle joints is economical and ethical. Samples are obtained from an abattoir that eliminates the need for researchers to sacrifice the animal.

Ex Vivo Work Examining the Loading Effects on the Knee

The majority of the previous work has used cartilage plugs to determine the relationship between mechanical loading and cartilage damage. Data from these studies

give good insight into the strength of cartilage, the conditions that create damage, and the patterns of damage observed through the thickness of the cartilage plug (Adams et al., 1998; Kerin et al., 2003; Palmoski & Brandt, 1984). Nonetheless, these data do not represent the joint as one organ, as many tissues comprise the knee joint and respond to external loads.

Load deformation curves (curves that plot deformation of a material on x and load it is subjected to on y) are commonly studied in *ex vivo* tissue work as they provide valuable information including: the stiffness of a material and its capability to resist deformation, the point at that deformations occur and micro injury takes place, and the failure point of a tissue (Aultman et al., 2004). When examining the load deformation curve, three points of interest should be addressed: 1) linear deformation 2) elastic limit 3) yield point (Nordin & Frankel, 2012). Originally, materials respond elastically, and all deformation can be recovered. Once the yield point is reached, further deformation is plastic and therefore full recovery cannot occur. This point is thought to be the beginning of micro-injury within a tissue (Aultman et al., 2004). Stiffness of the material is examined by computing the slope of the linear (elastic) portion of the curve (Nordin & Frankel, 2012). Compressive strength is the ability of a material to resist permanent deformation, and therefore damage, when under compression. Energy dissipation is calculated by subtracting the area under the unloading curve from the loading curve and represents energy lost within the tissue during loading (Korkusuz, 2016).

Cartilage damage has been successfully measured using macroscopic assessments (Cook et al., 2010; Kleemann et al., 2005). Mechanical measures, specifically cartilage

stiffness, histological assessment, and microscopic assessment of human tibial articular cartilage are related to the presence of knee OA (Kleemann et al., 2005). Therefore, all three are acceptable measures of cartilage quality as a result of mechanical load.

However, it is unclear whether these methods will be sensitive in relatively healthy cartilage with little damage. This information is important, as it validates the use of mechanical and macroscopic assessments, which are 2 forms of assessment used in this thesis.

Loading, Compressive Cartilage Strength, and Cartilage Damage

Load-induced water loss in bovine patellar articular cartilage reduces the compressive strength of cartilage, or its ability to resist damage under compressive load (Adams et al., 1998). Sustained loading, leading to tissue creep, causes a loss of water within the cartilage, which can reduce shock-absorbing properties and lead to cartilage fibrillation. Twenty pairs of specimens (40 in total) were tested. Cartilage plugs, which included 5 mm of underlying subchondral bone, were taken from the patellar groove, and their compressive strength was determined. However, 1 specimen from each pair was exposed to 30 minutes of static “creep” loading at 2 MPa prior to having its compressive strength and stiffness determined (“creep-loaded” specimens). These were compared to their paired counterparts, which did not receive pre-loading prior to testing and were known as the “fully-hydrated” specimens. The cartilage plugs were immersed in saline throughout static loading. To determine compressive strength and stiffness, specimens were embedded in dental plaster while a 5 N load was applied to the cartilage surface with a 5 mm metal indenter to ensure that the cartilage surface and indenter are parallel

once the plaster dried. A linear-ramp loading/unloading cycle was applied for 1 second once the plaster had set. This was done to mimic muscle action, specifically the force of the quadriceps acting on the patella, during knee bending. The load-deformation curve was obtained from the materials testing system after each cycle of loading and examined for signs of compressive failure including: 1) a decrease in stiffness and 2) an increase in the hysteresis indicating energy absorption due to failure mechanisms. If failure did not occur, the cartilage was allowed to recover in saline for one minute prior to further loading at a higher maximum displacement. This protocol was repeated until failure occurred and typically lasted 3-6 cycles. Specimens were stained with India ink following failure to assess damage. Staining revealed that the fully-hydrated specimens showed a smaller number of fissures, typically found around the initial indentation site. On the other hand, the creep-loaded specimens exhibited a larger number of fissures in a dense mosaic-like pattern that spread across the indentation site. In terms of mechanical results, creep-loaded specimens were 100% stiffer, and 21% stronger compared to their fully-hydrated counterparts, but, they absorbed 28% less energy at failure. Therefore, even though creep-loading strengthens cartilage, the fact that the energy to failure is reduced in creep-loaded specimens suggests that cartilage dehydration, as a result of water moving out of the tissue, results in poor shock absorption and less energy until failure. Additionally, soaking the samples in a saline solution can swell the cartilage beyond normal physiological conditions *in vivo*. This may impact the response of the cartilage to loading and the pattern of damage (Adams et al., 1998).

The effect of conditioning has also been demonstrated on cartilage *ex vivo*. In general, this theory suggests that cartilage is conditioned to the most predominant loads it incurs (Yao & Seedhom, 1993). If cartilage is conditioned to a low load, then damage, in the form of fibrillation, may occur in the presence of high loads. Fifteen pairs of human cadaveric knees were used to determine if the cartilage stress exposure is correlated to its compressive modulus. First, the average stress for the tibiofemoral compartments was determined. Dissected knee joints (soft tissue removed) were placed into a loading apparatus at 10% of flexion and were cyclically loaded at 1 Hz and three times body weight, as this most closely resembles the conditions experienced by the knee during gait. This was done with a partially intact knee joint, with the patella and meniscus removed, so that average stress could be obtained for all areas of the knee joint. To determine the cartilage compressive modulus, articular surfaces were indented at a variety of sites using a hemispherical indenter. The depth of this indent, representing cartilage thickness, was measured. The compressive cartilage modulus was calculated using the indentation value 2 seconds following load application, and the cartilage thickness at the test site. Following stress testing, the compressive modulus was surveyed on each joint surface. Each joint surface had varying levels of prevalent stresses and cartilage compressive moduli. Additionally, a positive relationship was found between the cartilage compressive modulus and the predominant stress that the cartilage was exposed to ($r = 0.889$, $p < 0.02$). This study illustrates that the functional (joint stress) and mechanical (compressive modulus) properties of cartilage are related. Therefore, it may be possible

to gradually increase joint stress levels without causing cartilage degradation (Yao & Seedhom, 1993).

Cyclic loading can propagate cartilage fissures in bovine cartilage plugs (Kerin et al., 2003). Thirty five bovine knee cartilage plugs following loading to compressive failure (36 MPa on average). Cyclic loading was done at 40% of compressive strength and fissure width, length, and depth were measured throughout this time. This was chosen as 40% of compressive strength is the minimum value required to propagate damage while still being considered ‘physiological’ as this magnitude of load will not damage the cells and matrix of the cartilage (Kerin et al., 2003; Green et al., 1993). The loading wave used was a 2 second linear ramp up (1 second) and down (1 second). Specimens were ink-stained and photographed at various intervals to get a measure of surface damage. Most specimens were loaded for 4000 cycles, however, a few were taken to 9000 cycles. It was found that cyclic loading caused fissures to increase in width and length, but depth was unaffected. Fissure length rapidly increased in the first 75 cycles, but little change was documented after this point. A larger number of cycles were required to reach equilibrium for fissure width. This study demonstrated that cartilage fissures are able to mechanically propagate following initial damage. Furthermore, an additional 16 specimens were exposed to initial damage and propagation, as stated above, but were allowed to recover while unloaded in saline for 12-24 hours prior to examination (Kerin et al., 2003). Of these specimens, 6 were then cyclically loaded for an additional 2-3 hours to examine if the fissures would propagate following full hydration. Following unloaded rest in saline, fissure length did not change significantly, whereas fissure width

did. Loading following rest increased fissure width to a similar value measured following the first period of loading, and length was unaffected (Kerin et al., 2003).

Loading Effects on Collagen

Collagen maintains cartilage shape under load despite the osmotic pressure created by PGs, however, collagen response to load varies on the type of load (Kääb et al., 1998). Fifty three intact rabbit joints were randomized to 1 of 5 conditions that differed in loading type (static or cyclic) and loading magnitude (high or low). Unloaded joints were used as a form of control. Joints were loaded to 3 (high) or 1 (low) times body weight, to mimic quadriceps force, for a total of 30 minutes. For the cyclic loading condition, the tibia was free to move between 70° and 150° of flexion relative to the femur. Loading was applied at 1 Hz. Following loading, joints were unloaded and held at 90° for up to 30 minutes to examine recovery. Indentations of the tibial plateau that occur as a result of femur contact during loading were qualitatively studied using electron microscopy. Specimen collagen structure was examined for bending or crimping (periodic sinusoidal crimp) of the collagen fibers within the indented area. The outer edge, or circumference, of the indent was better defined following static loading rather than cyclical. The high force static loading condition caused collagen crimping. This was not observed in any other condition. Cartilage was also found to be thinner following static loading compared to cyclical loading. Larger magnitudes of load caused greater cartilage volume loss as well. Full recovery of cartilage volume occurred between four mins for cyclically loaded specimens to sixteen minutes for specimens exposed to static loading (Kääb et al., 1998). This work suggest that cartilage, and collagen in particular is

sensitive to the type and magnitude of load. Static loading may be more damaging than cyclical loading as the same regions are continuously exposed to load causing the tissue to creep (Kääb et al., 1998; Nordin & Frankel, 2012).

Loading Effects on Proteoglycan (PG) Synthesis

To examine the effects of static and intermittent cyclic loading and varying duty cycles on articular cartilage metabolism, specifically glycosaminoglycan (GAG) and protein synthesis, Palmoski and Brandt (1984) loaded cartilage plugs obtained from the knee joints of dogs. Samples were loaded at 3 times body weight for 2 hours statically or cyclically at 2 different duty cycles: 60 seconds of loading followed by 60 seconds of unloading, to mimic prolonged compressive loading, or, loading for 4 seconds followed by 11 seconds of unloading, to simulate joint loading during motion. During loading, samples were immersed in a medium to provide measurements of protein and GAG synthesis. Results were compared to a control sample that was a cartilage plug obtained from the same knee but cultured at atmospheric pressure. The 60/60 duty cycle suppressed GAG synthesis by 30-60% compared to controls for both cyclic and static loading conditions. Protein synthesis was decreased as well. However, the 4/11 duty cycle caused GAG synthesis to increase by 34% and had no effect on protein synthesis (Palmoski & Brandt, 1984).

1.1.8 Gaps in the Knowledge, Study Objectives and Study Benefits

Although work has been done to examine the effect of loading on cartilage, little work has examined the impact of rest on cartilage. Additionally, the majority of work done has involved the use of cartilage plugs, which may unrealistically represent cartilage

degeneration as all supporting joint structures and tissues have been removed. The main gaps in the literature include the following:

- 1) No proposed protocol for compressive loading of an intact porcine stifle joint. For example, it remains unknown how much loading (magnitude and duration) is required to damage cartilage in an intact porcine stifle joint.
- 2) Limited knowledge on the impact of rest on an intact joint and how cartilage damages while part of an intact joint.
- 3) The dose of rest required to reap beneficial effects (*i.e.* tissue recovery) remains unknown.

To address the gaps in the knowledge the following study objectives and hypotheses were determined:

- 1) To determine if there is a difference in the deformation and rate of deformation of the porcine stifle between 3 loading conditions (no rest, and work:rest of 3:2 and 1:1) that each produce the same cumulative load. The hypothesis was that the cumulative load will deform the joints in all 3 conditions; but there will be a difference in deformation and rate of deformation between conditions, with conditions including rest resulting in less deformation.
- 2) To determine if energy dissipation differs between the beginning and end of the loading protocol and between the 3 loading conditions. It was hypothesized that while energy dissipation will be smaller at the end, compared to beginning of the

loading protocol for all 3 conditions, less energy will be dissipated at both time points in conditions that include rest.

- 3) To determine if cartilage damage observed in the matched pair stifle, a surrogate for the pre-loading condition of a loaded stifle, is related to energy dissipation at the beginning of the loading protocol. A secondary purpose was to determine if final cartilage damage of the loaded stifle is related to energy dissipation at the end of the loading protocol. It was hypothesized that a positive relationship will exist between cartilage damage with energy dissipation observed in the loaded stifle at the beginning and end of the protocol.
- 4) To determine if there is a difference in cartilage damage between the stifle following loading and its unloaded matched pair. It was hypothesized that there will be a significant difference between the loaded stifle and its unloaded matched pair.
- 5) To compare cartilage damage between the 3 loading conditions. It was hypothesized that stifles exposed to rest will demonstrate less cartilage damage after the loading protocol, compared to joints that do not have rest.

This work can be a starting point for creating guidelines for work:rest, or duty cycles, within occupational and clinical settings in order to minimize cartilage degradation as a result of mechanical loading. These data can be used as a foundation for determining the efficacy rest breaks for exercises prescribed for rehabilitation purposes and in physically demanding jobs such as construction or agriculture. Therefore, data

obtained in this study are unique and can be used in the development of secondary OA prevention programs.

To make the primary study of this thesis possible, a pilot study was done to determine:

- 1) The variability in qualitative macroscopic scores, describing tibial and femoral cartilage quality, in 32 porcine stifles. This was used to assess the need for a paired limb model.
- 2) The intra and inter-rater reliability of the cartilage damage scoring system. The scoring system used was originally developed for a canine model, and thus, it was necessary to determine if it could produce reliable data regarding cartilage quality in a porcine model (Cook et al., 2010). This model was chosen because no other large animal scoring systems are available at this time.

In addition to providing a foundation for the primary thesis study, this pilot study also explored how alterations to restrictions in end range of motion, particularly extension, can impact cartilage quality as determined by cartilage damage score. This study tested the “kinematic” theory that suggests that restrictions in knee extension and flexion can initiate degenerative process in the joint by shifting load to cartilage surfaces that are infrequently loaded, and therefore, poorly conditioned, in a porcine model. This study also compared angle measurements, which were used to represent maximal extension angle, between 2 modalities: 1) goniometry, and 2) line bisection.

This pilot study provided a foundation for the primary thesis study by exploring the use of a paired porcine model, and determining the reliability of the qualitative macroscopic scoring system. Studying how aberrant joint extension is linked to cartilage damage can aid in the understanding of why OA develops, and thus has potential to be used in secondary prevention, particularly in a clinical setting.

1.2 References

- Adams, M. A., Kerin, A. J., & Wisnom, M. R. (1998). Sustained loading increases the compressive strength of articular cartilage. *Connective Tissue Research*, 39(4), 245–256.
- Akizuki, S., Mow, V. C., Müller, F., Pita, J. C., Howell, D. S., & Manicourt, D. H. (1986). Tensile properties of human knee joint cartilage: I. Influence of ionic conditions, weight bearing, and fibrillation on the tensile modulus. *Journal of Orthopaedic Research*, 4(4), 379-392.
- Andriacchi, T. P., Koo, S., & Scanlan, S. F. (2009). Gait mechanics influence healthy cartilage morphology and osteoarthritis of the knee. *The Journal of Bone & Joint Surgery*, 91(Supplement 1), 95-101.
- Andriacchi, T. P., Mündermann, A., Smith, R. L., Alexander, E. J., Dyrby, C. O., & Koo, S. (2004). A framework for the in vivo pathomechanics of osteoarthritis at the knee. *Annals of Biomedical Engineering*, 32(3), 447–457.
- Arthritis Alliance of Canada, the Impact of Arthritis in Canada: Today and Over the Next 30 Years (Fall 2011), 11.
- Arthritis Community Research and Evaluation Unit (ACREU): Arthritis in Canada (Prepared for The Arthritis Society, 2013) 3.
- Ateshian, G. A., Warden, W. H., Kim, J. J., Grelsamer, R. P., & Mow, V. C. (1997). Finite deformation biphasic material properties of bovine articular cartilage from confined compression experiments. *Journal of biomechanics*, 30(11), 1157-1164.

Aultman, C. D., Drake, J. D., Callaghan, J. P., & McGill, S. M. (2004). The effect of static torsion on the compressive strength of the spine: an in vitro analysis using a porcine spine model. *Spine*, 29(15), E304–E309.

Badley E, Glazier R. Arthritis and related conditions (2004). *ICES Research Atlas*. Toronto: Institute for Clinical Evaluative Sciences.

Bennell, K., Bowles, K., Wang, Y., Cicuttini, F., Davies-Tuck, M., Hinman, R. (2011). Higher dynamic medial knee load predicts greater cartilage loss over 12 months in medial knee osteoarthritis. *Annals of the Rheumatic Diseases*, 70, 1770-1774.

Birmingham, T. B., Hunt, M. A., Jones, I. C., Jenkyn, T. R., & Giffin, J. R. (2007). Test–retest reliability of the peak knee adduction moment during walking in patients with medial compartment knee osteoarthritis. *Arthritis Care & Research*, 57(6), 1012-1017.

Carter, D. R., & Wong, M. (2003). Modelling cartilage mechanobiology. *Philosophical Transactions of the Royal Society of London B: Biological Sciences*, 358(1437), 1461-1471.

Cheng, Y., Macera, C. A., Davis, D. R., Ainsworth, B. E., Troped, P. J., & Blair, S. N. (2000). Physical activity and self-reported, physician-diagnosed osteoarthritis: is physical activity a risk factor? *Journal of Clinical Epidemiology*, 53(3), 315–322.

Choi, J.A., & Gold, G. E. (2011). MR Imaging of Articular Cartilage Physiology. *Magnetic Resonance Imaging Clinics of North America*, 19(2), 249–282.

- Cook, J. L., Kuroki, K., Visco, D., Pelletier, J.-P., Schulz, L., & Lajeber, F. P. J. G. (2010). The OARSI histopathology initiative – recommendations for histological assessments of osteoarthritis in the dog. *Osteoarthritis and Cartilage*, *18*, S66–S79.
- Creaby, M. W., Wang, Y., Bennell, K. L., Hinman, R. S., Metcalf, B. R., Bowles, K. A., & Cicuttini, F. M. (2010). Dynamic knee loading is related to cartilage defects and tibial plateau bone area in medial knee osteoarthritis. *Osteoarthritis and Cartilage*, *18*(11), 1380-1385.
- Dore, D. A., Winzenberg, T. M., Ding, C., Otahal, P., Pelletier, J.-P., Martel-Pelletier, J. ... Jones, G. (2013). The association between objectively measured physical activity and knee structural change using MRI. *Annals of the Rheumatic Diseases*, *72*(7), 1170–1175.
- Eckstein, F., Hudelmaier, M., & Putz, R. (2006). The effects of exercise on human articular cartilage. *Journal of Anatomy*, *208*(4), 491–512.
- Eckstein, F., Tieschky, M., Faber, S., Englmeier, K.-H., & Reiser, M. (1999). Functional analysis of articular cartilage deformation, recovery, and fluid flow following dynamic exercise in vivo. *Anatomy and Embryology*, *200*(4), 419–424.
- Felson, D. T. (2004). An update on the pathogenesis and epidemiology of osteoarthritis. *Radiologic Clinics of North America*, *42*(1), 1–9.
- Felson, D. T., Lawrence, R. C., Dieppe, P. A., Hirsch, R., Helmick, C. G., Jordan, J. M., ... & Sowers, M. (2000). Osteoarthritis: new insights. Part 1: the disease and its risk factors. *Annals of internal medicine*, *133*(8), 635-646.

- Foroughi, N., Smith, R., & Vanwanseele, B. (2009). The association of external knee adduction moment with biomechanical variables in osteoarthritis: a systematic review. *The Knee*, *16*(5), 303-309.
- Freeman, M. (1975). The fatigue of cartilage in the pathogenesis of osteoarthritis. *Acta Orthopaedica Scandinavica*, *46*, 323.
- Fuss, F. K. (1991). Anatomy and function of the cruciate ligaments of the domestic pig (*Sus scrofa domestica*): a comparison with human cruciates. *Journal of Anatomy*, *178*, 11.
- Gooyers, C. E. (2014). Exploring interactions between force, repetition and posture on low back joint loading and intervertebral disc injury. Retrieved from <https://uwspace.uwaterloo.ca/handle/10012/8707>
- Green, T. P., Adams, M. A., & Dolan, P. (1993). Tensile properties of the annulus fibrosus. *European Spine Journal*, *2*(4), 209-214.
- Grimsby, O., & Rivard, J. (2008). *Science, Theory and Clinical Application in Orthopaedic Manual Physical Therapy: Applied Science and Theory* (Vol. 2).
- Han, H. S., Lee, J. Y., Kang, S. B., & Chang, C. B. (2016). The relationship between the presence of depressive symptoms and the severity of self-reported knee pain in the middle aged and elderly. *Knee Surgery, Sports Traumatology, Arthroscopy*, *24*(5), 1634-1642.

- Henriksen, M., Aaboe, J., & Bliddal, H. (2012). The relationship between pain and dynamic knee joint loading in knee osteoarthritis varies with radiographic disease severity. A cross sectional study. *The Knee*, *19*(4), 392-398.
- Hurwitz, D.E, Ryals, A. R., Block, J. A., & Sharma, L. (2000). Knee pain and joint loading in subjects with osteoarthritis of the knee. *Journal of Orthopaedic Research*, *18*(4), 572 - 579.
- Hurwitz, D. E., Sharma, L., & Andriacchi, T. P. (1999). Effect of knee pain on joint loading in patients with osteoarthritis. *Current Opinion in Rheumatology*, *11*(5), 422-426.
- Jackson, B. D., Teichtahl, A. J., Morris, M. E., Wluka, A. E., Davis, S. R., & Cicuttini, F. M. (2004). The effect of the knee adduction moment on tibial cartilage volume and bone size in healthy women. *Rheumatology*, *43*(3), 311-314.
- Jensen, L. K. (2008). Knee osteoarthritis: influence of work involving heavy lifting, kneeling, climbing stairs or ladders, or kneeling/squatting combined with heavy lifting. *Occupational and Environmental Medicine*, *65*(2), 72–89.
- Kääb, M. J., Gwynn, I., & Nötzli, H. P. (1998). Collagen fibre arrangement in the tibial plateau articular cartilage of man and other mammalian species. *Journal of anatomy*, *193*(01), 23-34.
- Kääb, M. J., Ito, K., Clark, J. M., & Nötzli, H. P. (1998). Deformation of articular cartilage collagen structure under static and cyclic loading. *Journal of Orthopaedic Research*, *16*(6), 743–751.

- Kerin, A. J., Coleman, A., Wisnom, M. R., & Adams, M. A. (2003). Propagation of surface fissures in articular cartilage in response to cyclic loading in vitro. *Clinical Biomechanics*, 18(10), 960–968.
- Kessler, M. A. (2005). Volume Changes in the Menisci and Articular Cartilage of Runners: An In Vivo Investigation Based on 3-D Magnetic Resonance Imaging. *American Journal of Sports Medicine*, 34(5), 832–836.
- Kessler, M. A., Glaser, C., Tittel, S., Reiser, M., & Imhoff, A. B. (2008). Recovery of the Menisci and Articular Cartilage of Runners after Cessation of Exercise: Additional Aspects of In Vivo Investigation Based on 3-Dimensional Magnetic Resonance Imaging. *The American Journal of Sports Medicine*, 36(5), 966–970.
- King L. K., March L., & Anandacoomarasamy A. (2013). Obesity & osteoarthritis. *The Indian Journal of Medical Research*, 138(2), 185-193.
- Kleemann, R. U., Krockner, D., Cedraro, A., Tuischer, J., & Duda, G. N. (2005). Altered cartilage mechanics and histology in knee osteoarthritis: relation to clinical assessment (ICRS Grade). *Osteoarthritis and Cartilage*, 13(11), 958–963.
- Korkusuz, F. (Ed.). (2016). *Musculoskeletal Research and Basic Science*. New York: Springer.
- Maly, M. R., Acker, S. M., Totterman, S., Tamez-Peña, J., Stratford, P. W., Callaghan, J. P. ... Beattie, K. A. (2015). Knee adduction moment relates to medial femoral and tibial cartilage morphology in clinical knee osteoarthritis. *Journal of Biomechanics*, 48(12), 3495–3501.

- Mansour, J. M. (2003). Biomechanics of cartilage. *Kinesiology: The Mechanics and Pathomechanics of Human Movement*, 66–79.
- McGill, S. (1997). The biomechanics of low back injury: implications on current practice in industry and the clinic, *30*(5), 465–475.
- Meyer, A. J., D’Lima, D. D., Besier, T. F., Lloyd, D. G., Colwell, C. W., & Fregly, B. J. (2013). Are external knee load and EMG measures accurate indicators of internal knee contact forces during gait? *Journal of Orthopaedic Research*, *31*(6), 921–929.
- Miyazaki, T., Wada, M., Kawahara, H., Sato, M., Baba, H., & Shimada, S. (2002). Dynamic load at baseline can predict radiographic disease progression in medial compartment knee osteoarthritis. *Annals of the rheumatic diseases*, *61*(7), 617-622.
- Mow, V. C., Holmes, M. H., & Lai, W. M. (1984). Fluid transport and mechanical properties of articular cartilage: a review. *Journal of biomechanics*, *17*(5), 377-394.
- Mow, V. C., Kuei, S. C., Lai, W. M., & Armstrong, C. G. (1980). Biphasic creep and stress relaxation of articular cartilage in compression: theory and experiments. *Journal of biomechanical engineering*, *102*(1), 73-84.
- Mündermann, A., Dyrby, C. O., & Andriacchi, T. P. (2005). Secondary gait changes in patients with medial compartment knee osteoarthritis: increased load at the ankle, knee, and hip during walking. *Arthritis & Rheumatism*, *52*(9), 2835-2844.

- Nordin, M., & Frankel, V. H. (Eds.). (2012). *Basic biomechanics of the musculoskeletal system* (4th Ed). Philadelphia: Wolters Kluwer Health/Lippincott Williams & Wilkins.
- Palmoski, M. J., & Brandt, K. D. (1984). Effects of static and cyclic compressive loading on articular cartilage plugs in vitro. *Arthritis & Rheumatism*, 27(6), 675-681.
- Pritzker, K. P. H., Gay, S., Jimenez, S. A., Ostergaard, K., Pelletier, J.-P., Revell, P. A., ... van den Berg, W. B. (2006). Osteoarthritis cartilage histopathology: grading and staging. *Osteoarthritis and Cartilage*, 14(1), 13–29.
- Proffen, B. L., McElfresh, M., Fleming, B. C., & Murray, M. M. (2012). A comparative anatomical study of the human knee and six animal species. *The Knee*, 19(4), 493–499.
- Radin, E. L., Burr, D., Caterson, B., Fyhrie, D., Brown, T., & Boyd, R. (1991). Mechanical determinants of osteoarthritis, *Seminars in arthritis and rheumatism*, 21(3), 12–21.
- Rossignol, M. (2005). Primary osteoarthritis of hip, knee, and hand in relation to occupational exposure. *Occupational and Environmental Medicine*, 62(11), 772–777.
- Sack, W.O. (1982). *Essentials of Pig Anatomy*. Veterinary Textbooks.
- Sandmark, H., Hogstedt, C., & Vingard, E. (2000). Finnish Institute of Occupational Health Danish National Research Centre for the Working Environment Norwegian National Institute of Occupational Health, 26(1), 20–25.

- Seedhom, B. B. (2005). Conditioning of cartilage during normal activities is an important factor in the development of osteoarthritis. *Rheumatology*, *45*(2), 146–149.
- Sharma, L., Hurwitz, D. E., Thonar, E. J. A., Sum, J. A., Lenz, M. E., Dunlop, D. D., & others. (1998). Knee adduction moment, serum hyaluronan level, and disease severity in medial tibiofemoral osteoarthritis. *Arthritis & Rheumatism*, *41*(7), 1233-1240.
- Toivanen, A. T., Heliövaara, M., Impivaara, O., Arokoski, J. P., Knekt, P., Lauren, H., & Kröger, H. (2010). Obesity, physically demanding work and traumatic knee injury are major risk factors for knee osteoarthritis—a population-based study with a follow-up of 22 years. *Rheumatology*, *49*(2), 308-314.
- Toussiro, E., Streit, G., & Wendling, D. (2007). The contribution of adipose tissue and adipokines to inflammation in joint diseases. *Current medicinal chemistry*, *14*(10), 1095-1100.
- Yao, J. Q., & Seedhom, B. B. (1993). Mechanical conditioning of articular cartilage to prevalent stresses. *Rheumatology*, *32*(11), 956-965.
- Zhao, D., Banks, S. A., Mitchell, K. H., D'Lima, D. D., Colwell, C. W., & Fregly, B. J. (2007). Correlation between the knee adduction torque and medial contact force for a variety of gait patterns. *Journal of Orthopaedic Research*, *25*(6), 789-797.

Chapter Two: The Presence of Articular Cartilage Damage is not associated with Restrictions in End-Range Extension in Porcine Stifles

Damjana Milicevic¹, Mamiko Noguchi², Joe Quadrilatero², Jack P. Callaghan², Monica R. Maly^{1,2}

¹ Department of Kinesiology, McMaster University, Hamilton, ON, Canada

² Department of Kinesiology, University of Waterloo, Waterloo, ON, Canada

2.0 Introduction

Osteoarthritis (OA) is a chronic joint condition characterized by loss of articular cartilage and pathological changes in the underlying subchondral bone (Radin et al., 1991). The knee is most commonly affected by OA (Felson, 2004). Thirteen percent of Canadians suffer from some form of OA, and this prevalence is only expected to grow with the aging population (ACREU, 2013). Knee OA is the most common form of OA, and it is a leading cause of lower limb disability, immobility, and pain (Felson, 2004), resulting in a diminished quality of life (Arthritis Alliance of Canada, 2011). In Canada, OA-related health care costs and lost productivity in the workplace cost an estimated \$33 billion per year (Arthritis Alliance of Canada, 2011). As there is currently no cure for OA, understanding the factors that contribute to the incidence and progression of the disease can be useful in prevention and treatment (Andriacchi et al., 2004; Mansour, 2003).

Varus knee alignment, typically assessed using radiography and goniometry, (Cooke et al., 2007) is linked to worsening knee OA in humans (Sharma et al., 2001). Knee malalignment creates joint laxity, alters joint motion, and increases joint contact stress, which impacts the mechanical function of articular cartilage (Andriacchi et al., 2004). However, literature examining the influence of varus knee alignment on the onset of knee OA remains equivocal, with evidence both against (Hunter et al., 2007) and for varus alignment predicting knee OA incidence (Cicuttini et al., 2004; Sharma et al., 2013). This inconsistency suggests that the onset of OA is complex and is likely a result of a combination of risk factors.

While the vast majority of knee OA literature focuses on frontal knee alignment, little has examined the role of sagittal knee mechanics in the incidence of knee OA. It has been theorized that restrictions in sagittal range of motion may contribute to the development of knee OA (Andriacchi et al., 2004). This “kinematic” theory suggests that new restrictions in the excursions of knee flexion and extension may initiate degenerative processes by shifting load to areas of the articular cartilage that are infrequently, therefore poorly conditioned, to tolerate loading (Andriacchi et al., 2004). Alterations in contact positions influenced degenerative changes in the knee post anterior cruciate ligament (ACL) injury (Andriacchi et al., 2004). However it is unclear whether joint degradation post ACL injury is the result of altered knee flexion and extension excursion, or other elements related to the injury such as joint laxity (Andriacchi, 2009; Andriacchi et al., 2004). It remains unclear whether the inability to fully extend the leg, which promotes weight-bearing on regions of knee cartilage that are not designed to tolerate large loads, is linked the degradation of articular cartilage within these regions and OA.

Animal models are ideal to explore this gap as they are cost-effective and can be easily controlled in laboratory settings. The porcine hind limb is comparable to the lower limb of a human in terms of its gross anatomy, composition of articular cartilage (Sack, 1982; Käab et al., 1998), and mechanical characteristics. One functional difference is that pigs cannot reach full knee extension (Fuss, 1991; Proffen et al., 2012). This is true for all quadrupeds (Proffen et al., 2012). In addition to the anatomical similarities, the porcine model may be ideal to study joint degeneration because pigs bred for consumption reach their target body weight (~80 kg) within the first 5-6 months of life,

before the skeleton has matured (Sack, 1982). This body weight on the immature skeletal structure causes the cartilage degradation and bone deformity of the stifle (Sack, 1982). Thus, the porcine model is useful to explore the overarching kinematic theory.

This study had 3 main purposes. The first purpose was to determine the magnitude of agreement between goniometry and line bisection measures of maximum knee extension angle in porcine stifles. It was hypothesized that these measures would agree moderately. The second purpose was to assess the intra-rater and inter-rater reliability of the macroscopic scoring system developed for the canine on a porcine model. It was hypothesized that the intra-rater reliability would be high and that the inter-rater reliability would be moderate. The final objective was to determine if there is a difference in tibial and femoral articular cartilage damage, as determined by a macroscopic cartilage damage scoring system, between stifles with minimal versus major restrictions in knee extension. It was hypothesized that stifles with major restrictions in knee extension will demonstrate greater severity of articular cartilage damage, as demonstrated by larger cartilage damage scores.

2.1 Methodology

A cross-sectional analysis was performed on 32 porcine stifle joints.

2.1.1 Specimen Preparation

Fresh porcine hind limbs were obtained from local abattoirs. Specimens were comprised of the entire femur, the intact stifle joint, the tibia and fibula, and all soft tissue. Once obtained, specimens were frozen and stored at -20° C. Prior to testing,

specimens were thawed overnight. Soft tissue was removed to ensure that only the osteoligamentous joint was left intact. The medial-most aspect of the femoral condyle and the femoral and tibial shafts were palpated and marked with stickers. Maximum sagittal extension angle was measured using two methods: 1) goniometry, and 2) line bisection via photography. Block randomization was used to determine whether extension angle would be measured by goniometer or photography first.

2.1.2 Goniometry

Maximum sagittal extension angle was measured using a universal goniometer. The axis of rotation was identified on the femur of each specimen. This point was located 1 cm anterior to the medial-most aspect of the femoral condyle to represent the center of the femur about that the tibia rotates. A hole was drilled into the femur at the point of rotation on the femoral aspect of the joint and the center of the goniometer was fixed to this location using a screw. The arms of the goniometer were attached to the femoral and tibial shafts in line with the marks drawn on the shafts. Modeling clay was placed on the arms of the goniometer to ensure the arms were parallel to the specimen. Maximum sagittal extension angle was measured 3 times by an experienced assessor (D.M.). Maximum extension was attained when the assessor reached a bony or hard end feel. This point was the anatomical limit of range, even when a reasonable force was applied, without damaging joint structures (*i.e.* ligaments). Mean maximum sagittal extension angle was computed using the 3 measures.

2.1.3 Line Bisection

A standardized photograph was taken of each specimen in the sagittal plane. A high resolution camera was used to capture the photos (Canon Rebel T3i EOS 600D, Tokyo, Japan). The camera was fixed onto a tripod and this setup was not disturbed during collections. The standardized photos of each limb were used to assess sagittal plane maximum extension angle in ImageJ (National Institutes of Health, Bethesda, Maryland). The line tool was used to draw straight lines along the shaft of the femur and tibia through the marks labeled on each shaft. The maximum sagittal extension angle was calculated about the point where the lines bisected.

2.1.4 Articular Cartilage Assessment

Following angle measurement, samples were dissected carefully to expose the femoral and tibial articular cartilage and standardized photography was taken of the exposed cartilage. A cartilage damage scoring system was used to grade both the femoral and tibial joint surfaces from these photographs. Cartilage damage was scored on a categorical scale developed for the canine by Osteoarthritis Research Society International (OARSI) (Cook et al., 2010). This is the only large animal model proposed by OARSI, which was developed by Outerbridge (1961), and modified by Mastbergen et al (2006) (Mastbergen et al., 2006; Outerbridge, 1961) (Table 2.1). The primary assessor (D.M.) developed a set of guidelines, with examples, for grading porcine stifle cartilage using a cartilage damage scoring system developed for canines (Appendix A).

Table 2.1: Macroscopic articular cartilage scoring for the medial and lateral tibial and femoral compartment of the canine stifle joint. Scores range from 0 to 4, where 0 representing no cartilage damage, and 4 representing large areas of severe damage.

Surface Description	Score
Smooth Surface	0
Slightly fibrillated/roughened surface	1
Fibrillated surface with focal partial thickness lesions	2
Deep lesions surrounding damage	3
Large areas of severe damage	4

The cartilage damage scoring system was originally developed for use in a canine model, thus its reliability was tested in the porcine model. Both intra-rater and inter-rater reliability were assessed to ensure that the cartilage damage scoring system produced reliable results within and between assessors. To examine intra-rater reliability, an experienced assessor (D.M.) scored the photos of the specimens that displayed the articular surface of the tibia and femur. The photos were de-identified and randomized by an independent research assistant. The photos were scored again by the same assessor, who was blinded to the photo order. To determine inter-rater reliability, a secondary trained assessor (M.N.) scored the randomized and blinded photo set.

2.1.5 Statistical Analyses

All statistical analyses were performed using SPSS software, version 23.0 (SPSS Inc., Chicago, Illinois, USA). To determine the level of agreement between the goniometer and line bisection measures of maximum knee extension angle, an Interclass Correlation Coefficients (ICC) (3, k aka two-way mixed, average measure in SPSS) and a

Bland-Altman plot were used. To determine intra-rater and inter-rater reliability of the cartilage damage scores, Spearman's Rho test was used.

For the final research question, stifles were categorized as either have a (i) minor restriction to reach full knee extension or a (ii) major restriction to knee extension by splitting the sample at the median value for each of the goniometry and line bisection techniques. To determine whether cartilage damage scores were different between stifles with minor versus major restrictions from full extension, a Kruskal-Wallis test was used. The primary rater's initial scores were compared to the secondary assessor's scores to assess inter-rater reliability.

2.2 Results

2.2.1 Goniometry and Line Bisection Measures of Maximum Extension

The sagittal maximum extension angles obtained by goniometry and line bisection were different (Table 2.2). A bias of 10° was present between mean maximum stifle extension angles determined using the goniometer (165° SD 6.33) and line bisection (155° SD 5.84). The mean difference between the two angle measures in the largest maximum extension angle was 10° . There was a 6° mean difference in the minimum extension angles recorded between goniometry and line bisection measurements. The median values obtained by goniometry (165° cut-off) and line bisection (155° cut-off) were not the same. The specimens were split into 2 groups (minor restriction in knee extension above the median; major restriction in knee extension below the median) for

each of goniometry (165° median) and line bisection (155° median). 81% of the specimens had the same group assignment with both approaches.

Table 2.2: Descriptive characteristics of maximum extension angle data obtained by goniometry and line bisection including: mean, median, minimum, and maximum angle for 32 porcine stifles.

	Goniometry	Line Bisection
Mean Angle	165	155
Median Angle	165	155
Minimum Angle	150	144
Maximum Angle	177	167

There was relatively poor agreement between the maximum extension angle measures obtained by goniometer and line bisection measures (ICC = 0.325, $p = 0.004$). This corresponds to the Bland-Altman plot that illustrates that the goniometer and line bisection measures demonstrated poor to moderate agreement (Figure 2.1). The majority of the measured angles fall within the upper and lower confidence limit, however, the spread of the data along the y-axis is large indicating variability between the goniometer and line bisection maximum sagittal extension angles.

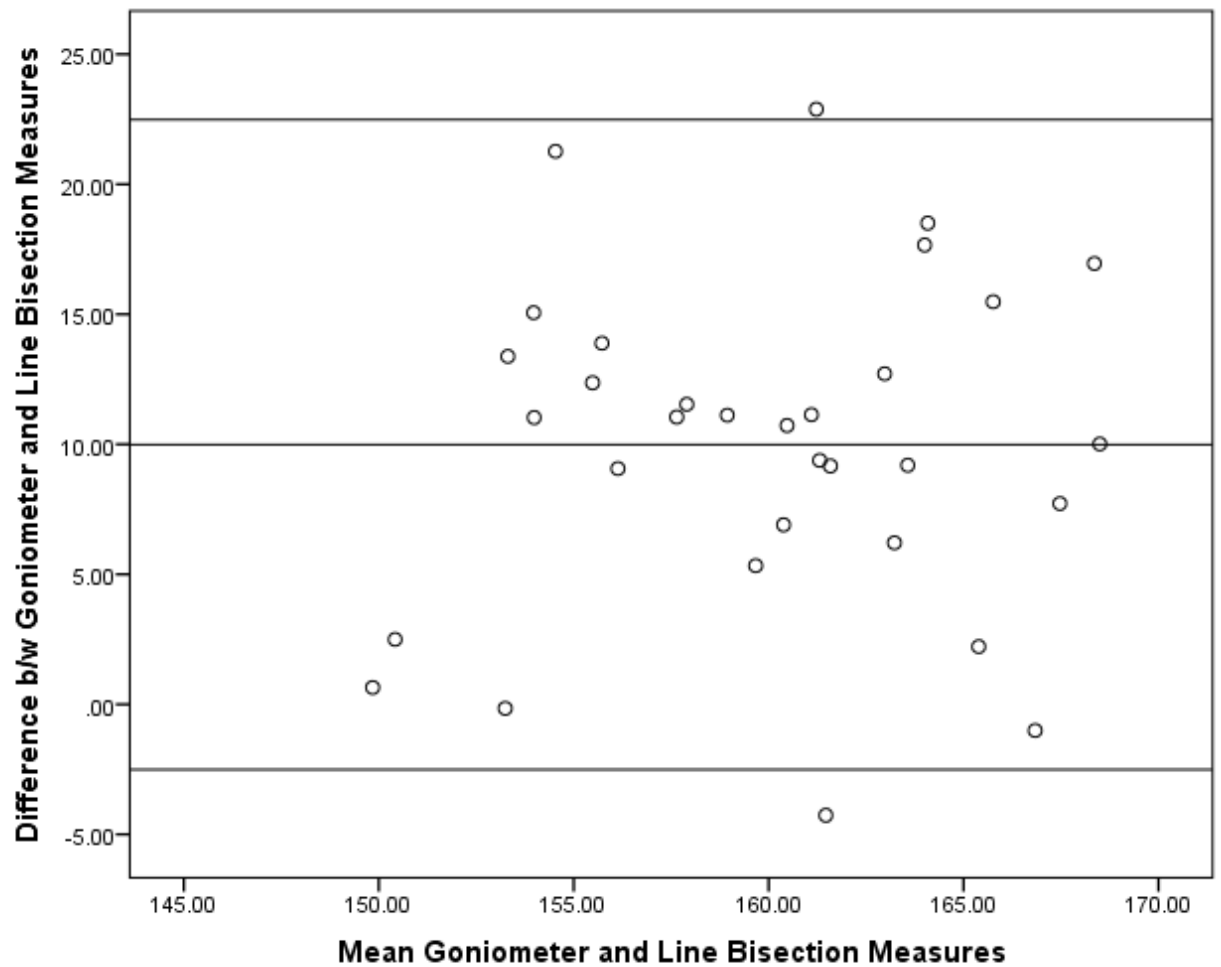


Figure 2.1: Goniometer and line bisection measures have poor agreement when measuring sagittal maximum extension angle. The Bland-Altman plot features a wide spread of data across the vertical axis (y), indicating large variance in angle measures.

2.2.2 Reliability of the Macroscopic Scoring System for Cartilage Damage

The cartilage damage scores ranged from 0 (smooth surface) to 4 (large areas of severe damage) (Table 2.3). The majority of the specimens scored between 0 and 2, indicating that cartilage fibrillation and focal partial thickness lesions were common, whereas deep lesions with surrounding damage were not.

For intra-rater reliability of cartilage damage scores, Spearman correlation coefficients were significant for the lateral tibia ($\rho = 0.812$, $p = 0.001$), medial tibia ($\rho = 0.759$, $p = 0.001$), lateral femur ($\rho = 0.808$, $p = 0.001$), and medial femur ($\rho = 0.858$, $p = 0.001$). For inter-rater reliability, significant correlations were found between the two raters scores in the lateral tibia ($\rho = 0.469$, $p = 0.007$), lateral femur ($\rho = 0.561$, $p = 0.001$), and medial femur ($\rho = 0.598$, $p = 0.001$). No significant relationship was found between raters' medial tibia scores ($\rho = 0.249$, $p = 0.169$).

Table 2.3: Cartilage damage scores of the medial and lateral tibia and femur, ranging between 0 (no damage/smooth surface) to 4 (large areas of damage including the presence of cartilage lesions and fibrillation). Scores from the primary assessor (D.M.) in this sample of 32 porcine stifles ranged from 0 – 4 with the majority of stifles receiving scores between 0 – 2.

Area	Score Frequency				
	0	1	2	3	4
Lateral Tibia	13	12	6	1	0
Medial Tibia	6	15	11	0	0
Lateral Femur	11	8	12	0	1
Medial Femur	10	14	4	1	3

2.2.3 Differences between Extension Groups in Cartilage Damage Scores

No difference existed in cartilage damage scores between the minor and major restricted extension groups in any joint region (lateral and medial tibia and femur), for both the goniometer and line bisection approaches ($p > 0.05$) (Table 2.4).

Table 2.4: Maximum extension angle representing minor and major restrictions in extension are not related to cartilage damage score for both goniometer and line bisection measures in a sample of 32 porcine stifle joints.

		Lateral Tibia	Medial Tibia	Lateral Femur	Medial Femur
Goniometry	Chi-Square	0.558	0.027	0.462	0.161
	Significance	0.455	0.870	0.497	0.688
Line Bisection	Chi-Square	1.567	0.071	2.956	1.551
	Significance	0.211	0.790	0.086	0.213

2.4 Discussion

The goniometry and line bisection measures of the maximum knee extension angle from a porcine stifle demonstrated poor to moderate agreement. It is likely that absolute values from these methods contain error; nonetheless, both methods classified restrictions in maximum extension similarly. As hypothesized, intra-rater reliability of cartilage damage scores was high and inter-rater reliability was moderate for most joint compartments. Cartilage damage scores reflecting tibial and femoral articular cartilage damage were not different between the stifles with minimal restrictions to extension, compared to those with substantial restrictions to extension.

Despite the poor agreement found between the goniometer and line bisection methods, the majority of the data was grouped similarly suggesting that both tools are acceptable for categorizing maximum extension angle in a porcine model. There was a bias between the two median cut-offs used for the goniometer (165°) and line bisection measures (155°), respectively. This difference can, at least in part, be explained by the fact that the line bisection method uses a two-dimensional representation of a three-dimensional object, and thus some data regarding limb position may be lost. Identifying a

single axis of flexion and extension for the goniometry measurement is a likely source of error as the instantaneous axis of rotation shifts throughout the range of motion.

Goniometry produces reliable knee extension ($r=0.86$) angles in humans (Watkins et al., 1991). However, this measurement of agreement is relatively high; goniometry depends upon user experience and standardized protocols. The use of a less conservative form of ICC (1, 1) likely also contributed to a higher reliability in the study by Watkins et al. (1991). Because the measurements produced by goniometry versus line bisection did not demonstrate strong agreement, reducing the continuous data to categorical data minimizes the likelihood that error within either measurement would affect the analyses. However, splitting the angle data into 2 categories, instead of examining it on a continuous scale, produces a loss of information when grouping data.

Assessing the reliability of data produced by the cartilage damage scoring system is crucial to determine if this scoring system is suitable for use in a porcine model. The intra-rater reliability was high for all 4 stifle compartments. Moderate inter-rater reliability was found for all joint compartments with exception to the medial tibia. This may be due to the sample size. This data suggest that the cartilage damage scoring system developed for assessing canine cartilage is reliable in a porcine model. As the porcine and canine stifles are similar, using the same cartilage damage scoring system may be an acceptable solution when using a porcine stifle model (Proffen et al., 2012).

Cartilage damage scores did not differ between the minor restriction and major restriction to extension groups. These data appear to contradict the kinematic theory proposed by Andriacchi et al. (2004) and suggests that maximum extension is not linked

to osteoarthritic changes in articular cartilage, at least in a porcine model of relatively young animals bred for consumption. It is possible that flexion, and not extension, angle plays a more important role in knee OA development. High knee flexion has been linked to higher knee loads and may play a role in disease pathogenesis (Creaby et al., 2013). On the other hand, flexion angles during gait are not different between healthy individuals and those with knee OA (Baliunas et al., 2002). However, some evidence does suggest that individuals with OA extend their leg more when making initial heel contact compared to their healthy counterparts (Mündermann et al., 2005). This may be an effort to reduce the knee adduction moment (KAM) during stance. It is possible that kinetics may, indeed be of greater importance to mechanisms underlying OA compared to kinematics, or that kinematics alone may not be sufficient to increase OA risk. The external KAM, which represents the load distribution between the medial and lateral portions of the knee, is implicated in knee OA and can be used to predict medial compartment knee OA presence, severity, and progression (Miyazaki et al., 2002; Mündermann et al., 2005). However the relationship between knee OA and KAM is complex with conflicting results reported in the literature, and still needs to be verified in a porcine model.

Cartilage damage scores ranged from 0, indicating healthy smooth articular cartilage, to 4 indicating large areas of severe damage among the specimens in this study. This is consistent with data that suggest pigs experience degradation of articular cartilage within the stifle joint due to over-loading skeletally immature joints and bones (Sack, 1982). The large range in scores may be due to differences in environmental stimuli as

pigs from varying farms were obtained from the abattoir. The threshold at that the tissue fails, and damage occurs, is determined by the most prevalent stresses to that joints are exposed (Seedhom, 2005). As the loading history of the specimens remains unknown, it was important to use a paired model when conducting experiments using the porcine stifle joint. This approach assumes that both the right and the left stifles have been exposed to the same frequency and magnitude of loading, and similar tissue characteristics.

A few limitations should be considered. First, details of the animals from that the specimens arose were unavailable. The conditions in that the pigs were raised, their sex, body mass, and the age at that they were slaughtered are unknown. Second, the gold standard for kinematic measures (motion capture) and knee alignment assessment (radiograph) were not used. Kinematic data obtained from motion capture would examine all three planes (x, y, and z). Additionally, the bony structure of the stifle joint was exposed because the soft tissue was removed; from this perspective, radiography may not have provided more information than the photography protocol used in this study.

2.5 Conclusion

Goniometry and line bisection measures yield different results when measuring maximum extension angle in porcine stifles, however specimen grouping was unaffected by this. Therefore, careful consideration of the advantages and limitations of each should be considered prior to choosing a measurement tool. Intra-rater reliability for the cartilage damage scoring system was high and intra-rater reliability was moderate. This suggests that the scoring system used, although developed for the canine, is acceptable for

use in a porcine model. Finally, cartilage damage was not different between stifles with only minor restrictions in knee extension, compared to those with major restrictions; these data suggest that an inability to achieve knee extension is not linked with greater OA.

Author Contributions

Damjana Milicevic designed the study, collected data, performed the analysis, and prepared the manuscript. Mamiko Noguchi assisted with study design, data collection, and inter-rater reliability analysis. Jack Callaghan and Joe Quadrilatero guided study design and provided the necessary equipment for data collection. Monica Maly designed the study, guided the analysis and prepared the manuscript.

2.6 References

- Andriacchi, T. P., Koo, S., & Scanlan, S. F. (2009). Gait mechanics influence healthy cartilage morphology and osteoarthritis of the knee. *The Journal of Bone & Joint Surgery, 91*(Supplement 1), 95-101.
- Andriacchi, T. P., Mündermann, A., Smith, R. L., Alexander, E. J., Dyrby, C. O., & Koo, S. (2004). A framework for the in vivo pathomechanics of osteoarthritis at the knee. *Annals of Biomedical Engineering, 32*(3), 447–457.
- Arthritis Alliance of Canada, the Impact of Arthritis in Canada: Today and Over the Next 30 Years (Fall 2011), 11.
- Arthritis Community Research and Evaluation Unit (ACREU): Arthritis in Canada (Prepared for The Arthritis Society, 2013) 3.
- Baliunas, A. J., Hurwitz, D. E., Ryals, A. B., Karrar, A., Case, J. P., Block, J. A., & Andriacchi, T. P. (2002). Increased knee joint loads during walking are present in subjects with knee osteoarthritis. *Osteoarthritis and cartilage, 10*(7), 573-579.
- Cicuttini, F., Wluka, A., Hankin, J., & Wang, Y. (2004). Longitudinal study of the relationship between knee angle and tibiofemoral cartilage volume in subjects with knee osteoarthritis. *Rheumatology, 43*(3), 321-324.
- Cook, J. L., Kuroki, K., Visco, D., Pelletier, J.-P., Schulz, L., & Lajeber, F. P. J. G. (2010). The OARSI histopathology initiative – recommendations for histological assessments of osteoarthritis in the dog. *Osteoarthritis and Cartilage, 18*, S66–S79.

- Cooke, T. D. V., Sled, E. A., & Scudamore, R. A. (2007). Frontal plane knee alignment: a call for standardized measurement. *Journal of Rheumatology*, 34(9), 1796-1801.
- Creaby, M. W., Hunt, M. A., Hinman, R. S., & Bennell, K. L. (2013). Sagittal plane joint loading is related to knee flexion in osteoarthritic gait. *Clinical Biomechanics*, 28(8), 916-920.
- Felson, D. T. (2004). An update on the pathogenesis and epidemiology of osteoarthritis. *Radiologic Clinics of North America*, 42(1), 1–9.
- Fuss, F. K. (1991). Anatomy and function of the cruciate ligaments of the domestic pig (*Sus scrofa domestica*): a comparison with human cruciates. *Journal of Anatomy*, 178, 11.
- Hunter, D. J., Niu, J., Harvey, W. F., McCree, P., Gross, K. D., & Zhang, Y. (2007). Knee alignment does not predict incident osteoarthritis. *Arthritis and Rheumatism*, 54(9), S155.
- Kääb, M. J., Gwynn, I., & Nötzli, H. P. (1998). Collagen fibre arrangement in the tibial plateau articular cartilage of man and other mammalian species. *Journal of anatomy*, 193(01), 23-34.
- Mansour, J. M. (2003). Biomechanics of cartilage. *Kinesiology: The Mechanics and Pathomechanics of Human Movement*, 66–79.
- Mastbergen, S. C., Marijnissen, A. C., Vianen, M. E., van Roermund, P. M., Bijlsma, J. W., & Lafeber, F. P. (2006). The canine “groove” model of osteoarthritis is more

than simply the expression of surgically applied damage. *Osteoarthritis and Cartilage*, 14(1), 39–46.

Miyazaki, T., Wada, M., Kawahara, H., Sato, M., Baba, H., & Shimada, S. (2002).

Dynamic load at baseline can predict radiographic disease progression in medial compartment knee osteoarthritis. *Annals of the rheumatic diseases*, 61(7), 617-622.

Outerbridge, R. E. (1961). The etiology of chondromalacia patellae. *Journal of Bone and Joint Surgery*, 43.

Proffen, B. L., McElfresh, M., Fleming, B. C., & Murray, M. M. (2012). A comparative anatomical study of the human knee and six animal species. *The Knee*, 19(4), 493–499.

Radin, E. L., Burr, D., Caterson, B., Fyhrie, D., Brown, T., & Boyd, R. (1991).

Mechanical determinants of osteoarthritis, *Seminars in arthritis and rheumatism*, 21(3), 12–21.

Sack, W.O. (1982). *Essentials of Pig Anatomy*. Veterinary Textbooks.

Seedhom, B. B. (2005). Conditioning of cartilage during normal activities is an important factor in the development of osteoarthritis. *Rheumatology*, 45(2), 146–149.

Sharma, L., Chmiel, J. S., Almagor, O., Felson, D., Guermazi, A., Roemer, F. ... &

Hietpas, J. (2013). The role of varus and valgus alignment in the initial development of knee cartilage damage by MRI: the MOST study. *Annals of the rheumatic diseases*, 72(2), 235-240.

Sharma, L., Hurwitz, D. E., Thonar, E. J. A., Sum, J. A., Lenz, M. E., Dunlop, D. D., & others. (1998). Knee adduction moment, serum hyaluronan level, and disease severity in medial tibiofemoral osteoarthritis. *Arthritis & Rheumatism*, *41*(7), 1233-1240.

Watkins, M. A., Riddle, D. L., Lamb, R. L., & Personius, W. J. (1991). Reliability of goniometric measurements and visual estimates of knee range of motion obtained in a clinical setting. *Physical therapy*, *71*(2), 90-96.

Chapter Three: The Effect of Mechanical Cyclical Loading on Porcine Stifle Deformation and Cartilage Quality

Damjana Milicevic¹, Mamiko Noguchi², Joe Quadrilatero², Jack P. Callaghan², Monica
R. Maly^{1,2}

¹ Department of Kinesiology, McMaster University, Hamilton, ON, Canada

² Department of Kinesiology, University of Waterloo, Waterloo, ON, Canada

3.0 Introduction

Knee osteoarthritis (OA) is a mechanical disease that damages all tissues within the joint, including but not limited to articular cartilage and the underlying subchondral bone (Radin et al., 1991). Knee OA has a heavy cost on the individual through chronic pain, immobility and disability; and a heavy cost on the economy in healthcare costs (Felson, 2004). Further, knee OA can be problematic for industry. In fact, knee OA costs the economy \$33 billion per year in indirect costs including lost productivity in the workplace (Arthritis Alliance of Canada, 2011).

Exposure to large and repetitive mechanical knee loads and flexed postures in the workplace predicts development of knee OA in epidemiological studies (Jensen, 2008; Rossignol et al., 2005). Occupations that involve repetitive exposure to kneeling, lifting, bending, and stair- or ladder-climbing are linked to a higher risk of developing OA (Jensen, 2008; Rossignol et al., 2005). Once osteoarthritic changes are present, it appears that further exposure to physical activity can worsen knee OA (Cheng et al., 2000; Dore et al., 2013). For example, walking more than 10,000 steps per day was associated with increased risk of meniscal and cartilage pathology and damage in individuals with pre-existing knee structural abnormalities (Dore et al., 2013).

Compressive loading of the knee causes cartilage deformation, largely as a result of fluid flow out of the cartilage extracellular matrix (ECM) into the joint capsule (Choi & Gold, 2011). As cartilage volume decreases from fluid expulsion, the density of proteoglycans (PG) increases. These PGs are negatively charged; thus increasing the density of PGs also increases the repulsive force within cartilage. This repulsive force, or

swelling pressure, contributes to stiffening cartilage under loaded conditions. Upon the removal of load, fluid flows back into the cartilage and the tissue recovers. Fluid flow is key in dictating the deformations of knee articular cartilage under load, in both *in vivo* and *ex vivo* experiments. In *in vivo* experiments of the human knee, even seemingly low intensity activities, such as during gait, produce significant cartilage deformation detected using magnetic resonance imaging (MRI) (Eckstein et al., 2006). This deformation is largely driven by the flow of fluid out of the cartilage and into the synovial space during loading (Choi & Gold, 2011).

In *ex vivo* experiments exploring deformations of cartilage plugs in response to loads, excessive fluid loss and alterations in collagen orientation as a result of mechanical loading reduced cartilage thickness but also decreased compressive strength and increased energy dissipation, surface damage, and micro-injury (Adams et al., 1998; Kääh et al., 1998; Aultman et al., 2004). Excessive fluid loss can occur as a result of cartilage damage causing increased permeability (Nordin & Frankel, 2012). Stiffness reflects a tissue's rigidity, or its ability to resist deformation. Strength refers to a tissue's capacity to resist micro-injury or damage when compressed. It is the point at that a tissue crosses the yield point and its deformations become plastic in nature. These results were likely influenced by the use of cartilage plugs – the cartilage may have been more prone to failure as it was removed from the joint and the support of adjacent tissues within the joint (*i.e.* surrounding cartilage, muscle, and bone).

Rest may mitigate the potential for excessive fluid flow within cartilage as a result of repetitive mechanical loading by allowing the tissue to recover. Intermittent rest (*i.e.*

non-loading) stimulates PG synthesis, which promotes effective responses to loading (Choi & Gold, 2011; Palmoski & Brandt, 1984). Unloading cartilage plugs for 12-24 hours in a saline solution reduces cartilage fissure width, thus demonstrating that the tissue has potential for recovery (Kerin et al., 2003). During repetitive loading, adding periods of rest may allow for fluid to flow back into the tissue, minimizing alterations in cartilage morphology and composition. This in turn may enable knee articular cartilage to be more resilient to loading and therefore minimize tissue degradation. Knowledge regarding the impact of altering work:rest , or duty cycles, remains limited. Such evidence is necessary to identify optimal work:rest that minimize the breakdown of cartilage under conditions of repeated loading.

Thus, the overarching purpose of this study was to examine the effect of rest on joint mechanics and cartilage damage in an intact porcine model. To achieve this goal, three different loading conditions were developed to expose an intact porcine stifle to the same cumulative load (7200 cycles of loading) with varying exposures to rest. The primary purpose was to determine if there is a difference in the deformation and rate of deformation of the porcine stifle between three loading conditions (no rest, and work:rest of 3:2 and 1:1) that each produce the same cumulative load. The hypothesis was that the cumulative load would deform the joints in all 3 conditions; but there will be less deformation and a slower rate of deformation in conditions incorporating rest, in a dose-response manner. Secondary purposes included the following:

- 1) To determine if energy dissipation differs between the beginning and end of the loading protocol and among the 3 loading conditions. It was hypothesized that

while energy dissipation will be smaller at the end, compared to beginning of the loading protocol for all 3 conditions, less energy will be dissipated at both time points in conditions that include rest.

- 2) To determine if cartilage damage observed in the matched pair stifle, a surrogate for the pre-loading condition of a loaded stifle, is related to energy dissipation at the beginning of the loading protocol. A secondary purpose was to determine if final cartilage damage of the loaded stifle is related to energy dissipation at the end of the loading protocol. It was hypothesized that a positive relationship will exist between cartilage damage with energy dissipation observed in the loaded stifle at the beginning and end of the protocol.
- 3) To determine if there is a difference in cartilage damage between the stifle following loading and its unloaded matched pair. It was hypothesized that there will be a significant difference between the loaded stifle and its unloaded matched pair.
- 4) To compare cartilage damage between the 3 loading conditions. It was hypothesized that stifles exposed to rest will demonstrate less cartilage damage after the loading protocol, compared to joints that do not have rest.

These fundamental data will provide some evidence necessary to inform a program of research aimed at developing guidelines for work duty cycles within occupational settings, which can benefit many workers who are at risk of developing OA.

3.1 Methodology

A randomized control trial was performed to assess the impact of rest on 18 pairs of porcine stifle joints (Figure 3.1). From each pair, 1 stifle was randomly selected for exposure to an intervention (a loading protocol); the matched pair served as a control. This element of design assumes similar tissue properties in stifles acquired from the same animal. Intervention joints were randomized into 1 of 3 loading protocols: no rest, or a work:rest of 3:2 or 1:1. Data on deformation, rate of deformation and energy dissipation were obtained from the loading apparatus in the intervention joints; and categorical data (cartilage damage score) were collected from both intervention and control stifles. The sample size was determined *a priori* ($\alpha = 0.05$, power = 0.8; $N = 36$, minimum per group = 6). This is the minimum sample size required to observe a moderate effect, based on means and standard deviations from studies examining porcine cervical loading (Callaghan & McGill, 2001).

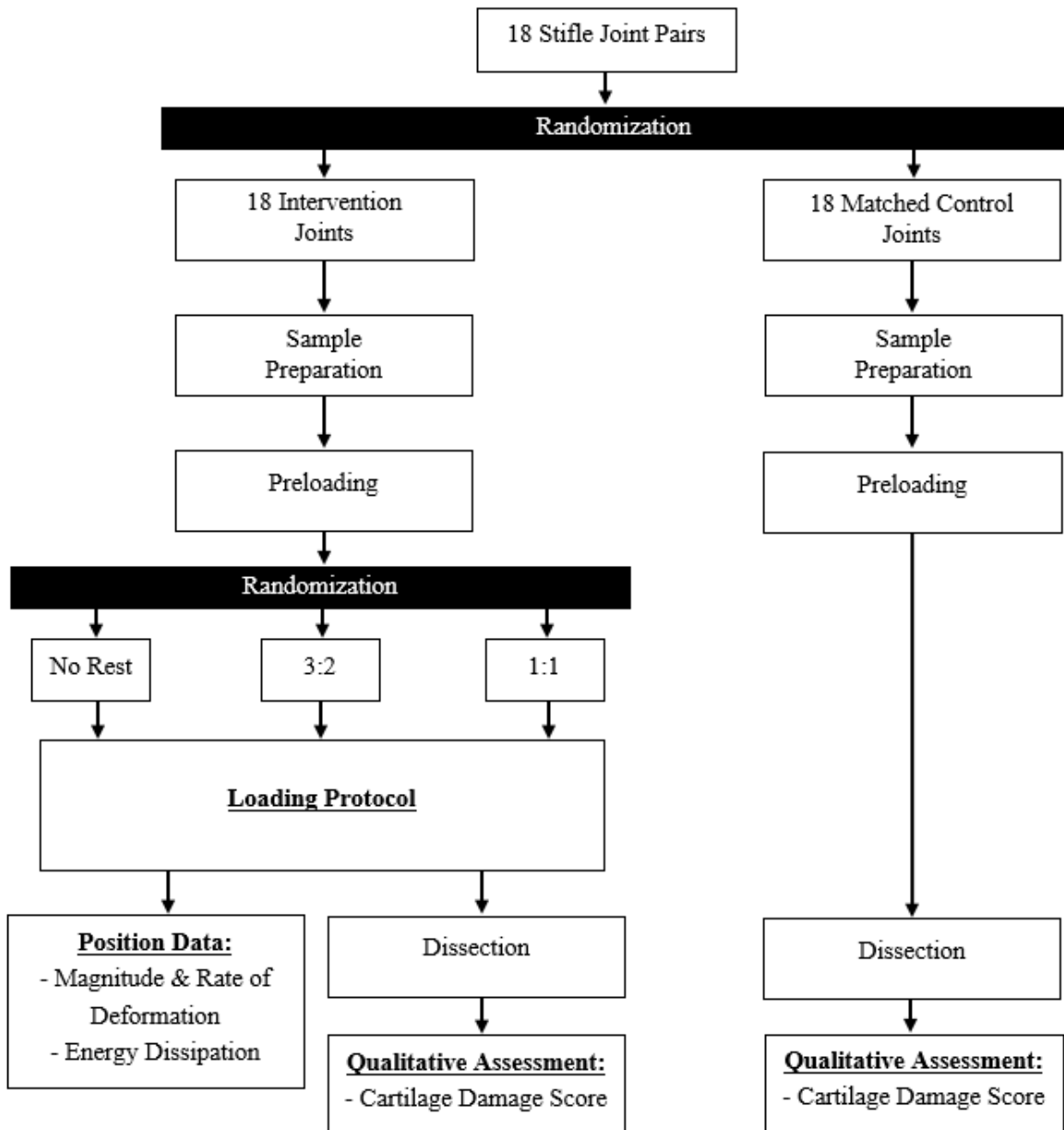


Figure 3.1: A methodological outline depicting the study protocol. Paired stifles were randomized to either the control or intervention groups. All specimens were dissected, mounted, and preloaded at 200 N. Intervention joints were randomized into 1 of 3 loading protocols that all produced 7,200 cycles of the same loading curve. Throughout the protocol, position data were obtained. Qualitative cartilage damage scores were also obtained for both control and intervention joints.

3.1.1 Specimen Preparation

Eighteen pairs of fresh porcine hind limbs were obtained from three local abattoirs. The specimens were comprised of the entire femur, tibia and fibula with an intact stifle joint (Figure 3.2). The soft tissue (muscle, adipose tissue, joint capsule) was intact. Specimen pairs were labelled and immediately frozen and stored -20°C immediately following pickup.

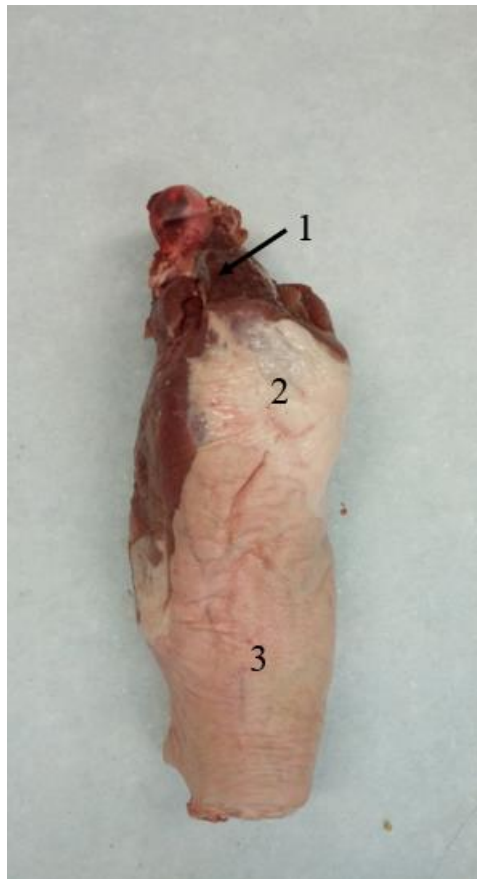


Figure 3.2: Anterior view of a specimen prior to dissection. This includes the entire limb and in intact joint, from the head of the femur to the distal portion of the tibia and fibula. The marked numbers denote anatomical landmarks where: 1) femur, 2) patella, 3) tibia and fibula.

Prior to testing, each pair of hind limbs was removed from the freezer and left to thaw overnight. One of the right or left limbs from one animal were randomly assigned to be the intervention limb. The intervention limb was exposed to the loading protocol, whereas the opposing limb from the same animal was used as the control (*i.e.* no loading). Both the intervention and control limbs were dissected using the same procedure once thawed; the soft tissue surrounding the stifle joint, including muscle and fat, were removed using a scalpel, leaving only the osteoligamentous joint structures intact (Figure 3.3). If the joint capsule was compromised, the specimen and its control pair were excluded from the experiment. Throughout the dissection, the specimen was sprayed with a saline solution (0.9 % weight/volume solution) every 15 minutes to maintain tissue hydration.

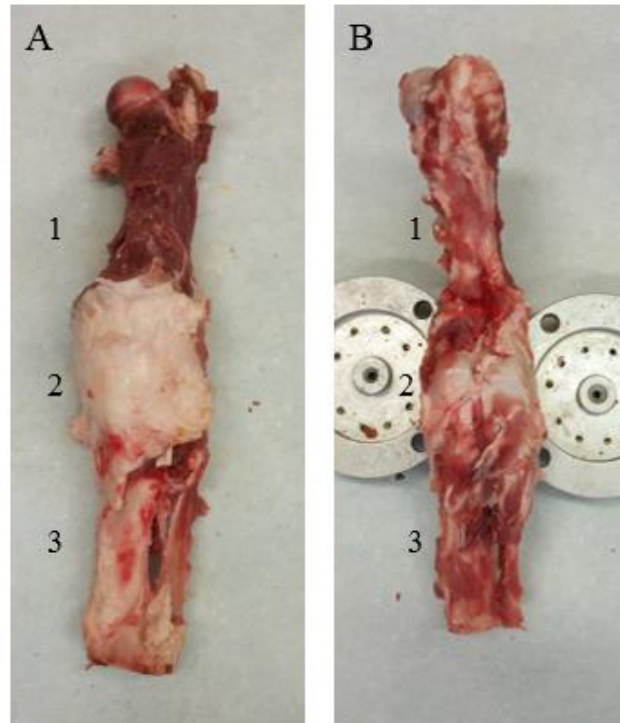


Figure 3.3: Example of a specimen following dissection. (A) Anterior view. This includes the entire limb and intact joint, from the head of the femur to the distal portion of the tibia and fibula. The marked numbers denote anatomical landmarks where: 1) femur, 2) patella, 3) tibia and fibula. (B) Posterior view of a specimen following dissection where: 1) femur, 2) intact posterior joint capsule, 3) tibia and fibula.

Following dissection, specimens were prepared to be mounted in aluminum cups for loading. First, each specimen was placed in a custom-built vice (Figure 3.4A) to ensure that the bones were cut parallel to one another. The proximal aspect of the femur was sawed off just superior to the attachment of the quadriceps. The patella was not disturbed, as removing it would compromise the joint capsule. The distal aspect of the tibia and fibula were sawed off at the base of the tibial crest (Figure 3.4B).

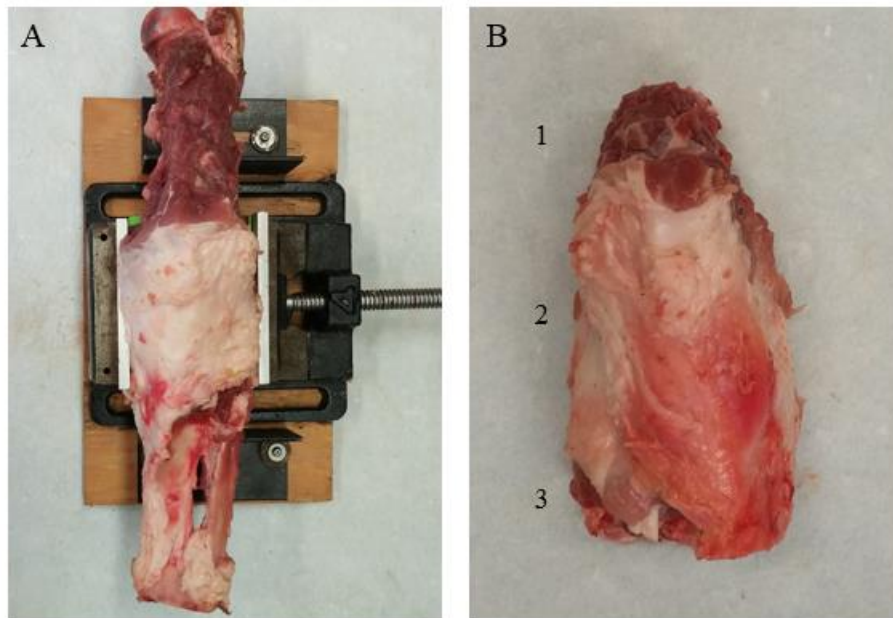


Figure 3.4: (A) Anterior view of a dissected specimen resting in a custom-built vice prior to removal of excess bone. This was used to ensure that the shaft of the femur, tibia, and fibula are parallel with one another to maximize sawing accuracy and to obtain a parallel cut for mounting. (B) Anterior view of a dissected and sawed specimen where the femoral, tibial, and fibular shafts have been cut down to prepare for mounting. The anatomical landmarks are as follows: 1) femur, 2) patella, 3) tibia and fibula.

The proximal and distal aspects of the femur and tibia, respectively, were then mounted into custom-made aluminum cups using wire, screws and plaster. Anatomical landmarks including the lateral and medial tibial condyles were identified and marked on the ends of the femur and tibia. Holes were drilled into each bone obliquely to the anatomical landmarks, with a total of eight holes (*i.e.* four on the femur and four on the tibia) made to facilitate mounting. Nineteen-gauge wire was fed through each hole (Figure 3.5), and each wire was fed through one of the eight holes in the aluminum mounting cup.

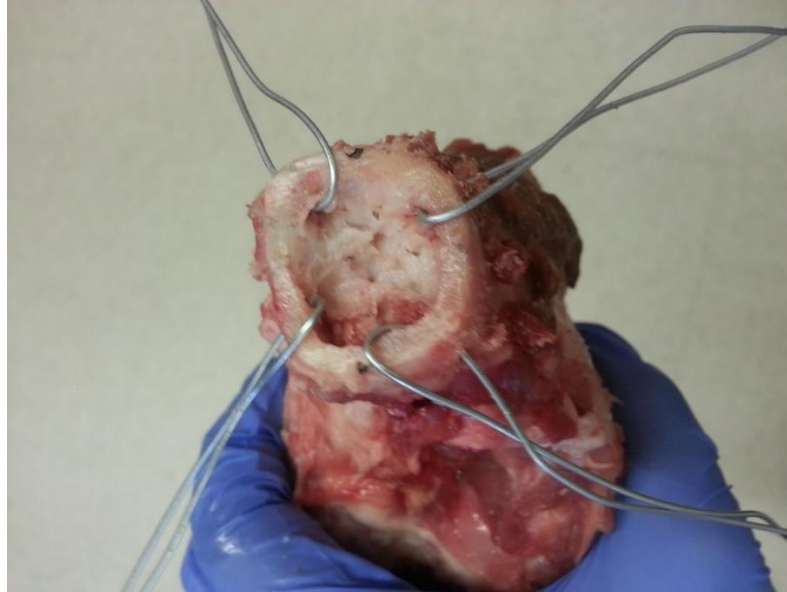


Figure 3.5: The femur from a superior view. Holes have been drilled obliquely relative to the anterior/posterior portions of the joint and the tibial condyles. Wire was inserted into these holes and folded in preparation for mounting the specimen into an aluminum cup.

The joint was secured by tightening wire pairs. Care was taken to ensure that the specimen was placed in the center of the cup and that the cups were aligned to avoid generating a torque during compression. Following wiring, holes were drilled into the posterior aspect of the tibia and femur, both medial and lateral sides of the femur, and the medial tibia, through holes in the aluminum cup. Wood screws were fastened with nuts and washers in order to adjust the length and to hold the screw firmly in place against the aluminum cup (Figure 3.6A). To finalize the mount, non-exothermic dental plaster (Denstone; Miles, Southbend, IN, USA) was poured into the cups and left to dry (Figure 3.6B).

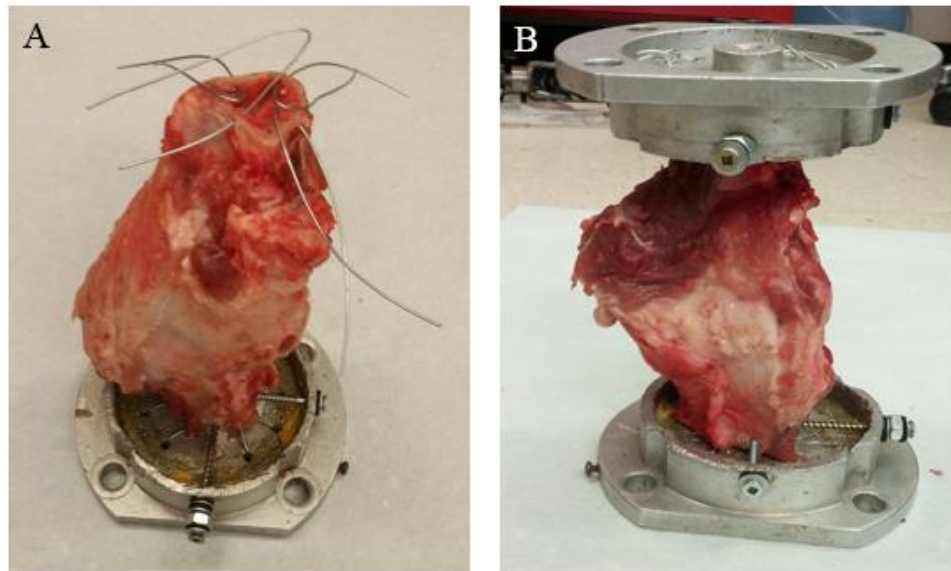


Figure 3.6: (A) Lateral view of a dissected specimen who's mounted on the femoral side (bottom). Wire and wood screws hold the specimen in place. Wood screws were drilled into the sides and posterior aspect of the bone. (B) Lateral view of a fully dissected and mounted specimen prior to the addition of dental plaster.

Once the specimen was securely mounted into the cups, it was placed into a servo-hydraulic materials testing system (Model 8872; Instron, Canton, MA, USA). The femur was placed superior to the tibia, and the cups were aligned to avoid the generation of a torque (Figure 3.7). A custom jig, which comprised of the loading head, two rods, and a vice grip, was attached to the Instron. This jig fixed the top aluminum cup firmly into place and guided the movement of the specimen to eliminate horizontal translation of the specimen and cup.



Figure 3.7: Anterior view of a fully mounted specimen, including dental plaster, placed in the Instron for loading where: 1) femur and 2) patella. The femur is placed superiorly to the tibia such that the top cup holds the femur.

No guidelines regarding the preloading of the porcine stifle exist; thus, a preloading protocol that was developed for porcine cervical spine models to counter post-mortem swelling without producing excessive amounts of creep (Callaghan & McGill, 2001) was used. The specimen was then preloaded at 200 N of compression (1/4 of the total body weight) for 15 minutes. Following preloading, the control joint was removed from the loading apparatus and dissected; whereas the intervention joint was subjected to 1 of 3 randomly assigned loading protocols.

3.1.2 The Loading Jig

A specialized jig was custom made for this study (Figure 3.7) in order to eliminate the translation of the bottom cup and generation of a torque. The jig included a head piece that was directly attached to the loading arm of the loading apparatus. The superior aluminum cup containing the mounted femur was attached to the head piece using screws with washers and nuts to prevent translation of the top cup. The weight of the jig prevented translation of the bottom cup. Two rods were attached to the head piece of the jig in parallel to the specimen. The rods included a small compartment filled with frictionless balls that guided the vertical motion of the specimen during loading and unloading. The rods were attached to the side of the loading apparatus using a vice grip. The jig allowed for specimen translation to be eliminated and ensured that the specimen was only exposed to axial compression throughout the protocol. Additionally, this jig prevented the deflection of force through the loading arm.

3.1.3 Loading Protocols

The intervention stifles were randomized into 1 of 3 loading conditions: No rest, a 3:2 work-to-rest ratio, or a 1:1 work-to-rest ratio. Each condition included 6 intervention stifles. All conditions resulted in exposure to the same cumulative load. Conditions that included rest (3:2 and 1:1) alternated between one-minute periods of work and periods of rest. The length of the rest period depended upon the loading protocol, as the 1:1 condition included more rest than the 3:2 condition. Details of the loading protocols are summarized in Table 3.1.

Table 3.1: Details of the loading protocol for each condition (no rest, 3:2, 1:1) including cumulative exposure to work and rest, the work to rest ratio, and the overall duration of each loading protocol. Work, or cumulative load exposure is constant for all 3 loading protocols. The cumulative exposure to rest varies between protocols and increases from zero rest in the no rest condition to equal amounts of work and rest in the 1:1 condition.

Characteristics of the Loading Protocols				
Condition	Cumulative Load Exposure (# of cycles)	Work to Rest Ratio	Cumulative Rest Exposure (# of cycles)	Duration of Loading Protocol (min)
No rest	7200	Work only	0	120
3:2	7200	1 min work:40 s rest	2880	200
1:1	7200	1 min work: 1 min rest	7200	264

No rest was chosen to assess the effects of loading on the joint. The 1:1 ratio was chosen as it represents the same amount of joint loading (work) and unloading (rest). The 3:2 condition was chosen to assess if the benefits of rest on the joint can be seen with a shorter total duration of unloading.

All 3 conditions used the same loading curve to produce a loading exposure. No data on porcine gait were identified in the literature. Thus, this loading curve was derived from vertical ground reaction force (GRF) data obtained from one representative human participant of the 50th percentile with symptomatic knee OA from an existing dataset (n=25) (Maly et al., 2015). The GRF curves were obtained from a force plate (OR6-7, AMTI) during over ground normal gait trials. These data were interpolated and low-pass filtered using a Butterworth filter with a cut-off frequency of 6 Hz. Five GRF curves were exported from commercial software (Visual 3D, C-Motion Inc., Germantown, MD, USA) and averaged to obtain one mean GRF curve. As these data were obtained with a

force plate, there is no data during the swing portion of the curve. Instead, 10 N was continuously applied throughout the swing phase of the gait curve. This value was chosen as the actual joint contact forces in the knee do not approach zero (Meyer et al., 2013). The joint reaction force present during swing results from forces produced by the muscles and ligaments surrounding the knee joint. The vertical GRF curve was time normalized to last one second. To normalize the amplitude, each point on the curve was divided by the maximum value, making the new maximum value one. Each specimen was loaded to 3 times body weight (2400 N), which is at a magnitude that is seen in many everyday tasks, and is therefore applicable to real life scenarios in humans (Mündermann et al., 2008). Although this magnitude of loading is high for a porcine model, it ensured that the cumulative load would be large enough to cause damage within a reasonable duration. This loading magnitude has also previously been used in *ex vivo* models to damage cartilage (Palmoski & Brandt, 1984; Kääh et al., 1998). The loading curve that was used was multiplied by -1, as compression is programmed to be negative in the materials testing system (Figure 3.8). Note that this curve, including swing and stance, represents one single cycle of work.

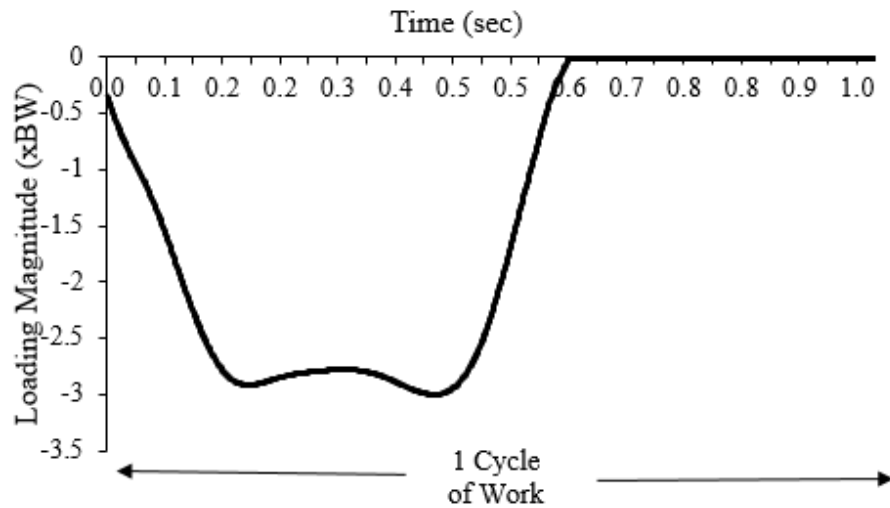


Figure 3.8: One cycle of work. The loading cycle is a vertical GRF curve for one entire stride obtained from one representative human subject with knee OA. Loading begins at 10 N of compression and the peak load is 2400 N, or three times body weight. Ten N of compression were applied during the swing phase. The cycle was normalized to be 1 sec in duration.

For the conditions that involved rest, a constant load of 10 N was applied for the rest period (Figure 3.9). This value was chosen for rest as the knee joint always experiences a joint reaction force (Meyer et al., 2013); however, the 10 N force used was assumed to have a negligible effect on the joint.

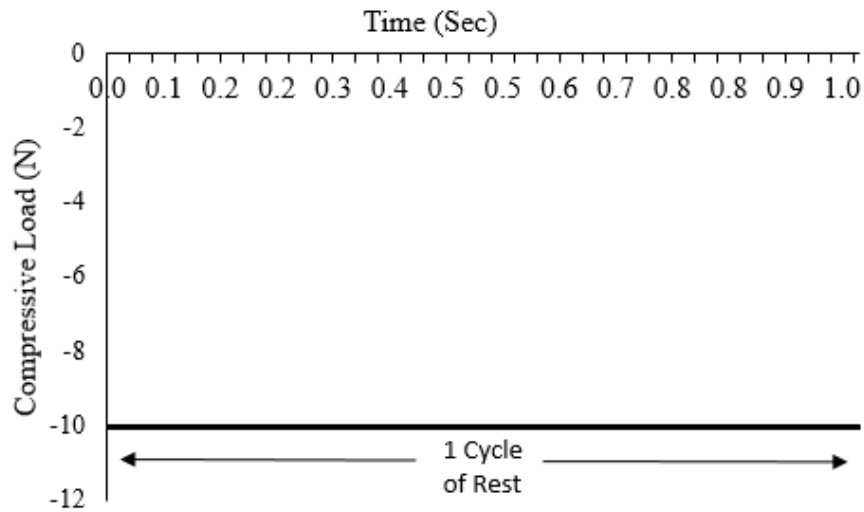


Figure 3.9: One cycle of rest where a constant load of 10 N is applied. The cycle was time normalized to be 1 s in duration.

As previously mentioned, loading exposure was normalized in all 3 conditions. All joints were loaded for 7200 cycles. This was broken down into 120 periods of work. Each work period contained 60 cycles of work and thus, each period lasted 1 minute (1 cycle = 1 second). A similar approach was used for rest, where each rest period contained repeated cycles of rest. The number of cycles in each rest period depended upon the loading protocol (3:2 or 1:1). Protocols that included rest alternated between periods of work and rest. In the 3:2 and 1:1 protocols, joints were exposed to 1 period of work followed by 1 period of rest.

For the no rest condition, the work curve was repeated for 7200 cycles for a total loading duration of 2 hours (120 minutes) (Palmoski & Brandt, 1984). Specifically, 120 periods of work, each containing 60 cycles of work, were repeated continuously in this protocol (Figure 3.10):

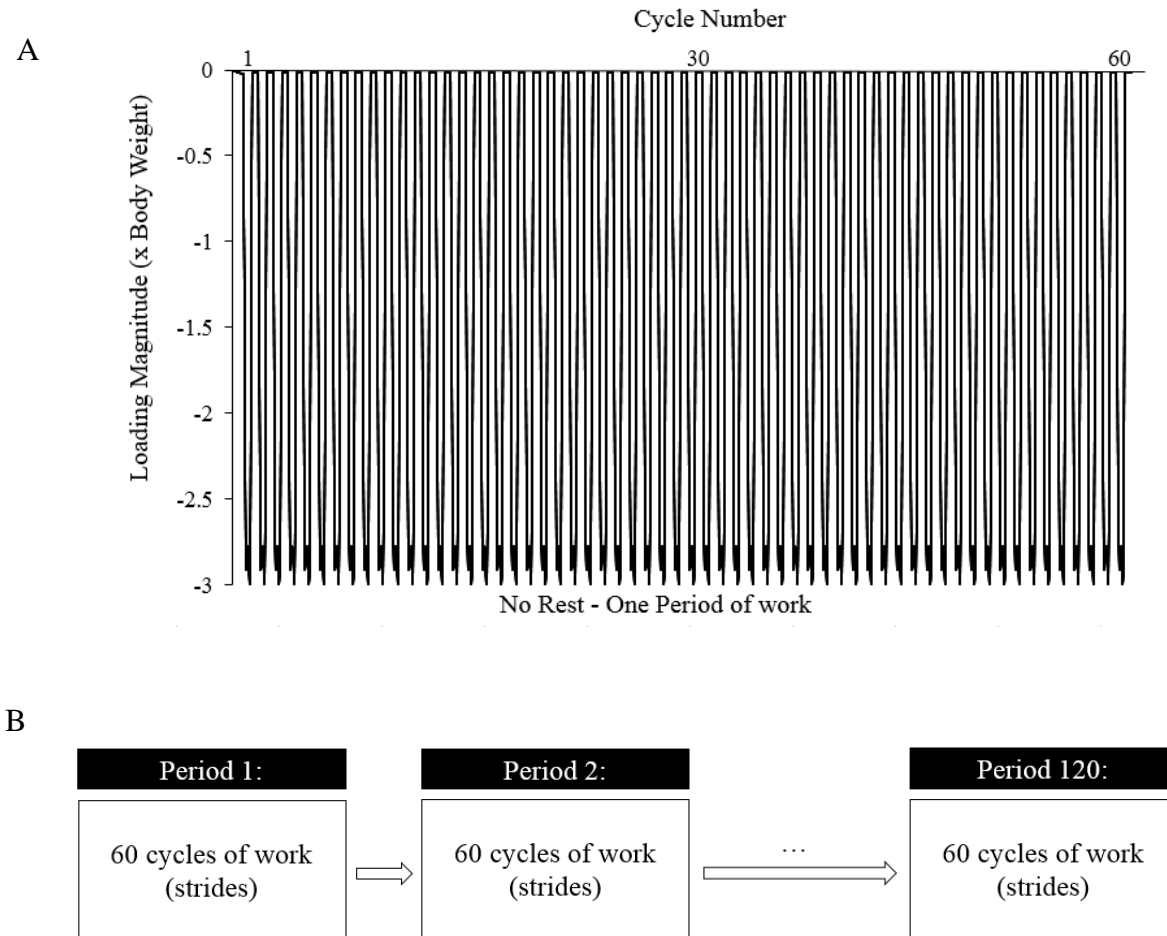


Figure 3.10: (A) One loading period for the no rest condition. This includes 60 repetitions of individual work cycles with no rest, which equals 1 min of loading. 120 periods of work, which each include 60 cycles of work, are repeated in the no rest loading protocol. This yields a cumulative load of 7,200 work cycles. (B) A schematic of the no rest condition. One period of work includes 60 repetitions of the work loading curve with no rest that equals 1 min of loading. This is repeated 120 times for a total cumulative load of 7200 work cycles.

For the other two conditions (3:2 and 1:1), alternating periods of rest were added. In the 3:2 condition, specimens were exposed to a period (60 cycles) of work, immediately followed by a period of rest that included 40 cycles of rest at a constant 10 N load (Figure 3.11). This is equivalent to 40 seconds of rest per period. Thus, alternating periods of work and rest were repeated until a specimen was exposed to 120 periods of work (7200 work cycles in total) and 120 periods of rest (2880 rest cycles in total). The total duration of the 3:2 protocol was 200 minutes.

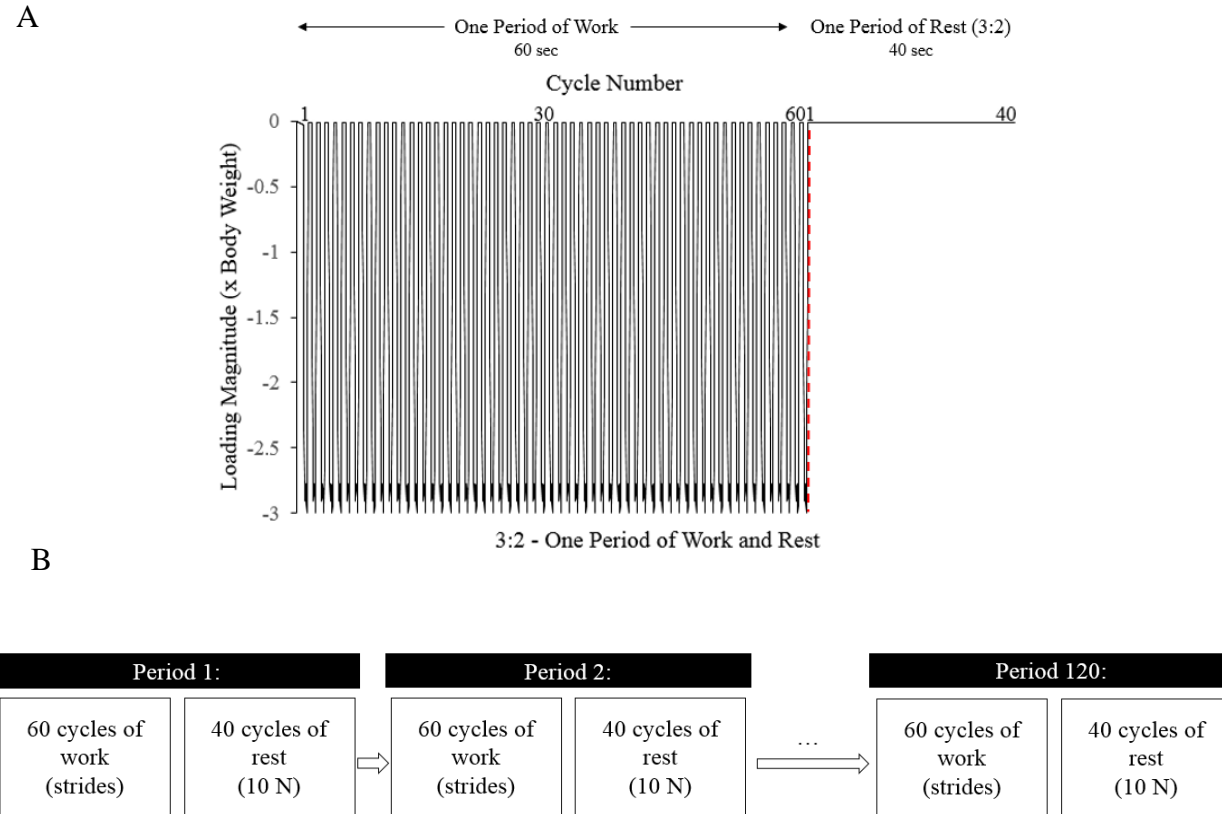


Figure 3.11: (A) One work-rest period for the 3:2 condition. This includes 60 repetitions of individual work cycles, followed by 40 repetitions of the rest cycle. Both are repeated 120 times, in an intermittent fashion (work-rest-work-rest...). However, cumulative exposure to work and rest is disproportionate with this condition having 7,200 cycles of work and 2,880 cycles of rest exposure overall. (B) A schematic of the 3:2 condition. One period of work includes 60 repetitions of the work loading curve with no rest that equals 1 min of loading. This is repeated 120 times for a total cumulative load of 7,200 work cycles. Each period of work is followed by a period of rest where 40 rest cycles are repeated for each period resulting in 40 s of rest per period. This protocol includes 120 periods of rest, with 40 rest cycles in each period. Work and rest are intermittent such that the specimen is exposed to 1 min of work followed by 40 s of rest.

In the 1:1 condition, specimens were once again exposed to 1 period of work (contains 60 individual cycles of work). This was again followed by a period of rest (Figure 3.12). However, in the 1:1 condition rest cycles were repeated 60 times in each period, which resulted in one minute of rest per period. These work:rest periods were alternated until 120 periods of work and rest were completed. Therefore, specimens in this condition were exposed to equivalent cumulative work (7200 cycles of work) and rest (7200 cycles of rest). The total duration of this protocol was 264 minutes.

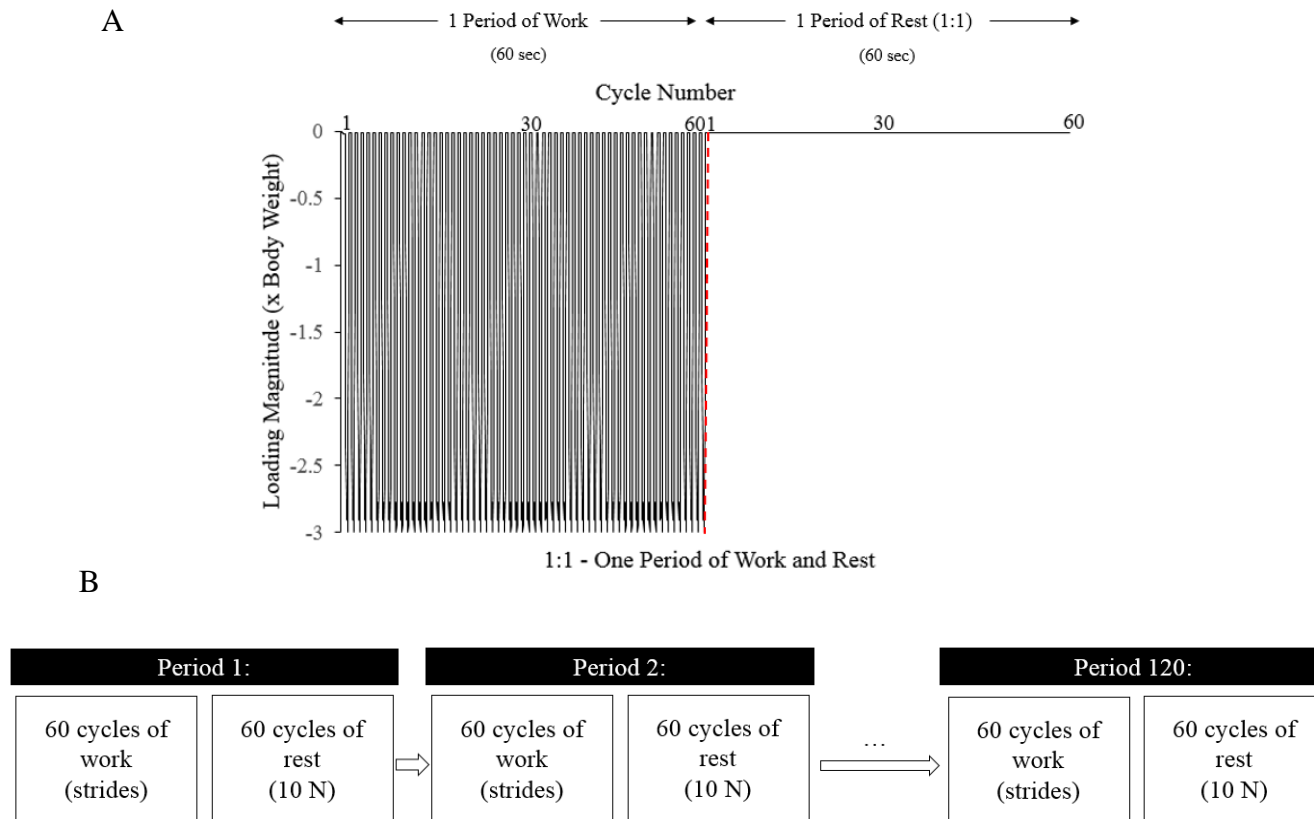


Figure 3.12: (A) One work-rest period for the 1:1 condition. This includes 60 repetitions of individual work cycles, followed by 60 repetitions of the rest cycle. Both are repeated 120 times, in an intermittent fashion (work-rest-work-rest...) so that cumulative exposure to work and rest is identical (a total of 7200 cycles of work and rest). (B) A schematic of the 1:1 condition. One period of work includes 60 repetitions of the work loading curve with no rest that equals 1 min of loading. This is repeated 120 times for a total cumulative load of 7,200 work cycles. Each period of work is followed by a period of rest where 60 rest cycles are repeated for each period resulting in 1 min of rest per period. This protocol includes 120 periods of rest, with 60 rest cycles in each period. Work and rest are intermittent such that the specimen is exposed to 1 min of work followed by 1 min of rest.

Regardless of condition, each specimen was removed from the loading apparatus and dissected after completion of loading. The joint capsule was cut carefully to avoid damaging the cartilage. The patella, collateral and cruciate ligaments, and the menisci were dissected and removed to expose the articular surface of the tibia and femur. The dissected samples (separate femur and tibia) remained mounted. The same process was followed for the control joint following preloading.

3.1.4 Outcome Measures

1) Position data

Cross-head position and load data were obtained from the servo-hydraulic materials testing system (Model 8872; Instron, Canton, MA, USA) for each specimen in each of the 3 intervention groups (no rest, 3:2, 1:1). Data were sampled at 25 Hz and data during work were exported and sorted into periods. Each loading condition included 120 work periods that were each comprised of 60 cycles of work. All data were processed using a custom code in Matlab (Matlab, Natick, MA, USA).

To obtain the mean change in position (*i.e.* deformation) over the course of the loading protocol, the mean position value for each period of work was obtained from each period of work. Thus, each data point represented the average position value for the specimen over 60 cycles (1 period). This represents deformation of the entire structure including bone, the stifle tissues (cartilage, ligaments, meniscus, connective tissue), and the equipment (cross-head, aluminum cups, dental plaster), and will be referred to as deformation throughout the remainder of the text. Although equipment deformation was

possible, the custom jig minimized deformation of the stifle joint in terms of malalignment by preventing translation of the specimen and eliminated deflection of force through the cross-head during loading.

Mean deformation across all cycles was obtained and plotted for each intervention joint (Figure 3.13). These curves were separated into (i) the initial period of rapid, non-linear deformation, which is defined as stage I; (ii) a slower, relatively linear deformation, or stage II. The distinction between stage I and II was determined by calculating the instantaneous slope of the loading curve and subsequently identifying the point at that the slope stopped changing by 20%. Separating the curve allowed for deformation to be assessed all together as a whole and separately as 2 distinct regions. As the specimen was expected to respond differently prior to and immediately following stage I, analyzing these areas separately was anticipated to provide further insight into mechanical behaviour of the joint.

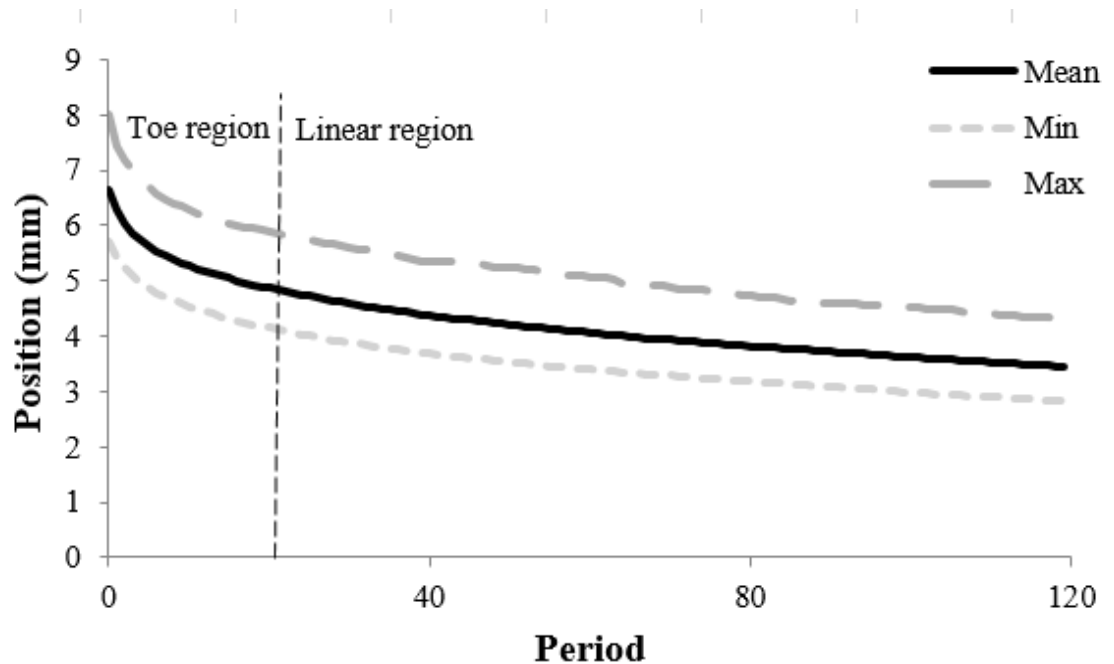


Figure 3.13: Change in position, or displacement of a representative of mean deformation over the loading protocol (120 periods)

The overall mean deformation across all cycles was obtained by subtracting the mean position at period 120 from the mean position at period 1. Deformation during stage I was calculated by subtracting the final mean position of stage I from the mean position at period 1. Similarly, deformation of stage II was calculated by subtracting the mean position at period 120 from the mean position of the first period of stage II. The slope of the curve, representing the rate of deformation, was calculated from stage II. The average mean deformations and rates of deformation were computed for each loading condition (no rest, 3:2, 1:1).

Energy dissipated by the joint during the loading protocol was computed. To obtain this measure, load deformation curves of the last cycle of each work period were collected for a total of 120 load deformation curves for each intervention joint. These

curves include both loading and unloading of the specimen. Energy dissipation was calculated by subtracting the area under the unloading portion of the curve from the area under the loading portion of the curve. The area under the loading portion of the curve was defined as the area from the starting point (nearing 10 N of compression) to the maximum point (2400 N of compression). The area under the unloading curve began at this maximum point and ended at the final point of the curve. A cumulative trapezoidal integration method was used to find the area under the loading and unloading curves, respectively. These areas were then subtracted to reveal the energy dissipated by the tissue during loading (Figure 3.14).

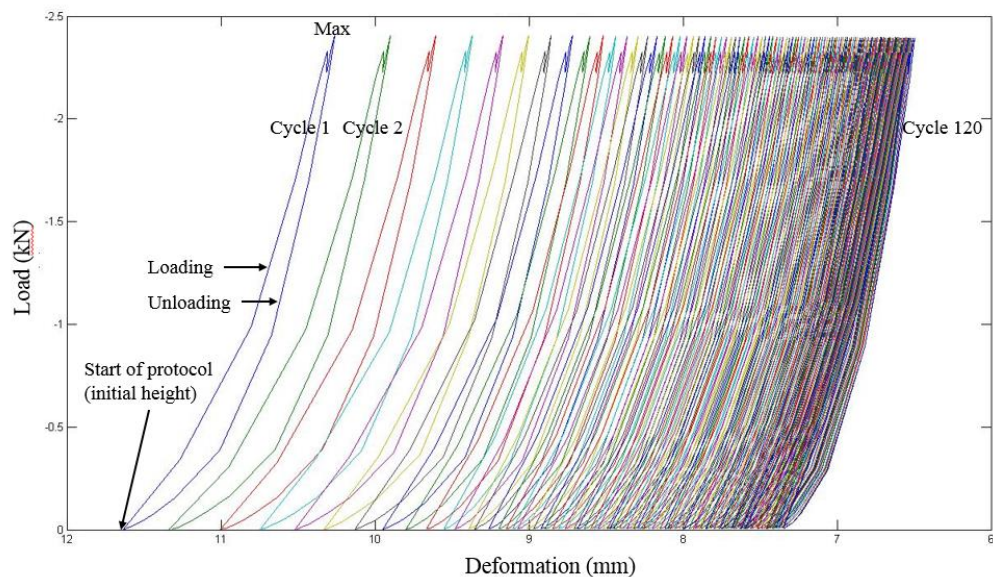


Figure 3.14: A typical load deformation curve for a representative specimen. The loading portion of the curve, beginning at the start of each cycle and ending at the peak loading magnitude (2,400 N), represents a specimen's response to loading. The unloading portion of the curve, beginning after the peak compressive value and ceasing at the end of a cycle, represents a specimen's response to unloading. The hysteresis, or area under each curve, represents energy dissipation. Dissipated energy can be calculated by subtracting the area under the unloading region from the loading region

To calculate the energy dissipated at the beginning of the loading protocol, the average energy dissipated during the first 10 periods was obtained. Energy dissipated at the end of the loading protocol was calculated by computing the average energy dissipated during the final 10 periods of the loading protocol.

2) Cartilage Damage Score

Following dissection, the articular surfaces were exposed and standardized photographs were taken. A high-resolution camera (Canon Rebel T3i EOS 600D, Tokyo, Japan) was fixed onto a tripod that was angled downward to capture the articular surface of each specimen. The camera mount and sample preparation setup was not disturbed between collections. A custom white balance was also done prior to each collection to standardize the photograph lighting. Creating a custom white balance allows for the colour white to be defined prior to each collection. All colours are compared to this definition of white, which removes ‘unrealistic’ colours from the image and allows for an object’s true colour to be depicted in the photograph. Photographs included a white background, the specimen, and a colour chart.

A blinded, experienced assessor did a visual assessment on the photographs. Damage of the articular surface of the tibia and femur were scored using 4 categories that reflect smoothness of the cartilage surface and the presence of lesions. Separate scores were given for each of the medial and lateral femur and tibia. Macroscopic scoring was done using the Osteoarthritis Research Society International (OARSI) histopathology initiative recommendations for histological assessments of OA in the dog (Cook et al., 2010), as shown in the table below (Table 3.2). The model for the dog was used as this is

the only large animal model proposed by OARSI, and there is currently no endorsed criteria for the pig.

Table 3.2: Categorical scores and articular cartilage surface descriptions for the qualitative macroscopic scoring system, representing cartilage damage, for a canine model (Cook et al., 2010). Scores range from 0-4, with higher scores being associated with greater cartilage damage

Surface Description	Score
Smooth Surface	0
Slightly fibrillated/roughened surface	1
Fibrillated surface with focal partial thickness lesions	2
Deep lesions surrounding damage	3
Large areas of severe damage	4

The foundation for this scoring system was developed by Outerbridge (1961), and modified by Mastbergen et al (2006). The articular surface was given a score ranging between 0 and 4, with 0 being a healthy smooth surface and 4 representing large areas of severe damage (Mastbergen et al., 2006; Outerbridge, 1961). Cartilage damage was scored for every stifle in the control and intervention groups. Cartilage damage scores for the control joint were used as a surrogate measure of initial joint damage pre-loading.

3.1.5 Statistical Analysis

All statistical analyses were performed using SPSS software, version 23.0 (SPSS Inc., Chicago, Illinois, USA). To determine if there is a difference in the change in deformation and rate of deformation of the joint between three loading conditions (no rest, 1:1, and 3:2), 4 separate between-groups one-way analyses of variance (ANOVAs) were performed for each of the 4 outcome variables (*i.e.* overall deformation, deformation during stage I and II, and rate of deformation). All applicable assumptions were tested

(*i.e.* normality, homoscedasticity, independent random sampling, and interval data).

Normality was assessed with the Kolmogorov-Smirnov test and homogeneity of variance was checked using Levene's test. Tukey's post hoc tests were used to identify the location of group differences, where applicable.

A 3x2 (condition x time) mixed ANOVA was performed to determine if energy dissipation differs with time (*i.e.* between the beginning and the end of the loading protocol) and between the three loading conditions. This statistical method was chosen over performing t-tests and one-way ANOVAs to reduce family-wise error (type 1 error). All applicable assumptions were tested (*i.e.* normality, homoscedasticity, independent random sampling, and interval data). The Kolmogorov-Smirnov test was used to test normality, and Levene's test was used to investigate homoscedasticity. Tukey's post hoc tests were used to identify the location of group differences, where applicable.

The relationships between energy dissipation and cartilage damage were explored using bivariate correlation analyses. Initial cartilage damage scores from the control joint were compared to energy dissipation at the start of the loading protocol (Figure 3.15). Final cartilage damage scores following loading within the intervention joints were compared to energy dissipation at the end of loading.

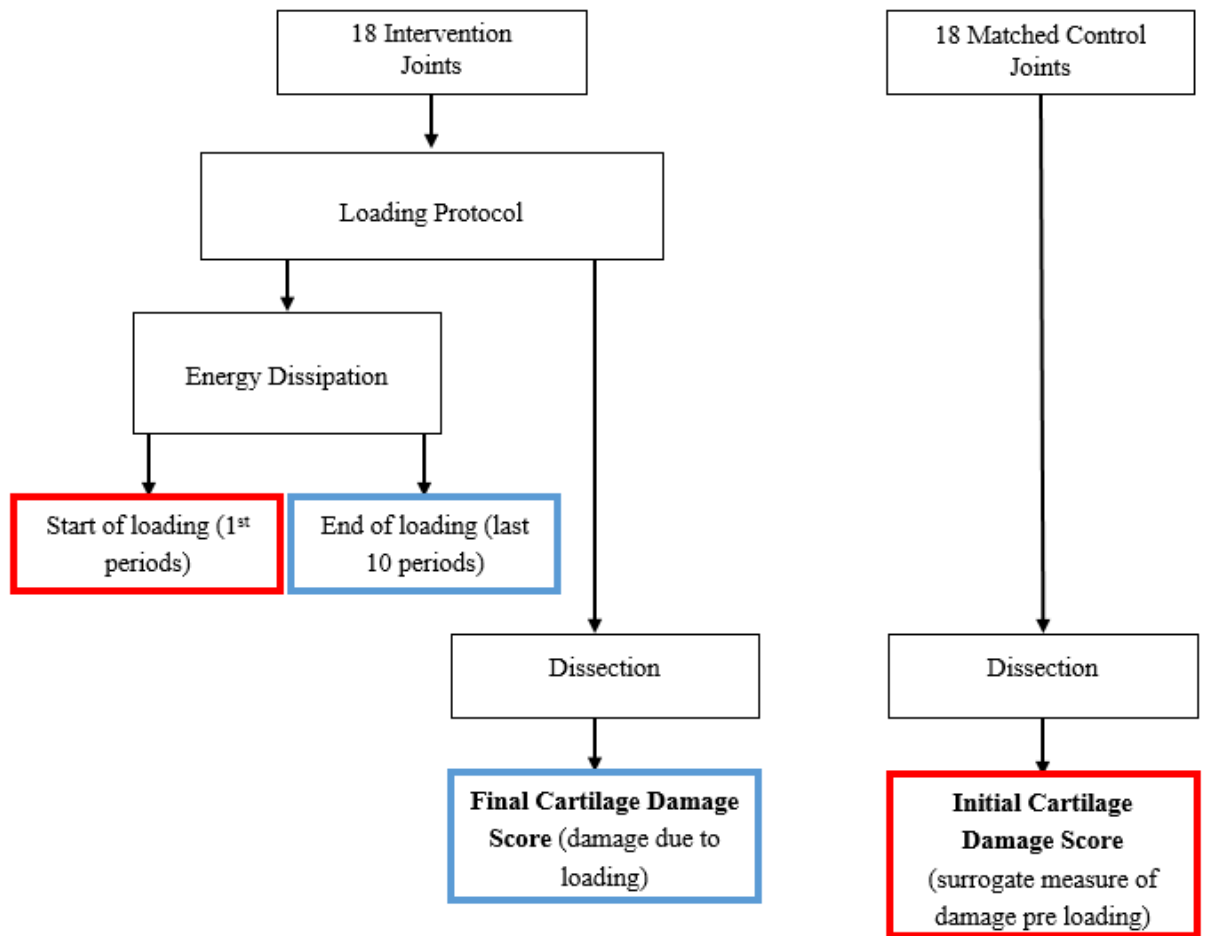


Figure 3.15: To address the third purpose, Spearman’s Rho correlations were computed between energy dissipation at the start of the protocol and initial cartilage damage (obtained from the cartilage damage scores from the control joint – a surrogate measure of initial damage) (seen in red). Correlations were also done for energy dissipation at the end of the loading protocol and final cartilage damage (obtained from the cartilage damage scores of the intervention limb) (seen in blue).

Spearman’s Rho correlations were computed between energy dissipation at the start of loading (mean of first 10 periods) and cartilage damage scores for the control joints, representing initial damage prior to loading. This was also done between energy

dissipation at the end of loading (mean of last 10 periods) and cartilage damage scores for the intervention joints, representing damage induced by loading.

To determine if there is a difference in cartilage damage scores between intervention and control limbs, a Kruskal-Wallis test was performed on each of the four knee compartments (medial and lateral tibia and femur). Also, to assess differences in cartilage damage scores between the intervention limbs within each of the 3 experimental groups (no rest, 3:2, and 1:1), a Kruskal-Wallis test was performed. Mann-Whitney U post-hocs were used to identify the location of group differences, where applicable.

3.2 Results

All 36 specimens had intact joint capsules and were used in data analysis. No specimens were excluded from the study.

3.2.1 Stifle Deformation within the No Rest, 3:2, and 1:1 Conditions throughout Loading

All assumptions for a one-way ANOVA were met for all 4 ANOVAs. Homogeneity of variance was met for all three outcomes ($p > 0.05$). The dependent variables were also normally distributed ($p > 0.05$). There was no difference in the change in overall deformation, or in deformation in stage I or II, between loading conditions (no rest, 3:2, and 1:1) (overall deformation $p = 0.206$, deformation in stage I $p = 0.109$, deformation in stage II $p = 0.641$) (Figure 3.16). There were also no differences in slope, or rate of deformation, between the three conditions ($p = 0.649$) (Figure 3.16).

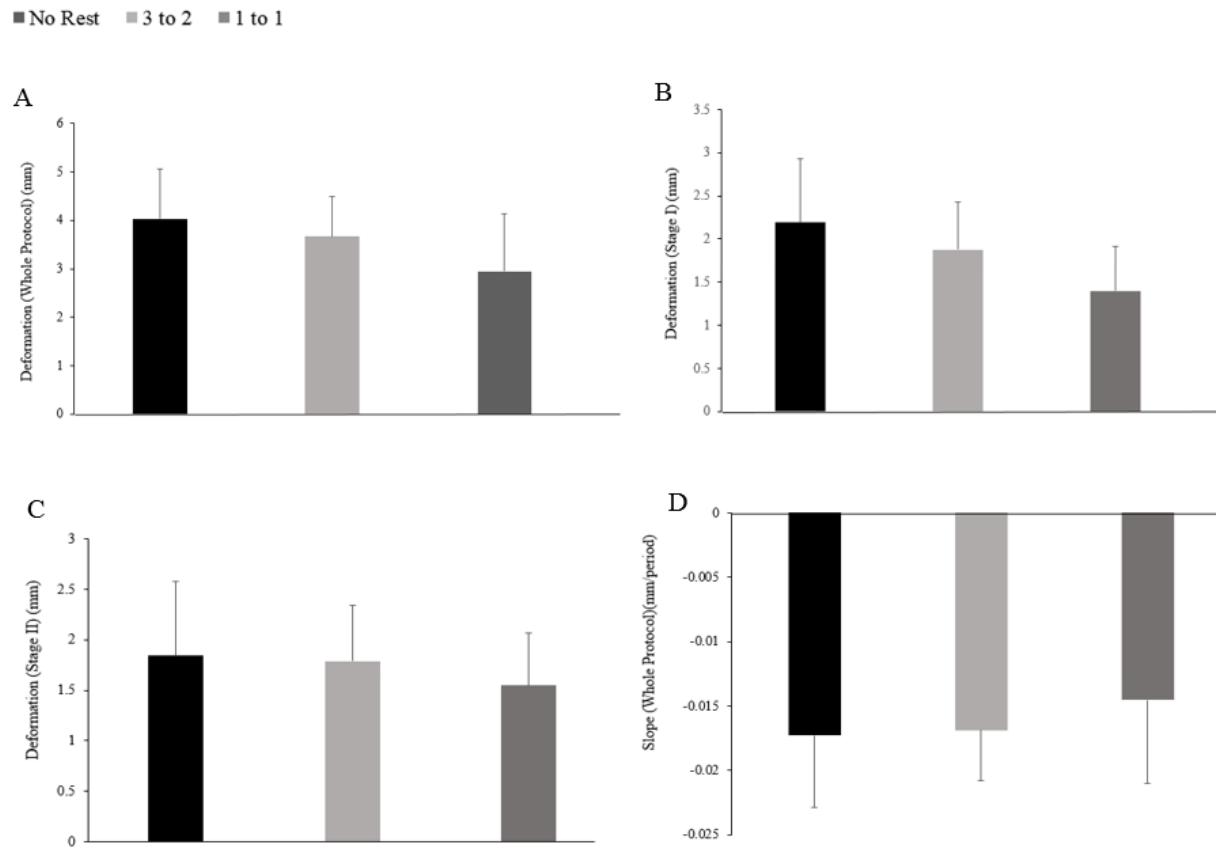


Figure 3.16: Mean deformation over (A) the entire loading protocol, (B) stage I, and (C) stage II for all intervention stifles in all 3 loading conditions is not affected by rest. Mean rate of deformation (D) for all intervention stifles in all 3 loading conditions is not affected by rest.

3.2.2 Energy Dissipation within the No Rest, 3:2, and 1:1 Conditions throughout Loading

The assumptions for a mixed ANOVA were met. Homogeneity of variance was met ($p > 0.05$). The data was also normally distributed ($p > 0.05$). Two outliers were found by examining box plots: 1 outlier was found in energy dissipated at the start of loading, and another was found at the end of loading. These outliers were kept in the model as their values were still within physiological range. Additionally, ANOVAs are robust statistical tests; therefore, leaving these data points in should not affect the statistical analysis. There was a main effect of time on energy dissipation such that energy dissipation decreased between the beginning (first 10 periods) and end (last 10 periods) of the loading protocol ($F= 3.615$, $p = 0.001$) (Figure 3.17). No differences were found in energy dissipation between the loading conditions ($p > 0.05$). However, a trend was visible once again in energy dissipation at the end of the loading protocol, as adding rest (from no rest to 1:1) appeared to decrease energy dissipation.

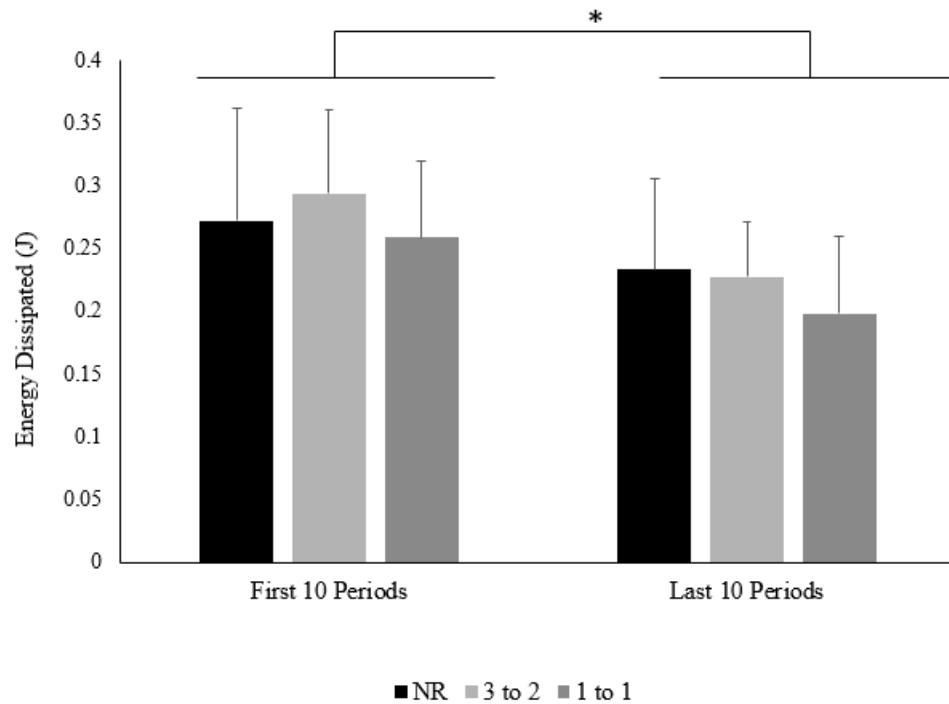


Figure 3.17: Mean energy dissipation decreased as a function of time for all intervention stifles in all 3 loading conditions. Energy dissipation, both at the start and end of the loading protocol was not mitigated by rest.

3.2.3 Energy Dissipation and Cartilage Damage within the No Rest, 3:2, and 1:1

Conditions

A significant, negative relationship was found between the cartilage damage score for the medial femur of the control joint and energy dissipation at the beginning of the loading protocol ($\rho = -0.493$, $p = 0.038$) (Table 3.3A). However, a moderate positive relationship was found between cartilage damage scores for the medial tibia of the intervention joint and energy dissipation at the end of the loading protocol ($\rho = 0.5$, $p = 0.035$) (Table 3.3B).

Table 3.3A: Medial femur damage scores were negatively associated with energy dissipation at the beginning of the loading protocol

Correlation Between Initial Cartilage Damage Score and Energy Dissipation at the Start of Loading				
	Cartilage Damage Score – Control Joint			
Energy Dissipation	Lateral Tibia	Medial Tibia	Lateral Femur	Medial Femur
Start (first 10 periods)	Spearman's Rho = -0.064 p value= 0.800	Spearman's Rho = -0.086 p value = 0.734	Spearman's Rho = 0.006 p value = 0.982	Spearman's Rho = -0.493 p value = 0.038*

Table 3.3B: Medial tibia damage scores were positively associated with energy dissipation at the end of the loading protocol

Correlation Between Final Cartilage Damage Score and Energy Dissipation at the End of Loading				
	Cartilage Damage Score – Intervention Joint			
Energy Dissipation	Lateral Tibia	Medial Tibia	Lateral Femur	Medial Femur
End (last 10 periods)	Spearman's Rho = 0.079 p value = 0.756	Spearman's Rho = 0.500 p value = 0.035*	Spearman's Rho = 0.043 p value = 0.866	Spearman's Rho = 0.058 p value = 0.819

3.2.4 Initial and Post-Loading Cartilage Damage Scores for No Rest, 3:2, and 1:1

Conditions

A large range in cartilage damage scores was found across all specimens. Frequency plots for all 4 joint compartments and both control and intervention limbs are listed in the appendix (Appendix B). The lateral compartments of the tibia and femur both begin with a higher frequency of higher scores, indicating more damage, than their medial counterparts as shown in the control limb data. A comparison of the cartilage damage scores across the 3 loading groups is also summarized in Appendix B.

Cartilage damage scores differed between control and intervention limbs (Table 3.4). Intervention limbs had higher scores (*i.e.* greater damage) than the control limbs across all 4 knee compartments.

Table 3.4: Cartilage damage scores were significantly higher in intervention joints compared to control joints across all 4 joint compartments indicating that the loading protocol induced cartilage damage

Damage Score Differences Between Intervention and Control Joints					
		Lateral Tibia	Medial Tibia	Lateral Femur	Medial Femur
Intervention vs Control	Chi-Square	6.257	11.030	20.666	10.716
	Significance	0.012*	0.001*	0.001*	0.001*

Cartilage damage scores for the lateral femur were different between groups (Table 3.5). No other differences in cartilage damage scores were observed between groups. The Mann-Whitney U post-hoc test determined that differences in lateral femur scores lie between the 3:2 and 1:1 groups ($U = 7.5$, $p = 0.043$). There was a trend towards differences in cartilage damage scores in the lateral femur between no rest and 3:2, however, this failed to reach significance ($U = 9$, $p = 0.056$).

Table 3.5: Lateral femur damage scores differed between the 3:2 and 1:1 loading conditions

Damage Score Differences Between Loading Groups (NR, 3:2, 1:1)					
		Lateral Tibia	Medial Tibia	Lateral Femur	Medial Femur
Group Differences	Chi-Square	1.976	3.766	6.650	3.176
	Significance	0.372	0.152	0.035*	0.204

3.3 Discussion

While all joints experienced deformation as a result of loading, rest did not substantially mitigate deformation or rate of deformation in this sample. Thus, the first

hypothesis was not found to be true. Energy dissipated by the stifles decreased at the end of the protocol in comparison to the beginning. However, no significant differences were found in energy dissipation at the start or end of loading between loading conditions. Given the use of the control joints as a surrogate to represent the magnitude of cartilage damage without exposure to loading, less energy was absorbed by stifles that showed greater initial damage. Interestingly, the opposite was noted at the end of the protocol such that stifles that dissipated more energy at the end of the protocol demonstrated the greatest severity of cartilage damage. As anticipated, a significant difference in joint damage was identified between the control and intervention joints. However, the only significant between-group difference in damage scores was found in the lateral tibia between the 3:2 and 1:1 conditions. Therefore, rest may not be the most effective target when considering interventions to reduce the risk of cartilage damage in occupations that involve repetitive loading of the knee.

This protocol for the stifle is a corollary to the functional unit of the spine, used to explore joint tissue responses in the presence of intact osteoligamentous structures. This protocol was developed based on existing literature examining the effects of loading on cartilage plugs (Palmoski & Brandt, 1984; Yao & Seedhom, 1993). The loading protocol and intact porcine stifle model demonstrated efficacy, as intervention specimens deformed in a predictable manner for a viscoelastic material and cartilage was damaged (Adams et al., 1998; Özkaya; 1998). These results mimic the physiological processes occurring in the joint during loading: fluid is rapidly excreted from the ECM of the cartilage, into the joint cavity, as cartilage is loaded (Choi & Gold, 2011; Nordin &

Frankel, 2012). Fluid extrusion gradually diminishes until the cessation of flow occurs due to a decrease in cartilage permeability that accompanies prolonged compression (Choi & Gold, 2011; Mansour, 2003). This is seen in the linear portion of the deformation curve, or stage II. The loading magnitude (3x body weight or 2400 N) was chosen as this load was shown to deform cartilage plugs and interrupt cellular processes (Palmoski & Brandt, 1984; Yao & Seedhom, 1993). This magnitude of loading is also seen in many everyday tasks (*i.e.* stair ascent and descent, rising from a chair etc.) and is therefore applicable to real life scenarios (Mündermann et al., 2008). Specimens were exposed to 7200 cycles over two hours, a duration that damages cartilage (Palmoski & Brandt, 1984). This duration of exposure and magnitude of load were also found to be effective in damaging cartilage of an intact stifle in this work, demonstrating that the protocols used to damage cartilage plugs *ex vivo* are also appropriate for an intact stifle.

Given an equal cumulative load between 3 loading conditions, injecting rest did not substantially alter deformation, rate of deformation, energy dissipation, or cartilage damage in these intact stifles. There are several explanations for why rest was ineffective in this study. First, significance may not have been achieved due to the sample size as trends in the data were observed, with less total deformation and energy dissipation occurring with increasing rest. A *post hoc* sample size calculation was performed using mean deformation data (primary research question). Effect size (Cohen's *d*) was determined using loading group means and standard deviations ($d = 0.4297$). To obtain a power of 0.8, 57 joints would need to be loaded as intervention joints (114 pairs in total). Second, the rest protocol may not have been long enough to allow for significant recovery

of the joint to occur, as joints were rested for either 40 seconds (3:2 protocol) or 1 minute (1:1 protocol). Fifty percent of cartilage volume recovery following repetitive knee loading in live humans *in vivo* requires roughly 45 minutes of rest, and full recovery takes over 90 minutes (Eckstein et al., 1999). Kääb et al. (1998) demonstrated that cartilage deformations that occur as a result of mechanical loading were able to completely recover; however, this required 30 minutes of unloaded rest in rabbit stifles. However, in other models even 12-24 hours of rest in a saline solution had little impact on cartilage damaged by loading, as rest did not alter cartilage fissure length in cartilage plugs (Kerin et al., 2003). Soaking the loaded specimen in saline may have also influenced the results. Cartilage explants immersed in physiologic saline is capable of recovering following removal of the load (Nordin & Frankel, 2012). As the external tissues of the joint were only sprayed by saline occasionally in this study, recovery may require a longer period of time, however, the specific timeframe of recovery is unclear. Caution must be taken as soaking samples in a saline solution can also cause cartilage to swell beyond normal physiological conditions (Adams et al., 1998).

Additionally, as loading was carried out on deceased specimens in the current study, the ability of the tissue to respond may have been hindered due to the disruption of biological and physiological processes post mortem (Bolton et al., 2015). The breakdown of PGs on a molecular scale occurs within the first three weeks of death (Bolton et al., 2015). This may impact the mechanical properties of cartilage during loading and may limit recovery during rest. To minimize the effect this phenomenon may impose, fresh joints were obtained and frozen immediately to minimize decomposition. Death and

freezing of the knee joint have relatively small effects on the mechanical properties of articular cartilage (Adams et al., 1998).

Finally, rest may have been ineffective because cumulative loading exposure is of greater importance than rest. Previous observations have suggested that cumulative loading exposure is an important contributor to cartilage degradation, and ultimately knee OA development (Vignon et al., 2006). The pathomechanics of knee OA involves abnormal, excessive, and repetitive loading. Therefore, cumulative loading exposure is an important risk factor in OA development (Felson et al., 2000). Epidemiological studies clearly identify that repetitive loading of the knee in the workplace predicts the incidence of knee OA (Jensen, 2008; Rossignol et al., 2005). Thus, cumulative load may trump rest.

Interestingly, the severity of cartilage damage following loading (intervention stifle) in the lateral femur was greater in stifles exposed to the 3:2 work:rest condition (average score = 3) compared to the 1:1 group (average score = 2). However, a trend towards significance was observed between the no rest and 3:2 conditions, which suggests that rest may mitigate the degenerative effects of loading in the lateral femur in a larger sample. Three factors may help to explain this result. First, the lateral femur of the control joints, and in fact the entire lateral compartment, had a larger frequency of cartilage damage in the control stifles compared to the medial compartment, representing greater initial damage in the lateral aspect of the joint. Damaged cartilage may respond negatively to load (Andriacchi, 2009). Joint and tissue fatigue is sensitive to imperfections on the cartilage surface. The presence of discontinuities on the cartilage

surface may also lead to stress concentrations and would result in damage propagation (Nordin & Frankel, 2012).

Second, the larger overall surface area of the articular surface of the femur in comparison to the tibia may have contributed to the higher degree of damage observed on the femur. The area of the femur that is loaded depends on the position of the femur and that aspect of the femoral cartilage is in contact with the tibial surface. In this study specimens were mounted in extension, which may have altered the contact area of the femur, perhaps loading areas that were not previously conditioned to tolerate such large loads (Seedhom, 2005; Gatti, 2015). Contact forces obtained from an instrumented knee suggest that knee loading is greatly reduced following toe off, signifying that when the limb begins to move into extension, loading is reduced (Meyer et al., 2013). Therefore, the areas of the femur that come into contact with the tibia during extension may not be well conditioned to tolerate large loads, as they are not as commonly exposed to them, resulting in greater damage to the femur.

Last, this result may simply be due to chance as there is a 5% chance of making an error with an alpha level of 0.05. Thus, these data on their own may not be meaningful. This may help to explain why differences were found between the 2 conditions that included rest (3:2 and 1:1), while no significant differences were found between conditions with no rest and those that incorporate rest. Increasing sample size may alter these results and further significance may be found, particularly as there was near significance between the lateral femur scores in the no rest and 3:2 conditions.

Energy dissipation was correlated with cartilage damage. It is important to note that (i) correlations were calculated separately for the beginning and end of the loading protocol; (ii) in the absence of severity of cartilage damage scores from the intervention stifle, the matched pair was used; and (iii) the relationships between the beginning and end of the protocol were in the opposite directions. As viscoelastic tissues respond with an initial period of rapid deformation followed by a slower, steadier period of deformation, it may be unreasonable to expect the same relationships to persist across the entire loading protocol.

The data suggest that joints with damage are compromised in the ability to dissipate energy of loading at the outset of a loading exposure. This may be explained by the fact that damaged cartilage is unable to properly respond to loading resulting in the propagation of damage, whereas healthy cartilage is able to act positively and withstand load without damaging (Andriacchi, 2009). Cartilage damage is characterized by disruption and loss of the collagen and PGs (Freeman, 1975). Following disruption of the collagen-PG matrix within cartilage, damage is propagated due to: 1) decreased stiffness and increased permeability of the cartilage and 2) disrupted load distribution mechanisms that increase frictional shear on the surface of the cartilage (Nordin & Frankel, 2012). The use of an intact osteoligamentous stifle implies that all tissues of the stifle work together to ensure proper function of the joint. It is possible that when one section or compartment of the joint becomes compromised, the function of the joint system is also detrimentally affected.

A positive relationship was found between medial tibia damage scores in the intervention limb and energy dissipation at the end of the loading protocol. This increase in hysteresis, or energy dissipation, may represent failure of the joint as energy is dissipated by failure mechanisms in the specimen (Adams et al., 1998; Nordin & Frankel, 2012). Therefore, the medial tibia may have been approaching failure. As energy dissipation was reduced at the end of loading compared to at the beginning of loading, the joint as a whole did not reach failure; however, it may be that the medial tibia would be first to fail, as higher damage scores were associated with more energy dissipation. This may be explained by the large change in damage scores in the medial tibia between the control and intervention joints. Although the lateral compartment of the joint began with a larger frequency of higher damage scores (*i.e.* greater damage), final scores were not different between conditions. These observations may suggest that the medial tibia experienced a greater change in damage.

Alternatively, relationships between tibial cartilage damage scores and energy dissipation may have been identified, as loading of the medial compartment may have been favoured during the loading protocol. Although numerous precautions were developed to control specimen alignment (*i.e.* standardizing sawing of the long bones and specimen mounting), any remaining slight misalignment of the specimen in the loading apparatus may have contributed to increased medial loading of the stifle. Finally, these findings may also simply be due to chance, as there is a 5% chance of making a type I error for each statistical test that is run. As several correlations were computed and a small sample size was used, the chance of significance due to error rises.

While investigating the intact osteoligamentous stifle provides new data on the response of a whole knee joint to various mechanical loading protocols, we cannot infer how tissues within the joint function together. The bone is likely not principally responsible for the results as bone is strongest in compression (Nordin & Frankel, 2012) with a large capacity for storing energy due to its porous structure. It would take roughly 500,000 loading cycles to damage cortical bone and specimens in this study were only loaded for 7200 cycles (Nordin & Frankel, 2012). Deformation in the toe region is likely due to both deformation of the cartilage and soft tissues such as ligaments and menisci in response to loading. The soft tissues were likely not a source of failure or joint disruption in this study as no visible damage was observed during dissection. On the other hand, cartilage damage was visually present as cartilage damage scores increased from the control to intervention stifle. This may suggest that cartilage is the first tissue to fail in this organ. However, further work examining whole joint function and ligamentous and menisci contribution to joint dysfunction is required.

This study had several limitations that must be considered when interpreting these findings. First, a general limitation of animal models is their questioned relevance for application to human mechanics (Gooyers, 2014). Pigs, like all quadrupeds, cannot produce full extension, unlike their human counterparts (Fuss, 1991). Additionally, the anterior cruciate ligament (ACL) has a bipartite nature in the porcine model, causing the ACL to be divided (Fuss, 1991). Second, the specimens were post-mortem that alters the tissues response to loading and rest (Bolton et al., 2015). However, the effects of death were found to be minimal on the mechanical properties of porcine cartilage (Adams et al.,

1998). Third, the loading protocol itself was basic as only compression in maximal extension available at the stifle was used. The knee joint moves from roughly 60° of flexion to near extension through a gait cycle, and moments are generated at the joint as result (Winter, 1990). Keeping the knee extended throughout the loading protocol will influence the areas loaded, and will expose the same area of cartilage to load throughout the duration of the protocol that may maximize damage (Seedhom, 2005). Last, as previously eluded to, the sample size of the current study was relatively small, which may have limited the ability to detect the desired effects.

3.4 Conclusion

Cumulative loading may be more important than rest when it comes to stifle mechanics and articular cartilage damage. The loading protocol was able to cause significant stifle deformations and energy dissipation in an intact stifle model.

Author Contributions

Damjana Milicevic designed the study, collected data, performed the analysis, and prepared the manuscript. Mamiko Noguchi assisted with study design and gave input on data analysis. Jack Callaghan and Joe Quadrilatero guided study design and analysis in addition to providing the necessary equipment for data collection. Monica Maly designed the study, guided the analysis and prepared the manuscript.

3.5 References

- Adams, M. A., Kerin, A. J., & Wisnom, M. R. (1998). Sustained loading increases the compressive strength of articular cartilage. *Connective Tissue Research*, 39(4), 245–256.
- Andriacchi, T. P., Koo, S., & Scanlan, S. F. (2009). Gait mechanics influence healthy cartilage morphology and osteoarthritis of the knee. *The Journal of Bone & Joint Surgery*, 91(Supplement 1), 95-101.
- Arthritis Alliance of Canada, the Impact of Arthritis in Canada: Today and Over the Next 30 Years (Fall 2011), 11.
- Aultman, C. D., Drake, J. D., Callaghan, J. P., & McGill, S. M. (2004). The effect of static torsion on the compressive strength of the spine: an in vitro analysis using a porcine spine model. *Spine*, 29(15), E304–E309.
- Bolton, S. N., Whitehead, M. P., Dudhia, J., Baldwin, T. C., & Sutton, R. (2015). Investigating the Postmortem Molecular Biology of Cartilage and its Potential Forensic Applications. *Journal of Forensic Sciences*, 60(4), 1061–1067.
- Callaghan, J. P., & McGill, S. M. (2001). Intervertebral disc herniation: studies on a porcine model exposed to highly repetitive flexion/extension motion with compressive force. *Clinical Biomechanics*, 16(1), 28–37.
- Cheng, Y., Macera, C. A., Davis, D. R., Ainsworth, B. E., Troped, P. J., & Blair, S. N. (2000). Physical activity and self-reported, physician-diagnosed osteoarthritis: is physical activity a risk factor? *Journal of Clinical Epidemiology*, 53(3), 315–322.

- Choi, J.A., & Gold, G. E. (2011). MR Imaging of Articular Cartilage Physiology. *Magnetic Resonance Imaging Clinics of North America*, 19(2), 249–282.
- Cook, J. L., Kuroki, K., Visco, D., Pelletier, J.-P., Schulz, L., & Lafebber, F. P. J. G. (2010). The OARSI histopathology initiative – recommendations for histological assessments of osteoarthritis in the dog. *Osteoarthritis and Cartilage*, 18, S66–S79.
- Dore, D. A., Winzenberg, T. M., Ding, C., Otahal, P., Pelletier, J.-P., Martel-Pelletier, J. ... Jones, G. (2013). The association between objectively measured physical activity and knee structural change using MRI. *Annals of the Rheumatic Diseases*, 72(7), 1170–1175.
- Eckstein, F., Hudelmaier, M., & Putz, R. (2006). The effects of exercise on human articular cartilage. *Journal of Anatomy*, 208(4), 491–512.
- Eckstein, F., Tieschky, M., Faber, S., Englmeier, K.-H., & Reiser, M. (1999). Functional analysis of articular cartilage deformation, recovery, and fluid flow following dynamic exercise in vivo. *Anatomy and Embryology*, 200(4), 419–424.
- Felson, D. T. (2004). An update on the pathogenesis and epidemiology of osteoarthritis. *Radiologic Clinics of North America*, 42(1), 1–9.
- Felson, D. T., Lawrence, R. C., Dieppe, P. A., Hirsch, R., Helmick, C. G., Jordan, J. M., ... & Sowers, M. (2000). Osteoarthritis: new insights. Part 1: the disease and its risk factors. *Annals of internal medicine*, 133(8), 635-646.
- Fuss, F. K. (1991). Anatomy and function of the cruciate ligaments of the domestic pig (*Sus scrofa domestica*): a comparison with human cruciates. *Journal of Anatomy*, 178, 11.

- Gatti, A.A. (2015). How do running and bicycling affect your knees? Retrieved from https://macsphere.mcmaster.ca/bitstream/11375/18311/2/Gatti_Anthony_A_August_2015_MSc.pdf
- Gooyers, C. E. (2014). Exploring interactions between force, repetition and posture on low back joint loading and intervertebral disc injury. Retrieved from <https://uwspace.uwaterloo.ca/handle/10012/8707>
- Jensen, L. K. (2008). Knee osteoarthritis: influence of work involving heavy lifting, kneeling, climbing stairs or ladders, or kneeling/squatting combined with heavy lifting. *Occupational and Environmental Medicine*, 65(2), 72–89.
- Kääb, M. J., Gwynn, I., & Nötzli, H. P. (1998). Collagen fibre arrangement in the tibial plateau articular cartilage of man and other mammalian species. *Journal of anatomy*, 193(01), 23-34.
- Kerin, A. J., Coleman, A., Wisnom, M. R., & Adams, M. A. (2003). Propagation of surface fissures in articular cartilage in response to cyclic loading in vitro. *Clinical Biomechanics*, 18(10), 960–968.
- Maly, M. R., Acker, S. M., Totterman, S., Tamez-Peña, J., Stratford, P. W., Callaghan, J. P. ... Beattie, K. A. (2015). Knee adduction moment relates to medial femoral and tibial cartilage morphology in clinical knee osteoarthritis. *Journal of Biomechanics*, 48(12), 3495–3501.
- Mansour, J. M. (2003). Biomechanics of cartilage. *Kinesiology: The Mechanics and Pathomechanics of Human Movement*, 66–79.

- Mastbergen, S. C., Marijnissen, A. C., Vianen, M. E., van Roermund, P. M., Bijlsma, J. W., & Lafeber, F. P. (2006). The canine “groove” model of osteoarthritis is more than simply the expression of surgically applied damage. *Osteoarthritis and Cartilage*, *14*(1), 39–46.
- Meyer, A. J., D’Lima, D. D., Besier, T. F., Lloyd, D. G., Colwell, C. W., & Fregly, B. J. (2013). Are external knee load and EMG measures accurate indicators of internal knee contact forces during gait? *Journal of Orthopaedic Research*, *31*(6), 921–929.
- Mündermann, A., Dyrby, C. O., D’Lima, D. D., Colwell, C. W., & Andriacchi, T. P. (2008). In vivo knee loading characteristics during activities of daily living as measured by an instrumented total knee replacement. *Journal of Orthopaedic Research*, *26*(9), 1167–1172.
- Nordin, M., & Frankel, V. H. (Eds.). (2012). *Basic biomechanics of the musculoskeletal system* (4th Ed). Philadelphia: Wolters Kluwer Health/Lippincott Williams & Wilkins.
- Outerbridge, R. E. (1961). The etiology of chondromalacia patellae. *Journal of Bone and Joint Surgery*, *43*.
- Özkaya, N., Nordin, M., Goldsheyder, D., & Leger, D. (1998). *Fundamentals of biomechanics: Equilibrium, motion, and deformation*. New York: Springer Verlag.
- Palmoski, M. J., & Brandt, K. D. (1984). Effects of static and cyclic compressive loading on articular cartilage plugs in vitro. *Arthritis & Rheumatism*, *27*(6), 675-681.

- Radin, E. L., Burr, D., Caterson, B., Fyhrie, D., Brown, T., & Boyd, R. (1991). Mechanical determinants of osteoarthritis, *Seminars in arthritis and rheumatism*, 21(3), 12–21.
- Rossignol, M. (2005). Primary osteoarthritis of hip, knee, and hand in relation to occupational exposure. *Occupational and Environmental Medicine*, 62(11), 772–777.
- Seedhom, B. B. (2005). Conditioning of cartilage during normal activities is an important factor in the development of osteoarthritis. *Rheumatology*, 45(2), 146–149.
- Vignon, É., Valat, J. P., Rossignol, M., Avouac, B., Rozenberg, S., Thoumie, P. ... & Hilliquin, P. (2006). Osteoarthritis of the knee and hip and activity: a systematic international review and synthesis (OASIS). *Joint Bone Spine*, 73(4), 442-455.
- Winter, D., 1990. *Biomechanics and Motor Control of Human Movement*. New York: Wiley-Interscience Publication.
- Yao, J. Q., & Seedhom, B. B. (1993). Mechanical conditioning of articular cartilage to prevalent stresses. *Rheumatology*, 32(11), 956-965.

Chapter Four: Discussion

4.0 Thesis Summary

The overarching goal of this thesis was to explore the impact of rest on the mechanics and breakdown of an intact joint to understand if rest modifies these responses. Study one determined that extension end range of motion did not relate to cartilage damage indicating that damage scores in study 2 should not be impacted by joint extension capabilities. The measures (goniometry and line bisection) used to obtain extension angle measurements demonstrated poor agreement. Furthermore, the use of a cartilage damage scoring system developed for grading canine stifle cartilage is acceptable for use in a porcine stifle model, as intra and inter-rater reliability were moderate to high. The loading protocol used in study 2 was successful in producing changes in joint deformation, energy dissipation, and cartilage damage. Interestingly, relationships between cartilage damage and energy dissipation were also uncovered. The direction of this relationship was different at the beginning and end of the loading protocol, suggesting that the tissues response to load may be changing over time which alters mechanical functioning throughout the protocol. Additionally, this work suggests that rest may not mitigate cartilage damage in a porcine model as cumulative exposure to joint loading, regardless of rest, appeared most important in deforming intact stifles. However, the small sample size may have limited the ability to detect the impact of rest on stifles. This work has contributed to the development to a new protocol that investigated the response of a whole joint to loading, to show that rest did not appear to have a large effect in mitigating a cumulative load.

4.1 Scientific Contributions

Examining 2 differing durations of rest (3:2 and 1:1) on the stifle joint as a whole was a novel contribution to the scientific literature. Rest did not appear to mitigate the damaging effects of loading in this sample that may suggest that overexposure to physical activity may result in joint and cartilage damage, regardless of rest. However, as previously mentioned, this may have been influenced by the small sample size. To properly power this study to reach significant results, a sample size of 114 pairs would be required.

This work also provides a solid foundation in methodological procedures to inform future work done in this area of study. The methodological protocols for this work were developed as a result of a year of diligent pilot work. During development of the study protocol, 3 main issues were encountered: 1) translation of the bottom cup during loading 2) deflection of force through the Instron loading arm, and 3) secure mounting and alignment of specimens to minimize the generation of a torque. The creation of a custom built jig was a solution for concerns 1 and 2. This jig prevented posterior sliding of the bottom cup in addition to guiding the movement of the Instron arm during loading. The development of standardized protocols regarding specimen preparation (*i.e.* sawing of long bones, drilling and wire placement, careful alignment) was paramount in assuring the highest quality results were obtained. This careful and standardized preparation was able to solve issue 3. The use of a custom built jig and highly standardized protocols was imperative for this work and should be considered in future work examining stifle responses to loading.

The majority of published literature focuses on studying injury mechanisms in individual tissues *ex vivo* (*i.e.* articular cartilage plugs). For example, Kerin et al (2003) demonstrated that fissures can be produced, and propagated in bovine stifle articular cartilage plugs. Additionally, creep loaded cartilage fails sooner than non-creep loaded cartilage as a result of fluid flow out of the cartilage resulting in diminished shock absorption (Adams et al., 1998). Thus, *ex vivo* experiments have been successful in damaging articular cartilage and altering mechanical behavior. However, this work is limited as the response of only 1 tissue is studied. Cartilage may behave differently when loaded in its natural environment versus when it is removed from the joint (Armstrong et al., 1980). When injuries occur in the real world, injury mechanisms depend on the entire joint system, and failure of one tissue can impact the function of all other tissues in the system. Studying the joint as whole allows for injury mechanisms of the entire system to be examined, which represents how a joint would act under repetitive cyclical loading in a real life scenario. Examining the response of the joint under physiologically representative loads was also a unique contribution as a vertical ground reaction force curve was used to load specimens.

Common themes were found between study 1 and 2. A large range of cartilage damage sores existed prior to loading among this sample of porcine stifles, acquired from local abattoirs. This amount of variability between specimens illustrated the need for using matched pairs. It is important to note, however, that a design using matched pairs assumes that cartilage damage would be equivalent between both limbs of the same animal. This assumption has merit and been made before in previous work (Adams et al.,

1998). However, knee OA often presents unilaterally, which challenges this assumption. Radiography is an alternative method of assessing the presence and severity of knee OA. However, radiography is costly and major grading systems tend to focus on osteophyte formation and joint space narrowing that may not necessarily be representative of cartilage surface fibrillation (Altman et al., 2007; Cooke et al., 2007). Difficulty obtaining specimens in a timely manner drove researchers to obtain specimens from three separate abattoirs, which may contribute to the large range of cartilage damage scores. Animals from each source may have been exposed to different loading exposures, resulting in potential differences in cartilage tolerance in varying locations on the joint surface (Seedhom, 2005). Study 2 further expanded on this point by demonstrating that high initial cartilage damage may result in an altered response of the entire stifle during loading and increased cartilage damage following loading (Andriacchi, 2009). Thus, damage at 1 level of the joint (*i.e.* articular cartilage surface) may lead to altered responses in other joint tissues, like ligaments and bone.

4.2 Future Directions

Future work should aim to test longer periods of rest to further test whether cumulative loading is more important than injecting rest in determining the mechanical properties and cartilage damage of porcine stifles. A risk factor for the development of knee OA is joint overuse (Felson, 2004). Exposure to excessive joint loading, particularly of a damaged and vulnerable joint, can contribute to the development of OA. This is commonly seen in athletics and occupational activities, despite the fact that these individuals have intermittent rest breaks (Felson, 2004). Additionally, the ligaments and

menisci require further study and examination to determine their role in knee dysfunction as a result of repetitive loading. To answer this question, a collaborative research program is proposed where a diverse team (biologists, physiologists, kinesiologists, engineers) with expertise in various tissues work together to test each tissue in the knee joint (i.e. cartilage, ligament, tendon, muscle, bone, meniscus) following loading of an intact knee to identify how each tissue responds to load, and that tissues are contributing to joint failure. Future work should strive to load the stifle in different positions, such as varying levels of joint flexion. High flexion would be of particular interest as this knee posture is linked to knee OA development (Jensen, 2008; Rossignol et al., 2005). The effects of rest should also be examined in humans, *in vivo*, using MRI to assess how cartilage composition (*i.e.* determined by T2 relaxation time) is altered when rest is incorporated into a loading protocol.

4.3 References

- Adams, M. A., Kerin, A. J., & Wisnom, M. R. (1998). Sustained loading increases the compressive strength of articular cartilage. *Connective Tissue Research*, 39(4), 245–256.
- Altman, R. D., & Gold, G. E. (2007). Atlas of individual radiographic features in osteoarthritis, revised. *Osteoarthritis and cartilage*, 15, A1-A56.
- Andriacchi, T. P., Koo, S., & Scanlan, S. F. (2009). Gait mechanics influence healthy cartilage morphology and osteoarthritis of the knee. *The Journal of Bone & Joint Surgery*, 91(Supplement 1), 95-101.
- Armstrong, C. G., Bahrani, A. S., & Gardner, D. L. (1980). Changes in the deformational behavior of human hip cartilage with age. *Journal of Biomechanical Engineering*, 102(3), 214-220.
- Cooke, T. D. V., Sled, E. A., & Scudamore, R. A. (2007). Frontal plane knee alignment: a call for standardized measurement. *Journal of Rheumatology*, 34(9), 1796-1801.
- Felson, D. T. (2004). An update on the pathogenesis and epidemiology of osteoarthritis. *Radiologic Clinics of North America*, 42(1), 1–9.
- Jensen, L. K. (2008). Knee osteoarthritis: influence of work involving heavy lifting, kneeling, climbing stairs or ladders, or kneeling/squatting combined with heavy lifting. *Occupational and Environmental Medicine*, 65(2), 72–89.

- Kerin, A. J., Coleman, A., Wisnom, M. R., & Adams, M. A. (2003). Propagation of surface fissures in articular cartilage in response to cyclic loading in vitro. *Clinical Biomechanics*, 18(10), 960–968.
- Rossignol, M. (2005). Primary osteoarthritis of hip, knee, and hand in relation to occupational exposure. *Occupational and Environmental Medicine*, 62(11), 772–777.
- Seedhom, B. B. (2005). Conditioning of cartilage during normal activities is an important factor in the development of osteoarthritis. *Rheumatology*, 45(2), 146–149.

Appendix A

Macroscopic Cartilage Damage Score – A Guide to Scoring Images

- 1) All scoring will be done on standardized images captured at the time of data collection
- 2) Scores ranging from 0-4 will be given for each joint compartment (lateral and medial tibia and femur):

Surface Description	Score
Smooth Surface	0
Slightly fibrillated/roughened surface	1
Fibrillated surface with focal partial thickness lesions	2
Deep lesions surrounding damage	3
Large areas of severe damage	4

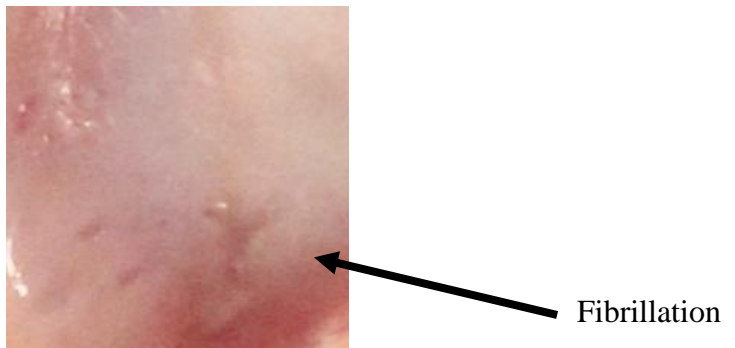
- 3) Assessors will be blinded to the specimen number and group allocation
- 4) Assessors will assume all visible damage is due to the loading protocol and will score what they see in the image
- 5) The entire compartment should be considered when scoring each specimen and the worst score for that compartment will be used to represent damage in that compartment
- 6) In case of uncertainty, assessors should take a more conservative approach when grading (ex. If unsure between 1 and 2 give a score of 2)
- 7) Assessors may use the zoom function to view the articular surface, and any damage present

Examples of damage in a porcine model (from thesis work):

0 – Smooth surface



1 – Slightly fibrillated/roughened surface



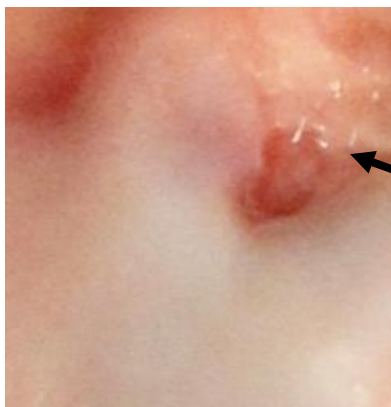
2 - Fibrillated surface with focal partial thickness lesions



Focal partial thickness lesion – the cartilage appears 'grooved'

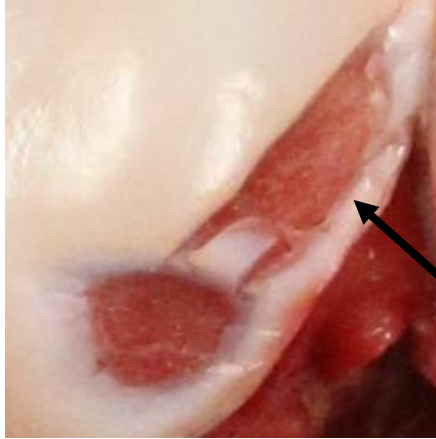
Fibrillation

3 - Deep lesions surrounding damage



Full thickness lesion – the cartilage appears to have a 'hole' in its surface

4 - Large areas of severe damage



Complete degeneration
of cartilage surface –
areas of subchondral
bone visible

Appendix B

Supplementary Figures and Tables

Table B.1: Cartilage damage scores for all intervention and control specimens and for all 4 joint compartments. Damage scores increase from no damage (0) to large areas of severe damage (4). Boxes coloured in green indicate a score of 0. Blue boxes represent scores of 1. Yellow boxes represent a score of 2, and orange represents a score of 3. The colour red represents a score of 4.

Specimen	Loading Protocol	Intervention Vs Control (I vs C)	Cartilage Damage Score			
			Lateral Tibia	Medial Tibia	Lateral Femur	Medial Femur
1	NR	C	2	1	2	1
		I	2	3	2	3
2	NR	C	1	1	2	2
		I	3	2	2	4
3	1:1	C	0	0	1	1
		I	1	1	2	3
4	3:2	C	1	0	1	0
		I	1	1	3	2
5	3:2	C	2	0	1	1
		I	3	1	2	4
6	NR	C	0	0	0	1
		I	2	2	2	2
7	3:2	C	2	1	2	0
		I	1	1	3	1
8	1:1	C	2	1	2	1
		I	2	1	2	2
9	NR	C	1	1	1	2
		I	2	1	2	3
10	3:2	C	1	0	1	1
		I	2	3	2	3
11	NR	C	1	0	1	0
		I	2	2	2	3
12	1:1	C	1	1	1	1
		I	1	2	1	1
13	3:2	C	0	0	1	0
		I	0	0	2	2
14	1:1	C	2	0	1	1
		I	2	1	2	2

15	3:2	C	1	1	2	1
		I	2	1	3	2
16	1:1	C	1	1	2	1
		I	4	1	2	2
17	NR	C	1	1	1	1
		I	2	1	2	2
18	1:1	C	2	1	3	1
		I	2	1	2	2

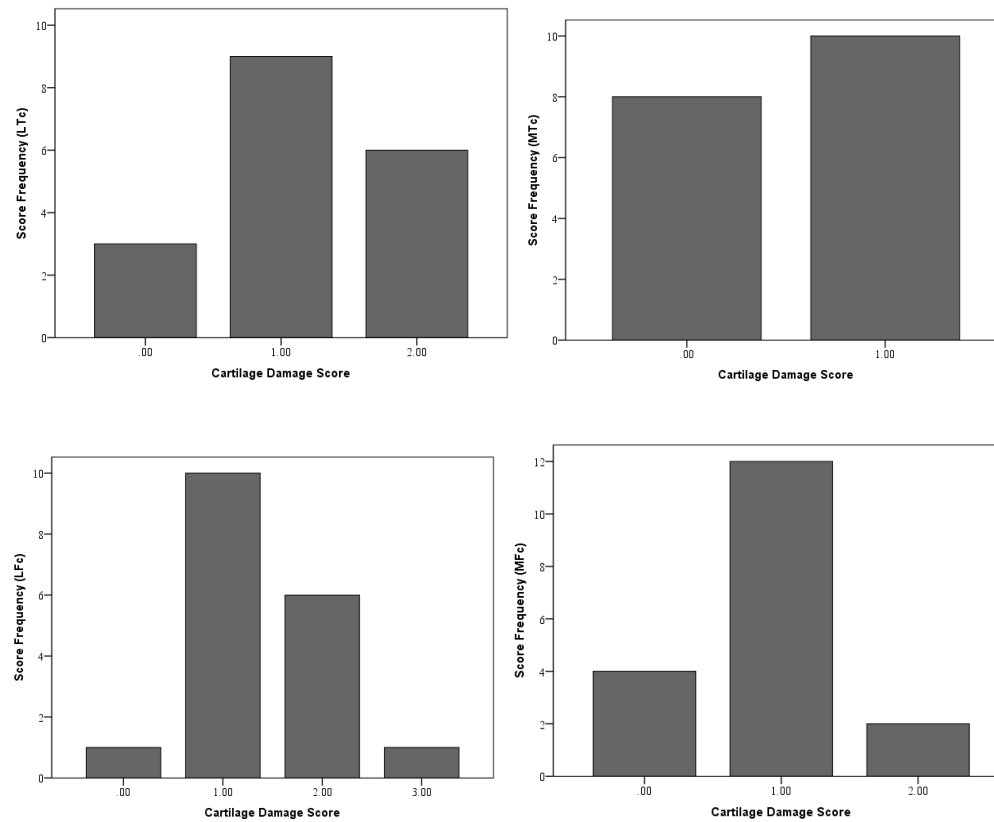


Figure B.1: The frequency of cartilage damage scores for all 4 joint compartments (LT = lateral tibia, MT = medial tibia, LF = lateral femur, MF = medial femur) in control (c) specimens. Damage scores increase from no damage (0) to large areas of severe damage (4).

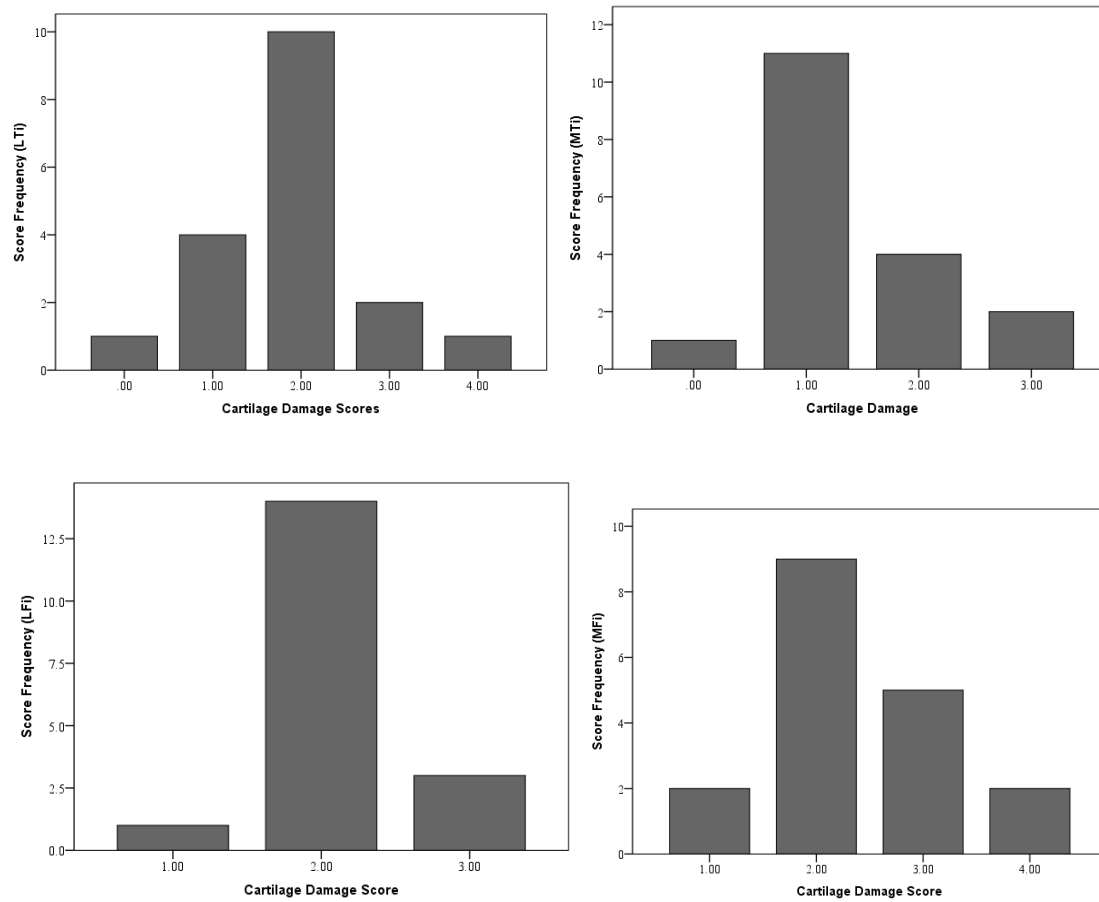


Figure B.2: The frequency of cartilage damage scores for all 4 joint compartments (LT = lateral tibia, MT = medial tibia, LF = lateral femur, MF = medial femur) in intervention (i) specimens. Damage scores increase from no damage (0) to large areas of severe damage (4).

Appendix C

Thesis Collection Sheet

Date: _____

Loading Protocol: _____

Right/Left: _____

Control/Intervention: _____

Overall Time: _____

Notes on specimen preparation (height, bone quality etc.):

1) Qualitative Assessment:

*Note: Remember to CLOSE all curtains. Use only room lighting.

Notes (amount/type of damage seen/drawings):

Image Names (* beside one to use):

Tibia: _____

Tibia: _____

Tibia: _____

Femur: _____

Femur: _____

Femur: _____

At time of assessment:

Smooth surface – Outerbridge 0	0
Slightly fibrillated/roughened surface – Outerbridge 1	1
Fibrillated surface with focal partial thickness lesions – Outerbridge 2	2
Deep lesions with surrounding damage – Outerbridge 3	3
Large areas of severe damage – Outerbridge 4	4

Lateral Tibia: _____ Medial Tibia: _____

Lateral Femur: _____ Medial Femur: _____

2) Laser Scan:

Notes:

Image Names (* beside one to use):

Tibia: _____ Femur: _____

Tibia: _____ Femur: _____

Tibia: _____ Femur: _____

3) Load Deformation:

File names

Work: _____

Rest: _____